

Structural and Chemical Biology of the Interaction of Cyclooxygenase with Substrates and Non-Steroidal Anti-Inflammatory Drugs

Carol A. Rouzer and Lawrence J. Marnett*

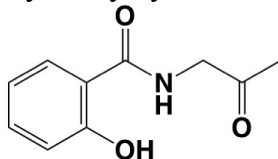
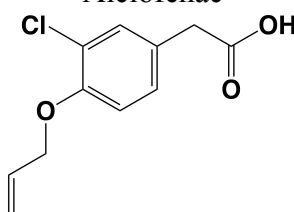
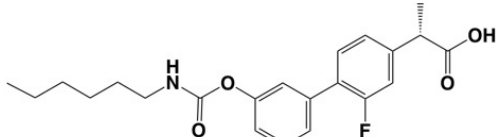
A. B. Hancock Jr. Memorial Laboratory for Cancer Research, Departments of Biochemistry, Chemistry, and Pharmacology, Vanderbilt Institute of Chemical Biology, Center in Molecular Toxicology, Vanderbilt-Ingram Cancer Center, Vanderbilt University School of Medicine, Nashville, Tennessee 37232

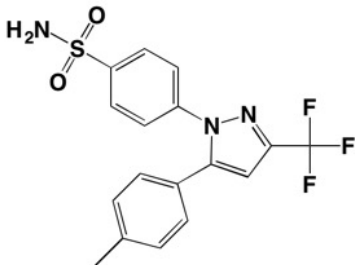
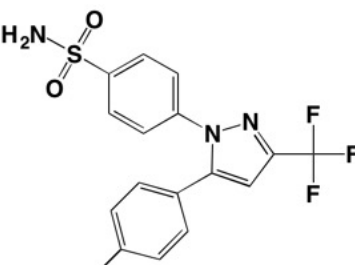
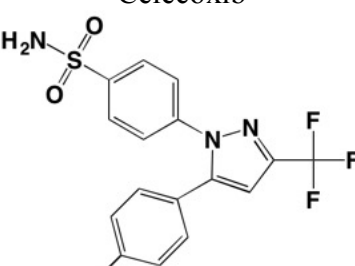
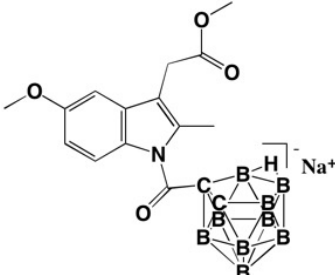
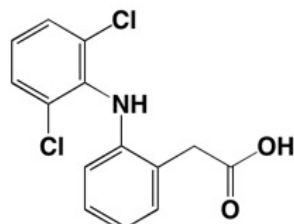
Supporting Information Table of Contents

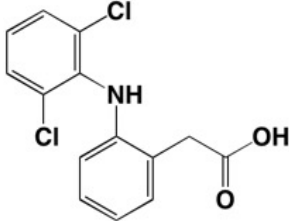
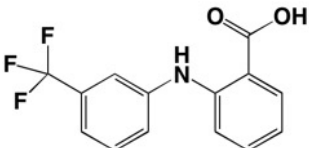
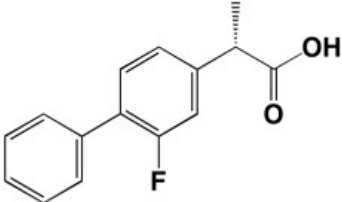
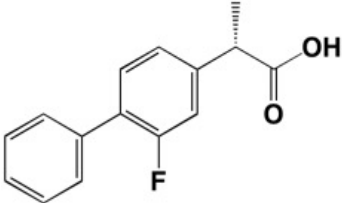
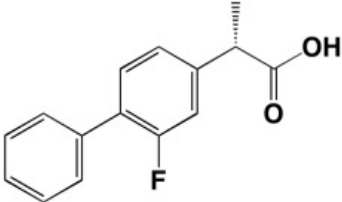
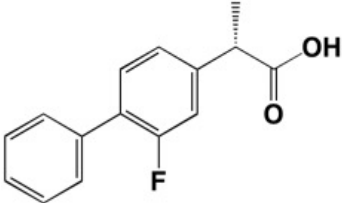
1. Table S1	Pages S2-S18
2. Table S2	Pages S19-S34
3. Figures S1-S20 Wall-Eyed Format	Pages S35-S63
4. Figures 1-22 Cross-Eyed Format	Pages S64-S100
5. Figures S1-S20 Cross-Eyed Format	Pages S101-S132

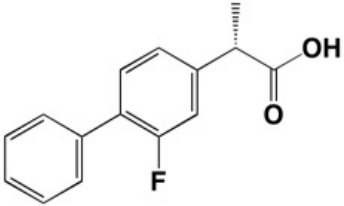
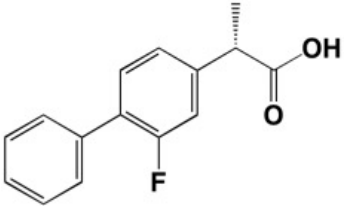
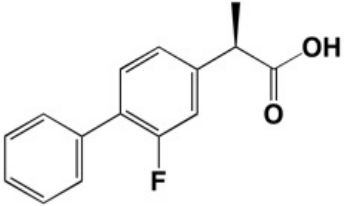
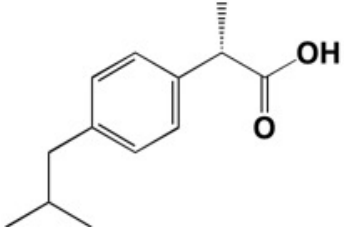
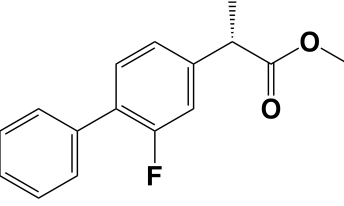
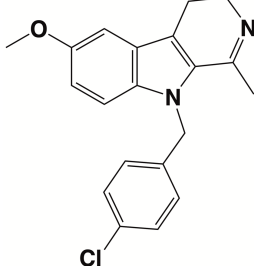
Table S1. Summary table of crystal structures.

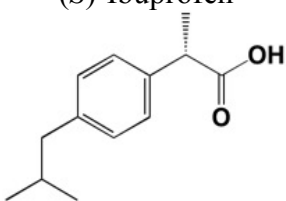
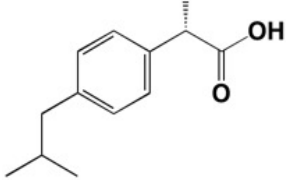
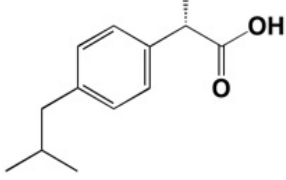
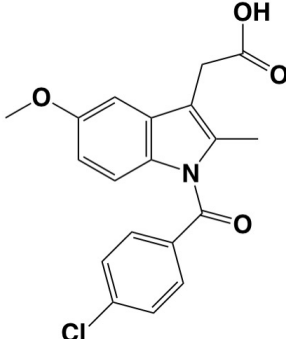
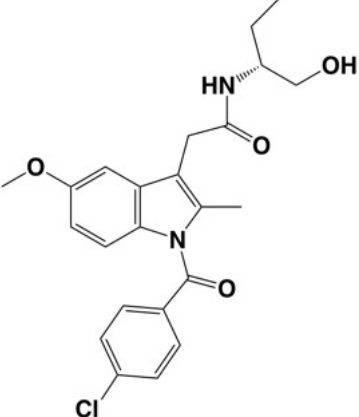
Data are listed in alphabetical order by ligand. Inhibitors are listed first followed by fatty acids. If more than one structure is available for a given ligand, data are provided for complexes containing COX-1 followed by COX-2. If more than one structure is available for a given enzyme-ligand complex, they are listed historically first for the wild-type enzyme followed by mutations of the enzyme created to study enzyme-ligand interactions. Sequence variations designate amino acids that differ from the NCBI reference sequence. These include intentionally and unintentionally engineered mutations and naturally occurring variants.

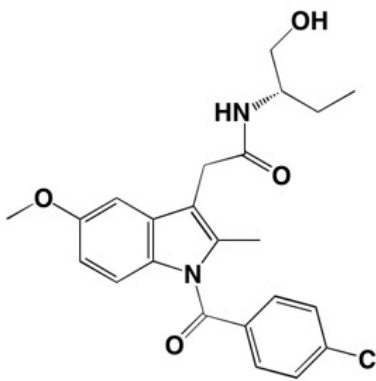
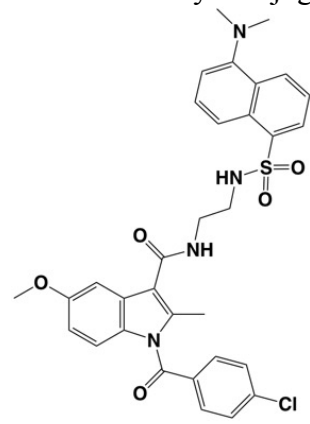
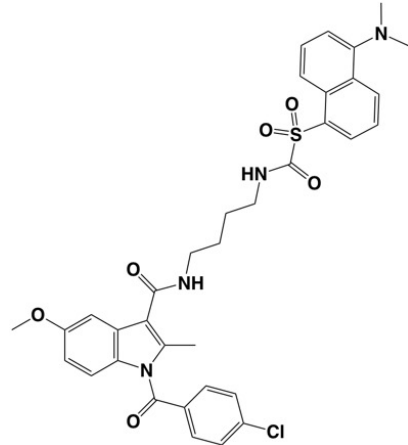
PDB#	Ref	Res	Isoform Cofactor Species Sequence variations	Asym Unit	Ligand Structure
5F19	1	2.04 Å	COX-2 Acetyl- Co ³⁺ -PPIX Human Δ586-612	1 dimer I222	Acetylated
1EBV	2	3.2 Å	COX-1 Acetyl- Fe ³⁺ -PPIX Sheep	1 monomer I222	<i>O</i> -Acetylsalicylhydroxamic Acid 
1HT8	3	2.69 Å	COX-1 Fe ³⁺ -PPIX Sheep	1 dimer I222	Alclofenac 
5W58	4	2.27 Å	COX-2 Fe ³⁺ -PPIX Mouse	1 monomer I4 22	ARN-2508 

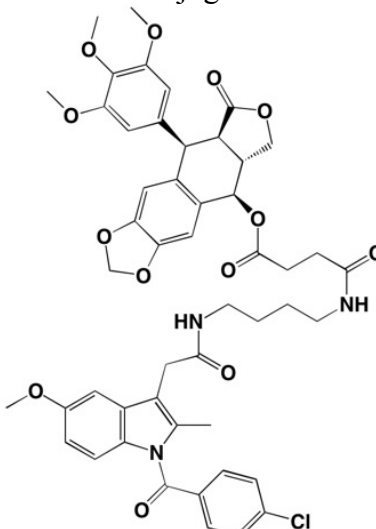
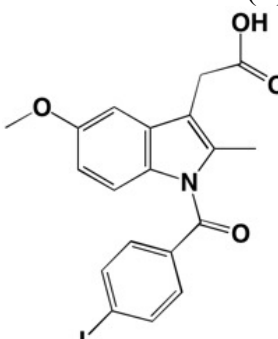
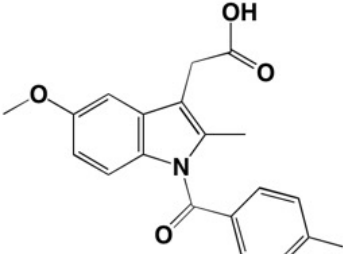
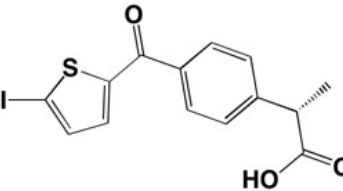
3KK6	5	2.75 Å	COX-1 Fe ³⁺ -PPIX Sheep	1 dimer P6 ₅	Celecoxib 
3LN1	6	2.4 Å	COX-2 Fe ³⁺ -PPIX Mouse	2 dimers P2 ₁ 2 ₁ 2	Celecoxib 
5JW1	7	2.82 Å	COX-2 Co ³⁺ -PPIX Mouse S121P	1 dimer I222	Celecoxib 
4Z0L	8	2.29 Å	COX-2 Fe ³⁺ -PPIX Mouse	2 dimers P2 ₁ 2 ₁ 2	<i>nido</i> -Dicarbaborate derivative of indomethacin methyl ester4Z0 
3N8Y	5	2.6 Å	COX-1 Acetyl- Fe ³⁺ -PPIX Sheep	1 dimer P6 ₅	Diclofenac 

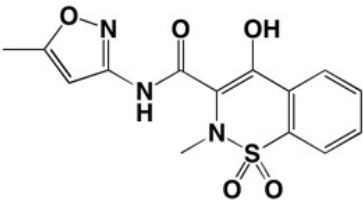
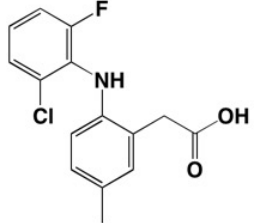
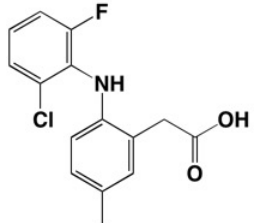
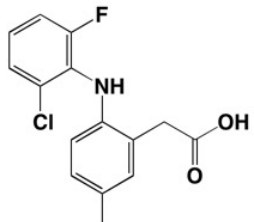
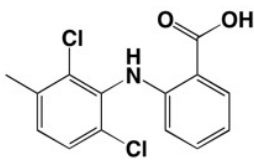
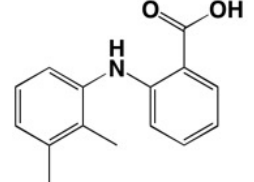
1PXX	9	2.9 Å	COX-2 Fe ³⁺ -PPIX Mouse	2 dimers P2 ₁ 2 ₁ 2	<p>Diclofenac</p> 
5IKV	10	2.51 Å	COX-2 Co ³⁺ -PPIX Human Δ586-612	1 dimer I222	<p>Flufenamic Acid</p> 
1CQE	11	3.1 Å	COX-1 Fe ³⁺ -PPIX Sheep	1 dimer I222	<p>(S)-Flurbiprofen</p> 
1EQH	3	2.7 Å	COX-1 Fe ³⁺ -PPIX Sheep	1 dimer I222	<p>(S)-Flurbiprofen</p> 
2AYL	12	2.0 Å	COX-1 Mn ³⁺ -PPIX Sheep	1 dimer I222	<p>(S)-Flurbiprofen</p> 
3N8Z	5	2.9 Å	COX-1 Fe ³⁺ -PPIX Sheep	1 dimer P6 ₅	<p>(S)-Flurbiprofen</p> 

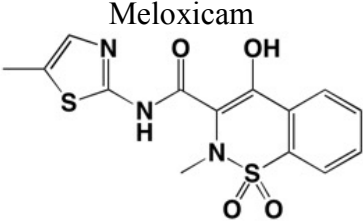
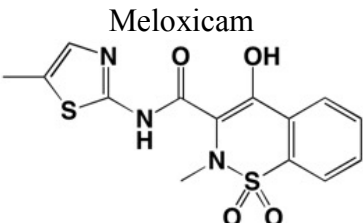
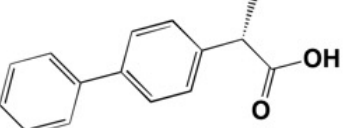
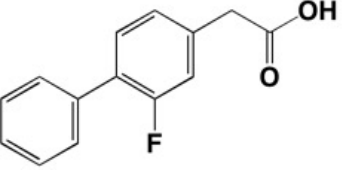
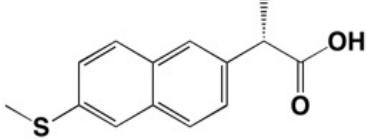
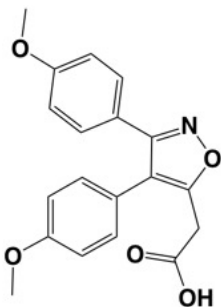
3N8W	5	2.75 Å	COX-1 Fe ³⁺ -PPIX Sheep R120Q/WT heterodimer	1 dimer P6 ₅	(S)-Flurbiprofen 
3PGH	13	2.5 Å	COX-2 Fe ³⁺ -PPIX Mouse N310Q R333K	2 dimers P2 ₁ 2 ₁ 2	(S)-Flurbiprofen 
3RR3	14	2.84 Å	COX-2 Fe ³⁺ -PPIX Mouse	2 dimers P2 ₁ 2 ₁ 2	(R)-Flurbiprofen 
5JVZ	7	2.62 Å	COX-2 Co ³⁺ -PPIX Mouse S121P	1 dimer I222	(S)-Flurbiprofen 
1HT5	3	2.75 Å	COX-1 Fe ³⁺ -PPIX Sheep	1 dimer I222	(S)-Flurbiprofen Methylenelester 
6V3R	15	2.66 Å	COX-2 Fe ³⁺ -PPIX Mouse	2 dimers C121	Harmaline Compound 3 

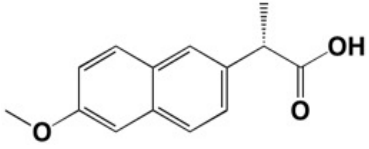
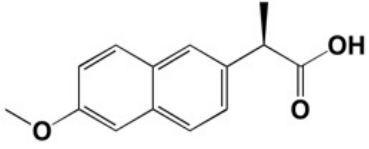
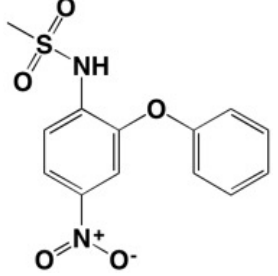
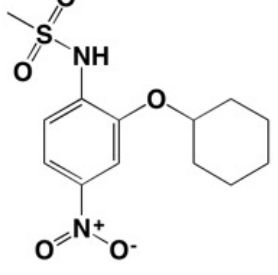
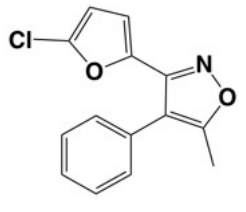
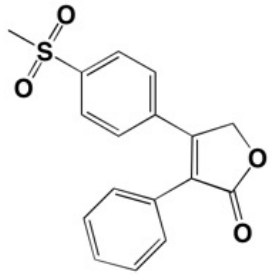
1EQG	3	2.61 Å	COX-1 Fe ³⁺ -PPIX Sheep	1 dimer I222	(S)-Ibuprofen 
4PH9	16	1.81 Å	COX-2 Fe ³⁺ -PPIX Mouse	1 dimer I222	(S)-Ibuprofen 
4RS0	17	2.81 Å	COX-2 Fe ³⁺ -PPIX Mouse H90W	1 monomer I4 ₁ 2 ₂	(S)-Ibuprofen 
4COX	13	2.9 Å	COX-2 Fe ³⁺ -PPIX Mouse N310Q R333K	2 dimers P2 ₁ 2 ₁ 2	Indomethacin 
2OYE	18	2.85 Å	COX-1 Fe ³⁺ -PPIX Sheep	1 monomer P6 ₅ 2 ₂	Indomethacin-(R)-α-ethyl- ethanolamide 

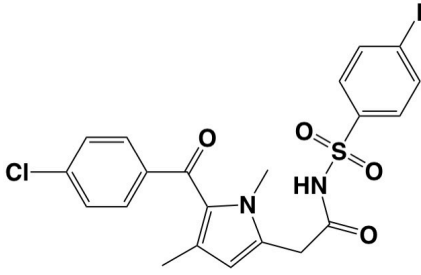
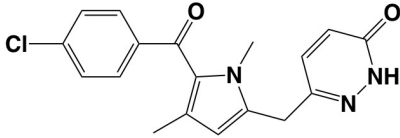
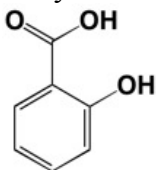
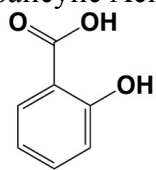
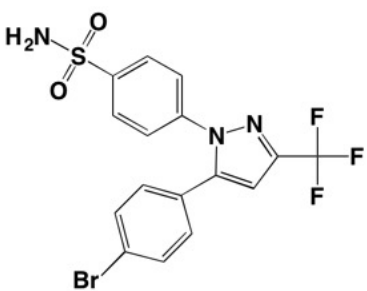
2OYU	18	2.7 Å	COX-1 Fe ³⁺ -PPIX Sheep	1 monomer P6 ₅ 22	Indomethacin-(S)-α-ethyl-ethanolamide 
6BL4	19	2.22 Å	COX-2 Fe ³⁺ -PPIX Mouse	2 dimers P2 ₁ 2 ₁ 2	Indomethacin-dansyl conjugate 1 
6BL3	19	2.22 Å	COX-2 Fe ³⁺ -PPIX Mouse	2 dimers P2 ₁ 2 ₁ 2	Indomethacin-dansyl conjugate 2 

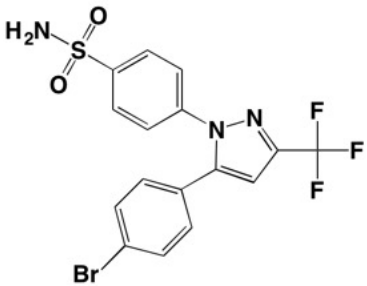
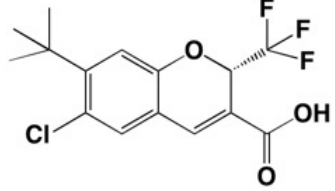
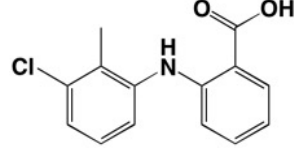
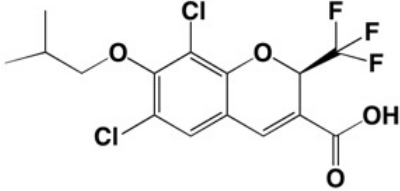
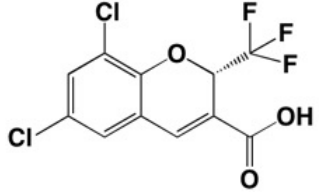
4OTJ	20	2.11 Å	COX-2 Fe ³⁺ -PPIX Mouse	2 dimers P2 ₁ 2 ₁ 2	Indomethacin-podophyllotoxin conjugate 
1PGF	21	4.5 Å	COX-1 Fe ³⁺ -PPIX Sheep	1 dimer I222	Iodoindomethacin (<i>E</i>) 
1PGG	21	4.5 Å	COX-1 Fe ³⁺ -PPIX Sheep	1 dimer I222	Iodoindomethacin (<i>Z</i>) 
1PGE	21	3.5 Å	COX-1 Fe ³⁺ -PPIX Sheep	1 dimer I222	(<i>S</i>)-Iodosuprofen 

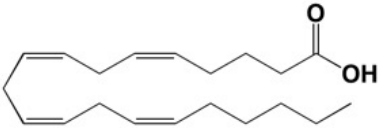
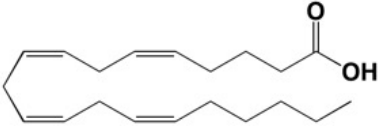
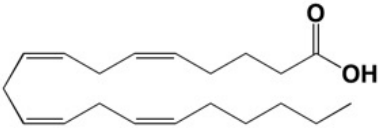
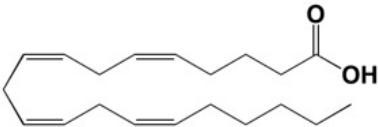
4M10	22	2.01 Å	COX-2 Fe ³⁺ -PPIX Mouse	2 dimers P22 ₁ 2 ₁	<p>Isoxicam</p> 
4OTY	23	2.35 Å	COX-2 Apo Mouse	1 dimer I222	<p>Lumiracoxib</p> 
4RRZ	17	2.57 Å	COX-2 Apo Mouse H90W	2 dimers C121	<p>Lumiracoxib</p> 
4RRX	17	2.78 Å	COX-2 Apo Mouse V89W	1 dimer I222	<p>Lumiracoxib</p> 
5IKQ	10	2.41 Å	COX-2 Co ³⁺ -PPIX Human Δ586-612	1 dimer I222	<p>Meclofenamic Acid</p> 
5IKR	10	2.34 Å	COX-2 Co ³⁺ -PPIX Human Δ586-612	1 dimer I222	<p>Mefenamic Acid</p> 

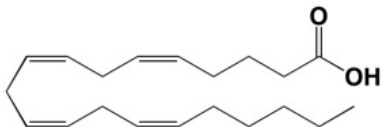
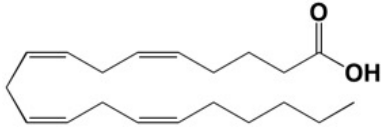
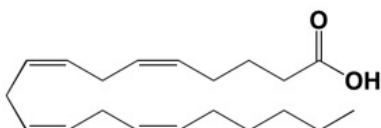
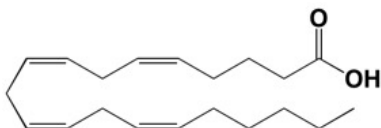
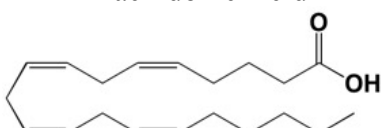
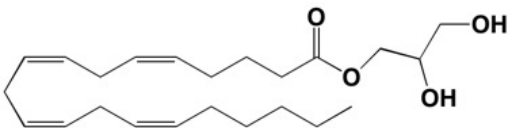
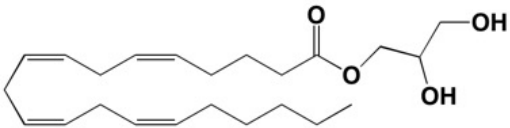
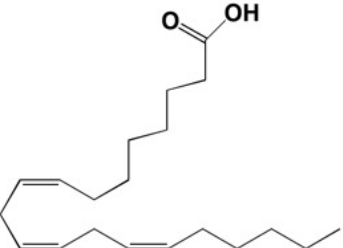
4O1Z	22	2.4 Å	COX-1 Fe ³⁺ -PPIX Sheep	1 dimer P6 ₅	Meloxicam 
4M11	22	2.45 Å	COX-2 Fe ³⁺ -PPIX Mouse	2 dimers P2 ₂ 1 ₂ 1	Meloxicam 
1Q4G	24	2.0 Å	COX-1 Fe ³⁺ -PPIX Sheep	1 dimer I222	(S)-α-Methyl-4-biphenylacetic Acid 
4FM5	25	2.81 Å	COX-2 Fe ³⁺ -PPIX Mouse	2 dimers P2 ₁ 2 ₁ 2	des-Methyl-flurbiprofen 
3NTB	26	2.27 Å	COX-2 Fe ³⁺ -PPIX Mouse	2 dimers P2 ₁ 2 ₁ 2	6-Methylthio-(S)-naproxen 
5WBE	27	2.75 Å	COX-1 Fe ³⁺ -PPIX Sheep	1 dimer P6 ₅	Mofezolac 

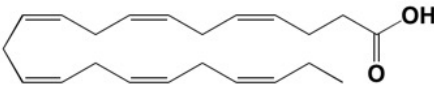
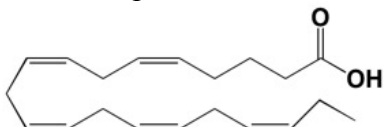
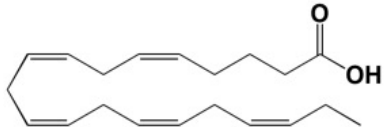
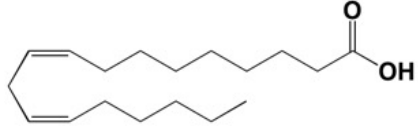
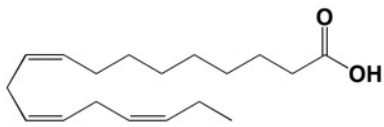
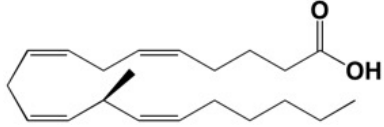
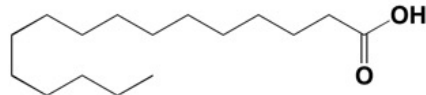
3NT1	26	1.73 Å	COX-2 Fe ³⁺ -PPIX Mouse	1 dimer I222	(S)-Naproxen 
3Q7D	14	2.4 Å	COX-2 Fe ³⁺ -PPIX Mouse	1 dimer I222	(R)-Naproxen 
3N8X	5	2.75 Å	COX-1 Fe ³⁺ -PPIX Sheep	1 dimer P6 ₅	Nimesulide 
3QMO	28	3.0 Å	COX-2 Co ³⁺ -PPIX Mouse N594A	1 dimer I222	NS-398 
5U6X	27	2.93 Å	COX-1 Fe ³⁺ -PPIX Sheep	1 dimer P6 ₅	P6 
5KIR	29	2.7 Å	COX-2 Co ³⁺ -PPIX Human Q350N Δ586-612	1 dimer I222	Rofecoxib 

NA	30	3.3 Å	COX-2 Fe ³⁺ -PPIX Human	1 dimer I222	RS104897 
NA	30	2.9 Å	COX-2 Fe ³⁺ -PPIX Human	1 dimer I222	RS57067 
1PTH	31	3.4 Å	COX-1 Br-acetyl- Fe ³⁺ -PPIX Sheep	1 dimer I222	Salicylic Acid 
5F1A	1	2.38 Å	COX-2 Co ³⁺ -PPIX Human Δ586-612	1 dimer I222	Salicylic Acid 
6COX	13	2.8 Å	COX-2 Fe ³⁺ -PPIX Mouse N310Q R333K	1 dimer I222	SC-558 

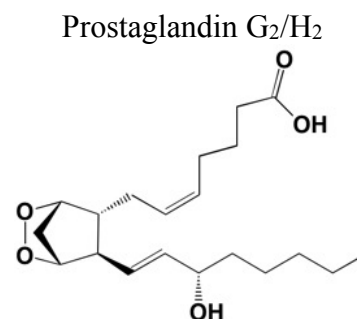
1CX2	13	3.0 Å	COX-2 Fe ³⁺ -PPIX Mouse N310Q R333K	2 dimers P2 ₁ 2 ₁ 2	<p>SC-558</p> 
3MQE	32	2.8 Å	COX-2 Fe ³⁺ -PPIX Mouse	2 dimers P2 ₁ 2 ₁ 2	<p>(S)-SC-75416</p> 
5IKT	10	2.45 Å	COX-2 Co ³⁺ -PPIX Human Δ586-612	1 dimer I222	<p>Tolfenamic Acid</p> 
3NTG	32	2.19 Å	COX-2 Fe ³⁺ -PPIX Mouse	2 dimers P2 ₁ 2 ₁ 2	<p>(R)-23d</p> 
3LN0	6	2.2 Å	COX-2 Fe ³⁺ -PPIX Mouse	2 dimers P2 ₁ 2 ₁ 2	<p>(S)-5c</p> 
3N8V	5	3.05 Å	COX-1 Fe ³⁺ -PPIX Sheep	1 dimer P6 ₅	No ligand
5COX	13	3.0 Å	COX-2 Fe ³⁺ -PPIX Mouse N310Q R333K	2 dimers P2 ₁ 2 ₁ 2	No ligand

4RRW	17	2.57 Å	COX-2 Apo Mouse	2 dimers C121	No Ligand
4RRY	17	2.43 Å	COX-2 Apo Mouse H90W	2 dimers P2 ₁ 2 ₁ 2	No Ligand
5FDQ	1	1.9 Å	COX-2 Co ³⁺ -PPIX Mouse S530T N594A	1 dimer I222	No Ligand
5JVY	7	2.36 Å	COX-2 Co ³⁺ -PPIX Mouse K82A N86Q I105V S121P	1 dimer I222	No Ligand
1DIY	33	3.0 Å	COX-1 Co ³⁺ -PPIX Sheep	1 monomer P6 ₅ 22	Arachidonic Acid 
1U67	18	3.1 Å	COX-1 Co ³⁺ -PPIX Sheep V349A W387F	1 monomer P6 ₅ 22	Arachidonic Acid 
1DDX	34	3.0 Å	COX-2 Apo Mouse	2 dimers P2 ₁ 2 ₁ 2	Arachidonic Acid 
1CVU	34	2.4 Å	COX-2 Apo Mouse H207A N310Q R333K	1 dimer I222	Arachidonic Acid 

3HS5	35	2.1 Å	COX-2 Co ³⁺ -PPIX Mouse N594A	1 dimer I222	Arachidonic Acid 
3KRK	35	2.4 Å	COX-2 Co ³⁺ -PPIX Mouse L531F N594A	1 dimer I222	Arachidonic Acid 
3OLT	36	2.45 Å	COX-2 Co ³⁺ -PPIX Mouse R513H	1 dimer I222	Arachidonic Acid 
3TZI	37	2.15 Å	COX-2 Co ³⁺ -PPIX Mouse G533V N594A	1 dimer I222	Arachidonic Acid 
6OFY	38	2.2 Å	COX-2 Co ³⁺ -PPIX Mouse V349I N594A	1 dimer I222	Arachidonic Acid 
3MDL	36	2.2 Å	COX-2 Co ³⁺ -PPIX Mouse N594A	1 dimer I222	1-Arachidonoyl Glycerol 
3OLU	36	2.35 Å	COX-2 Co ³⁺ -PPIX Mouse R513H	1 dimer I222	1-Arachidonoyl Glycerol 
1FE2	39	3.0 Å	COX-1 Co ³⁺ -PPIX Sheep	1 dimer P6522	Dihomo-γ-linolenic Acid 

3HS7	35	2.65 Å	COX-2 Co ³⁺ -PPIX Mouse N594A	1 dimer I222	Docosahexaenoic Acid 
1IGX	40	3.1 Å	COX-1 Co ³⁺ -PPIX Sheep	1 monomer P6522	Eicosapentaenoic Acid 
3HS6	35	2.4 Å	COX-2 Co ³⁺ -PPIX Mouse N594A	1 dimer I222	Eicosapentaenoic Acid 
1IGZ	40	2.9 Å	COX-1 Co ³⁺ -PPIX Sheep	1 monomer P6522	Linoleic Acid 
4E1G	37	2.1 Å	COX-2 Co ³⁺ -PPIX Mouse N594A	1 dimer I222	α -Linolenic Acid 
4RUT	41	2.16 Å	COX-2 Co ³⁺ -PPIX Mouse	2 dimers C121	13(S)-Methyl-arachidonic Acid 
3QH0	42	2.1 Å	COX-2 Co ³⁺ -PPIX Mouse N594A	1 dimer I222	Palmitic Acid 

1DDX 34 3.0 Å COX-2
Apo 2 dimers
Mouse P2₁2₁2



References

- (1) Lucido, M. J.; Orlando, B. J.; Vecchio, A. J.; Malkowski, M. G. *Biochemistry* **2016**, *55*, 1226.
- (2) Loll, P. J.; Sharkey, C. T.; O'Connor, S. J.; Dooley, C. M.; O'Brien, E.; Devocelle, M.; Nolan, K. B.; Selinsky, B. S.; Fitzgerald, D. J. *Mol Pharmacol* **2001**, *60*, 1407.
- (3) Selinsky, B. S.; Gupta, K.; Sharkey, C. T.; Loll, P. J. *Biochemistry* **2001**, *40*, 5172.
- (4) Goodman, M. C.; Xu, S.; Rouzer, C. A.; Banerjee, S.; Ghebreselasie, K.; Migliore, M.; Piomelli, D.; Marnett, L. J. *J Biol Chem* **2018**.
- (5) Sidhu, R. S.; Lee, J. Y.; Yuan, C.; Smith, W. L. *Biochemistry* **2010**, *49*, 7069.
- (6) Wang, J. L.; Carter, J.; Kiefer, J. R.; Kurumbail, R. G.; Pawlitz, J. L.; Brown, D.; Hartmann, S. J.; Graneto, M. J.; Seibert, K.; Talley, J. J. *Bioorg Med Chem Lett* **2010**, *20*, 7155.
- (7) Dong, L.; Yuan, C.; Orlando, B. J.; Malkowski, M. G.; Smith, W. L. *J Biol Chem* **2016**, *291*, 25641.
- (8) Neumann, W.; Xu, S.; Sarosi, M. B.; Scholz, M. S.; Crews, B. C.; Ghebreselasie, K.; Banerjee, S.; Marnett, L. J.; Hey-Hawkins, E. *ChemMedChem* **2016**, *11*, 175.
- (9) Rowlinson, S. W.; Kiefer, J. R.; Prusakiewicz, J. J.; Pawlitz, J. L.; Kozak, K. R.; Kalgutkar, A. S.; Stallings, W. C.; Kurumbail, R. G.; Marnett, L. J. *J Biol Chem* **2003**, *278*, 45763.
- (10) Orlando, B. J.; Malkowski, M. G. *J Biol Chem* **2016**, *291*, 15069.
- (11) Picot, D.; Loll, P. J.; Garavito, R. M. *Nature* **1994**, *367*, 243.
- (12) Gupta, K.; Selinsky, B. S.; Loll, P. J. *Acta Crystallogr D Biol Crystallogr* **2006**, *62*, 151.
- (13) Kurumbail, R. G.; Stevens, A. M.; Gierse, J. K.; McDonald, J. J.; Stegeman, R. A.; Pak, J. Y.; Gildehaus, D.; Miyashiro, J. M.; Penning, T. D.; Seibert, K.; Isakson, P. C.; Stallings, W. C. *Nature* **1996**, *384*, 644.
- (14) Duggan, K. C.; Hermanson, D. J.; Musee, J.; Prusakiewicz, J. J.; Scheib, J. L.; Carter, B. D.; Banerjee, S.; Oates, J. A.; Marnett, L. J. *Nat Chem Biol* **2011**, *7*, 803.
- (15) Uddin, M. J.; Xu, S.; Crews, B. C.; Ghebreselasie, K.; Banerjee, S.; Marnett, L. J. *ACS Med Chem Lett* **2020**, *in press*.
- (16) Orlando, B. J.; Lucido, M. J.; Malkowski, M. G. *J Struct Biol* **2015**, *189*, 62.
- (17) Blobaum, A. L.; Xu, S.; Rowlinson, S. W.; Duggan, K. C.; Banerjee, S.; Kudalkar, S. N.; Birmingham, W. R.; Ghebreselasie, K.; Marnett, L. J. *J Biol Chem* **2015**, *290*, 12793.
- (18) Harman, C. A.; Rieke, C. J.; Garavito, R. M.; Smith, W. L. *J Biol Chem* **2004**, *279*, 42929.
- (19) Xu, S.; Uddin, M. J.; Banerjee, S.; Duggan, K.; Musee, J.; Kiefer, J. R.; Ghebreselasie, K.; Rouzer, C. A.; Marnett, L. J. *J Biol Chem* **2019**, *294*, 8690.
- (20) Uddin, M. J.; Crews, B. C.; Xu, S.; Ghebreselasie, K.; Daniel, C. K.; Kingsley, P. J.; Banerjee, S.; Marnett, L. J. *ACS Chem Biol* **2016**, *11*, 3052.

- (21) Loll, P. J.; Picot, D.; Ekabo, O.; Garavito, R. M. *Biochemistry* **1996**, *35*, 7330.
- (22) Xu, S.; Hermanson, D. J.; Banerjee, S.; Ghebreselasie, K.; Clayton, G. M.; Garavito, R. M.; Marnett, L. J. *J Biol Chem* **2014**, *289*, 6799.
- (23) Windsor, M. A.; Valk, P. L.; Xu, S.; Banerjee, S.; Marnett, L. J. *Bioorg Med Chem Lett* **2013**, *23*, 5860.
- (24) Gupta, K.; Selinsky, B. S.; Kaub, C. J.; Katz, A. K.; Loll, P. J. *J Mol Biol* **2004**, *335*, 503.
- (25) Windsor, M. A.; Hermanson, D. J.; Kingsley, P. J.; Xu, S.; Crews, B. C.; Ho, W.; Keenan, C. M.; Banerjee, S.; Sharkey, K. A.; Marnett, L. J. *ACS Med Chem Lett* **2012**, *3*, 759.
- (26) Duggan, K. C.; Walters, M. J.; Musee, J.; Harp, J. M.; Kiefer, J. R.; Oates, J. A.; Marnett, L. J. *J Biol Chem* **2010**, *285*, 34950.
- (27) Cingolani, G.; Panella, A.; Perrone, M. G.; Vitale, P.; Di Mauro, G.; Fortuna, C. G.; Armen, R. S.; Ferorelli, S.; Smith, W. L.; Scilimati, A. *Eur J Med Chem* **2017**, *138*, 661.
- (28) Vecchio, A. J.; Malkowski, M. G. *J Struct Biol* **2011**, *176*, 254.
- (29) Orlando, B. J.; Malkowski, M. G. *Acta Crystallogr F Struct Biol Commun* **2016**, *72*, 772.
- (30) Luong, C.; Miller, A.; Barnett, J.; Chow, J.; Ramesha, C.; Browner, M. F. *Nat Struct Biol* **1996**, *3*, 927.
- (31) Loll, P. J.; Picot, D.; Garavito, R. M. *Nat Struct Biol* **1995**, *2*, 637.
- (32) Wang, J. L.; Limburg, D.; Graneto, M. J.; Springer, J.; Hamper, J. R.; Liao, S.; Pawlitz, J. L.; Kurumbail, R. G.; Maziasz, T.; Talley, J. J.; Kiefer, J. R.; Carter, J. *Bioorg Med Chem Lett* **2010**, *20*, 7159.
- (33) Malkowski, M. G.; Ginell, S. L.; Smith, W. L.; Garavito, R. M. *Science* **2000**, *289*, 1933.
- (34) Kiefer, J. R.; Pawlitz, J. L.; Moreland, K. T.; Stegeman, R. A.; Hood, W. F.; Gierse, J. K.; Stevens, A. M.; Goodwin, D. C.; Rowlinson, S. W.; Marnett, L. J.; Stallings, W. C.; Kurumbail, R. G. *Nature* **2000**, *405*, 97.
- (35) Vecchio, A. J.; Simmons, D. M.; Malkowski, M. G. *J Biol Chem* **2010**, *285*, 22152.
- (36) Vecchio, A. J.; Malkowski, M. G. *J Biol Chem* **2011**, *286*, 20736.
- (37) Vecchio, A. J.; Orlando, B. J.; Nandagiri, R.; Malkowski, M. G. *J Biol Chem* **2012**, *287*, 24619.
- (38) Dong, L.; Anderson, A. J.; Malkowski, M. G. *Biochemistry* **2019**, *58*, 3990.
- (39) Thuresson, E. D.; Malkowski, M. G.; Lakkides, K. M.; Rieke, C. J.; Mulichak, A. M.; Ginell, S. L.; Garavito, R. M.; Smith, W. L. *J Biol Chem* **2001**, *276*, 10358.
- (40) Malkowski, M. G.; Thuresson, E. D.; Lakkides, K. M.; Rieke, C. J.; Micielli, R.; Smith, W. L.; Garavito, R. M. *J Biol Chem* **2001**, *276*, 37547.
- (41) Kudalkar, S. N.; Nikas, S. P.; Kingsley, P. J.; Xu, S.; Galligan, J. J.; Rouzer, C. A.; Banerjee, S.; Ji, L.; Eno, M. R.; Makriyannis, A.; Marnett, L. J. *J Biol Chem* **2015**, *290*, 7897.
- (42) Dong, L.; Vecchio, A. J.; Sharma, N. P.; Jurban, B. J.; Malkowski, M. G.; Smith, W. L. *J Biol Chem* **2011**, *286*, 19035.

Table S2. Summary table of site-directed mutations of cyclooxygenase isoforms

Mutation	Isoform	%POX^a	%COX^b	Comments^c	Ref
R44A	COX-2	NR	42		1
R44Q	COX-2	NR	58		1
V50C/E3232C/ ΔC	COX-2	NR	63	Dimer is not cross-linked upon oxidation.	2
F74C/ΔC	COX-2	NR	50	Created for spin-label studies.	3
L75C/ΔC	COX-2	NR	70	Created for spin-label studies.	3
T76C/ΔC	COX-2	NR	60	Created for spin-label studies.	3
R77C/ΔC	COX-2	NR	50	Created for spin-label studies.	3
I78C/ΔC	COX-2	NR	70	Created for spin-label studies.	3
K79C/ΔC	COX-2	NR	70	Created for spin-label studies.	3
L80C/ΔC	COX-2	NR	70	Created for spin-label studies.	3
F81C/ΔC	COX-2	NR	50	Created for spin-label studies.	3
L82C/ΔC	COX-2	NR	40	Created for spin-label studies.	3
N87C/ΔC	COX-2	NR	60	Created for spin-label studies.	3
T88C/ΔC	COX-2	NR	40	Created for spin-label studies.	3
V89C/ΔC	COX-2	NR	60	Created for spin-label studies.	3
V89W	COX-2	77	100	K _{MS} : (AA) NC. k _{cat} S: (AA) NC. Potencies: Ibuprofen ↑>45-fold, becomes time-dependent; Naproxen ↑9.8-fold, becomes time-dependent; Indomethacin NC; Indomethacin-dansyl conjugate 1 ↓1.8-fold; Indomethacin-dansyl conjugate 2 ↓3-fold; Diclofenac ↓1.9-fold; Celecoxib ↑2-fold; Rofecoxib ↑2.4-fold.	4,5
V89W/H90W	COX-2	68	82	K _{MS} : (AA) ↓69%. k _{cat} S: (AA) ↓77%. Potencies: Ibuprofen ↑>97-fold, becomes time-dependent; Naproxen ↑15-fold, becomes time-dependent; Mefenamic acid ↑>54-fold, becomes time-dependent; Lumiracoxib ↑>150-fold, becomes time-dependent; Indomethacin ↓2.1-fold; Diclofenac NC; Flurbiprofen NC; Celecoxib ↓8-fold; Rofecoxib ↓4.5-fold.	4
V89W/S119W	COX-2	207	82	K _{MS} : (AA) ↓30%. k _{cat} S: (AA) ↓38%. Potencies: Ibuprofen ↑>55-fold, becomes time-dependent; Naproxen ↑7-fold, becomes time-dependent; Mefenamic acid ↑>85-fold, becomes time-dependent; Lumiracoxib ↑>130-fold, becomes time-dependent; Indomethacin ↓1.9-fold; Diclofenac ↓1.7-fold; Flurbiprofen NC; Celecoxib ↓1.5-fold; Rofecoxib NC.	4
H90C/ΔC	COX-2	NR	70	Created for spin-label studies	3

H90W	COX-2	122	84	K_{MS} : (AA) NC. k_{cat} : (AA) NC. Potencies: Ibuprofen \uparrow >10-fold, becomes time-dependent; Naproxen \uparrow 8-fold, becomes time-dependent; Indomethacin NC; Diclofenac NC; Celecoxib \downarrow 6-fold; Rofecoxib \downarrow 3.9-fold.	4
Y91C/ Δ C	COX-2	NR	70	Created for spin-label studies.	3
I92C/ Δ C	COX-2	NR	60	Created for spin-label studies.	3
L93C/ Δ C	COX-2	NR	30	Created for spin-label studies.	3
G98C/ Δ C	COX-2	NR	35	Created for spin-label studies.	3
F99C/ Δ C	COX-2	NR	50	Created for spin-label studies.	3
W100C/ Δ C	COX-2	NR	10	Created for spin-label studies.	3
N101C/ Δ C	COX-2	NR	50	Created for spin-label studies.	3
V102C/ Δ C	COX-2	NR	30	Created for spin-label studies.	3
V103C/ Δ C	COX-2	NR	30	Created for spin-label studies.	3
N104C/ Δ C	COX-2	NR	30	Created for spin-label studies.	3
N105C/ Δ C	COX-2	NR	20	Created for spin-label studies.	3
Y115L/ S119V/ F357L	COX-2	NR	~100	Potencies: SC-58125 NC.	6
S119A	COX-2	NR	NR	Potencies: Indomethacin \downarrow 2-fold; Indomethacin-dansyl conjugate 1 \uparrow 2-fold; Indomethacin-dansyl conjugate 2 NC.	5
S119W	COX-2	90	107	K_{MS} : (AA) NC. k_{cat} : (AA) NC. Potencies: Ibuprofen NC; Naproxen NC; Indomethacin \downarrow 3-fold; Diclofenac \downarrow 3-fold; Celecoxib NC; Rofecoxib NC.	4
R120E	COX-1	5 or 0	5 or 0	K_{MS} : (AA) \uparrow 120-fold. Potencies: Indomethacin \downarrow >270-fold; Flurbiprofen \downarrow >8000-fold; Ketoprofen \downarrow >400-fold; Ibuprofen \downarrow >2.4-fold; Diclofenac \downarrow 43-fold; Meclofenamic acid \downarrow 100-fold; DuP697 \uparrow 12-fold; L-746,483 \uparrow 12-fold. Residual activities: Aspirin 60%.	7-9
R120K	COX-1	62 or 120	15	K_{MS} : (AA) \uparrow 22-fold or 41-fold.	8,9
R120Q	COX-1	65 or 122	5	K_{MS} : (AA) \uparrow 820-fold or 2,700-fold. Reduced rate of suicide inactivation. Potencies: Ibuprofen \downarrow 200-fold; Flurbiprofen (instantaneous) \downarrow 200-fold and no longer time-dependent; <i>O</i> -acetylsalicylhydroxamic acid \downarrow ; aspirin \downarrow .	8-10

R120A	COX-2	92 or 99 104	23 or 50 or 106	K _{MS} : (AA) ↑3.4-fold. k _{cat} S; (AA) NC. Oxygenation: (LA) ↓; (αα) ↓; (SA) ↓; (EPA) ↓; (2-AG) ↓ but stimulated by 13-Me-AA. Potencies: Indomethacin ↓>12-fold or >240-fold; Indomethacin-dansyl conjugate 1 ↑2.7-fold; Indomethacin-dansyl conjugate 2 ↑4.7-fold; Ketorolac ↓ >380-fold; Piroxicam ↓110-fold; Naproxen ↓ 100%; Diclofenac ↓ 3.3-fold; Meclofenamic acid ↓3.2-fold or 4.7-fold; Ibuprofen ↓; Indomethacin esters/amides NC or ↓; Meclofenamic acid esters/amides NC. Aspirin acetylation: ↓>81%. Slow phase binding rate of a fluorescent indomethacin amide: ↑3.9-fold.	1, 5, 11-18
R120E	COX-2	NR	12	K _{MS} : (AA) ↑32-fold. Potencies: NS-398 ↓1000-fold; Flosulide ↓680-fold; Flurbiprofen ↓960-fold; Indomethacin ↓48-fold; L-761,066 ↓21-fold; Diclofenac ↓4.5-fold; Meclofenamic acid ↓5.5-fold; L-746,483 ↓2-fold; DuP697 NC; L-745,296 ↑4-fold; L588-983 ↑3-fold.	19
R120L	COX-2	17	20		20
R120Q	COX-2	79 or 132	86 or 100 or 174	K _{MS} : (AA) NC. Oxygenation: (2-AG) ↓90% but stimulated by 13-Me-AA; (AEA) ↓75%. Potencies: flurbiprofen (instantaneous) ↓500-fold, no longer time-dependent; NS-398 (instantaneous) ↑5-fold, no longer time-dependent; DuP697 ↑1,000-fold; SC-58125 ↑>400-fold; Indomethacin ↓12-fold or NC; Naproxen ↑2-fold; Indomethacin esters/amides NC. Indomethacin podophylotoxin conjugate ↑3.2-fold. Aspirin acetylation: ↓>73%. Slow phase binding rate of a fluorescent indomethacin amide: ↑3.5-fold.	11- 14,17, 20-24
R120A/G533A	COX-2	104	0	Oxygenation: (LA) ↓100%; (αLA) ↓100%; (SA) ↓100%; (EPA) ↓.	18
S121G	COX-2	NR	93		1
S121P	COX-2	NR	180	K _{MS} : (AA) NC; (DHLA) ↓1.3-fold. Potencies: Naproxen ↓; Flurbiprofen ↓; Diclofenac NC; Celecoxib NC.	1
H122N	COX-2	NR	110		1
H122P	COX-2	NR	53		1
L123A	COX-2	NR	120		1
I124A	COX-2	NR	75		1
D125A	COX-2	NR	65		1
D125P	COX-2	NR	53		1

S126C/ΔC	COX-2	NR	91 or 100	Dimer is not cross-linked upon oxidation.	1,2
S126C/A543C/ΔC	COX-2	NR	65	Dimer is cross-linked upon oxidation. Cross-linking inhibited by flurbiprofen.	2
P127C/ ΔC	COX-2	NR	80 or 89	Dimer is not cross-linked upon oxidation.	1,2
P127C/S541C/ΔC	COX-2	NR	56	Dimer is cross-linked upon oxidation. Cross-linking inhibited by flurbiprofen.	2
S138C/L334C/ΔC	COX-2	NR	NR	Dimer is not cross-linked upon oxidation.	2
Y148F	COX-2	70	100	K _{MS} : (AA) ↑1.5-fold. No effect on tyrosyl radical migration.	25
Y148F/Y348F/ Y404F/Y504F	COX-2	70	75	K _{MS} : (AA) ↑2.0-fold. Prevents tyrosyl radical migration.	25
Y148F/Y348F/ Y385/Y404F/ Y504F	COX-2	45	0	No tyrosyl radical signal detected.	25
Q203N	COX-2	109	55		26
Q203R	COX-2	2	3		26
Q203V	COX-2	1	NR		26
F205A	COX-1	90	28	K _{MS} : (AA) ↑1.5-fold. Oxygenation: (EPA) ↓1.9-fold; (LA) ↓12-fold; (DHLLA) ↓4.8-fold. Products: (AA) %11-HETE ↑4.4-fold, %15-HETE ↑2-fold.	9,27, 28
F205L	COX-1	106	65	Oxygenation: (EPA) NC; (LA) ↓2-fold; (DHLLA) ↓2.5-fold. Products: (AA) %11-HETE ↑2-fold, %15-HETE NC.	9,27, 28
F205A	COX-2	42	29	K _{MS} : (AA) NC. k _{catS} : (AA) ↓3.4-fold.	18
F205L	COX-2	137	71	K _{MS} : (AA) ↑1.8-fold. k _{catS} : (AA) ↓1.4-fold.	18
F205V	COX-2	89	51	K _{MS} : (AA) NC. k _{catS} : (AA) ↓2.0-fold.	18
H207A	COX-2	2	31	Peroxidase catalyzes predominantly one-electron reductions.	26
F209A	COX-1	55	15	K _{MS} : (AA) ↑5-fold. Oxygenation: (EPA) ↓50-fold; (LA) ↓25-fold; (DHLLA) ↓14-fold. Products: (AA) %11-HETE ↑5-fold, %15-HETE NC.	9,27, 28
F209L	COX-1	104	43	K _{MS} : (AA) ↑1.5-fold. Oxygenation: (EPA) ↓3-fold; (LA) ↓4.8-fold; (DHLLA) ↓2.1-fold. Products: (AA) %11-HETE ↑2-fold, %15-HETE NC.	9,27, 28
F209A	COX-2	88	37	K _{MS} : (AA) ↑1.6-fold. k _{catS} : (AA) ↓2.7-fold.	18
F209L	COX-2	207	129	K _{MS} : (AA) NC. k _{catS} : (AA) NC	18
F209V	COX-2	145	98	K _{MS} : (AA) ↑1.5-fold. k _{catS} : (AA) NC	18
K211A	COX-1	NR	8		29
K211E	COX-1	NR	2		29
K211A/K215A	COX-1	NR	8		29
K211E/K215E	COX-1	NR	5		29
K211A/K222A	COX-1	NR	5		29
K211E/K222E	COX-1	NR	3		29

K211A//K215A/ K222A	COX-1	NR	2		29
K211E//K215E/ K222E	COX-1	NR	3		29
K215A	COX-1	NR	75		29
K215E	COX-1	NR	110		29
K215A/K222A	COX-1	NR	55		29
K215E/K222E	COX-1	NR	45		29
K222A	COX-1	NR	78		29
K222E	COX-1	NR	90		29
V228F	COX-2	87	20	Products: (AA) %11-HETE NC, %15-HETE NC. Unable to make HETEs after acetylation.	30
R242H	COX-2	79	73	K _{MS} : (AA) NC; (EPA) NC. No effect on activation or inactivation.	31
Y254F	COX-1	94	104		32
Y262F	COX-1	66	73		32
C313S	COX-1	32	19	K _{MS} : (AA) ↓3.3-fold. Potencies: Flurbiprofen NC. No effect on dimer formation, glycosylation, or inactivation by maleimides.	33
C313S/C540S/ΔC	COX-2	NR	70 or 100	Created for spin-label studies. Dimer not cross-linked upon oxidation.	2,3
Y348F	COX-1	76	83	K _{MS} : (AA) NC. Products: (AA) %11-HETE NC, %15-HETE NC.	9
Y348L	COX-1	9	0		9
Y348W	COX-1	0	0		9
Y348F	COX-2	46 or 94 or 106	46 or 75 or 106	K _{MS} : (AA) ↑1.8-fold. Potencies: Diclofenac NC. Aspirin acetylation: ↓58%. Disrupts Y348-Y385 hydrogen bond. No effect on tyrosyl radical migration.	12,16, 25,34
Y348F/Y504F	COX-2	111	81	K _{MS} : (AA) ↑1.6-fold. Potencies: Nimesulide ↑4.8-fold. Disrupts Y348-Y385 hydrogen bond and radical transfer to Y504. Unable to make HETEs after acetylation.	34
V349A	COX-1	52	55	K _{MS} : (AA) NC; (EPA) ↑100-fold; (LA) ↑11-fold; (DHLA) ↑31-fold. Oxygenation: (EPA) ↓10-fold; (LA) ↓15-fold; (DHLA) ↓25-fold. Products: (AA) %11-HETE ↑21-fold (100% R), %15-HETE ↓100%.	9,27, 28,35
V349I	COX-1	NR	NR	Products: (AA) 15(R)-PGH ₂ :15(S)-PGH ₂ ↑, 15(R)-HETE:15(S)-HETE ↑, 11(R)-HETE:11(S)-HETE NC.	36

V349L	COX-1	117	63	K _{MS} : (AA) ↑3.5-fold; (EPA) ↑250-fold; (LA) ↑53-fold; (DHLA) ↑6.4-fold. Oxygenation: (EPA) ↓3.2-fold; (LA) ↓7.1-fold; (DHLA) ↓2.9-fold. Products: (AA) %11-HETE ↓100%, %15-HETE ↑9.6-fold (54% S), 15(R)-PGH ₂ :15(S)-PGH ₂ ↑.	9,27, 28,36
V349N	COX-1	NR	NR	Products: (AA) 15(R)-PGH ₂ :15(S)-PGH ₂ ↑, 11(R)-HETE:11(S)-HETE NC.	36
V349S	COX-1	94	43	K _{MS} : (AA) ↑7-fold. Products: (AA) %11-HETE ↑16-fold (100% R), %15-HETE ↓100%.	9
V349T	COX-1	136	39	K _{MS} : (AA) ↑7-fold. Products: (AA) %11-HETE ↑2.2-fold (100% R), %15-HETE ↓4-fold, 15(R)-PGH ₂ :15(S)-PGH ₂ NC.	9,36
V349A/S353T	COX-1	49	3	Oxygenation: (EPA) ↓100%; (LA) ↓100%; (DHLA) ↓100%. Products: (AA) %11-HETE ↑11-fold, %15-HETE ↑4.8-fold.	9,27, 28
V349A/W387F	COX-1	NR	NR	K _{MS} : (AA) NC. Products: (AA) 11-HETE >84% of total.	35
V349A/I523V	COX-1	NR	56	Oxygenation: (DHLA) ↓16-fold.	28
V349A/I434V/ H513R/I523V	COX-1	NR	50	K _{MS} : (AA) ↑1.5-fold; (DHLA) ↑60-fold. Oxygenation: (DHLA) ↓16-fold;	28
V349A	COX-2	NR	59	K _{MS} : (AA) NC; (DHLA) NC. Oxygenation: (DHLA) ↓ 2.2-fold; (2-AG) ↓ but stimulated by 13-Me-AA. Products: (AA) 15(R)-PGH ₂ :15(S)-PGH ₂ NC, 15-HETE ↓100%, 11(R)-HETE:11(S)-HETE NC; (2-AG) %HETE-G ↑; (AEA) %HETE-EA ↑. Potencies: Indomethacin ↑3.1-fold; 2- <i>des</i> -methyl-Indomethacin ↓>4-fold; Diclofenac ↓; Naproxen ↓4-fold; Lumiracoxib I.	11,14, 21,22, 28,36-38
V349I	COX-2	NR	NR	Products: (AA) 15(R)-PGH ₂ :15(S)-PGH ₂ ↑, 15(R)-HETE:15(S)-HETE ↑, 11(R)-HETE:11(S)-HETE NC. Potencies: Indomethacin ↓1.8-fold; 2- <i>des</i> -methyl-Indomethacin NC; Diclofenac NC; Lumiracoxib ↑>35-fold; Naproxen ↑3-fold.	11,36-38

V349L	COX-2	NR	NR	Products: (AA) 15(R)-PGH ₂ :15(S)-PGH ₂ ↑, 15(R)-HETE:15(S)-HETE ↑, 11(R)-HETE:11(S)-HETE NC; (2-AG) %HETE-Gs ↑. (AEA) %HETE-EAs ↑. Potencies: Indomethacin ↓8.0-fold or 16-fold; 2-Desmethyl-indomethacin ↓>4-fold; Diclofenac ↓; Indomethacin-podophylotoxin conjugate ↓>14-fold; Naproxen ↑4-fold.	11,21, 22,24, 36-38
V349N	COX-2	NR	NR	Products: (AA) 15(R)-PGH ₂ :15(S)-PGH ₂ ↑, 15(R)-HETE:15(S)-HETE ↑, 11(R)-HETE:11(S)-HETE NC.	36
V349T	COX-2	NR	NR	Products: (AA) 15(R)-PGH ₂ :15(S)-PGH ₂ NC, 15(R)-HETE:15(S)-HETE ↑, 11(R)-HETE:11(S)-HETE NC.	36
V349A/V523I	COX-2	NR	7.5	Oxygenation: (DHLA) ↓ 38-fold	28
L352V	COX-1	NR	34	Oxygenation: (EPA) ↓1.7-fold; (LA) ↓4.8-fold; (DHLA) ↓2.7-fold.	27,28
S353A	COX-1	60	56	Oxygenation: (EPA) ↓2.5-fold; (LA) ↓2.9-fold; (DHLA) ↓1.9-fold.	9,27, 28
S353G	COX-1	87	61	K _{MS} : (AA) NC. Oxygenation: (EPA) ↓2.9-fold; (LA) ↓7.7-fold; (DHLA) NC. Products: (AA) %11-HETE ↑1.5-fold, %15-HETE NC.	9,27, 28
S353T	COX-1	46	42	Oxygenation: (EPA) NC; (LA) ↓3.1-fold; (DHLA) ↓3.1-fold. Products: (AA) %11-HETE ↑5.5-fold, %15-HETE ↑4.8-fold.	9,27, 28
Y355A	COX-1	84	10	K _{MS} : (AA) ↑5-fold. Products: (AA) %11-HETE ↑3-fold, %15-HETE NC.	9
Y355F	COX-1	88 or 130	19	K _{MS} : (AA) ↑5-fold. Oxygenation: (EPA) ↓3-fold; (LA) ↓100%; (DHLA) ↓2.7-fold. Products: (AA) %11-HETE ↑2-fold, %15-HETE NC. Potencies: Ibuprofen NC but loss of stereoselectivity.	8,9,27, 28,32
Y355L	COX-1	82	10	K _{MS} : (AA) ↑1.9-fold. Products (AA) %11-HETE ↑1.6-fold, %15-HETE NC.	9
Y355A	COX-2	NR	NR	Oxygenation: (2-AG) ↓ but stimulated by 13-Me-AA. Binding of a fluorescent indomethacin amide: ↓100%.	14,17

Y355F	COX-2	90	47	K_{MS} : (AA) \uparrow 2.4-fold or NC; (2-AG) NC or \downarrow 3.1-fold; (AEA) \downarrow 1.7-fold. k_{catS} : (AA) \downarrow 2.1-fold or \downarrow 1.8-fold; (2-AG) \downarrow 1.8-fold or NC; (AEA) \downarrow 1.6-fold. Sigmoidal [S] vs V curve for AA. Oxygenation: (2-AG) \downarrow 20% but stimulated by 13-Me-AA; (AEA) NC. Potencies: Indomethacin \downarrow >16-fold, 24-fold, or 240-fold; Ketorolac \downarrow >380-fold; Meclofenamic acid \downarrow >23-fold or \downarrow >130-fold; Piroxicam \downarrow >110-fold; Ibuprofen \downarrow ; Indomethacin esters/amides I; Indomethacin-podophyllotoxin conjugate \downarrow >14-fold; Meclofenamic acid esters/amides I; Diclofenac \downarrow 1.8-fold; ARN-2508 \downarrow 2.5-fold. Binding of a fluorescent indomethacin amide: \downarrow 100%.	13-17,21,22,24,39-41
I377V	COX-1	110	72	K_{MS} : (AA) \downarrow 1.8. Oxygenation: (EPA) \downarrow 1.7-fold; (LA) \downarrow 1.8-fold; (DHLLA) \downarrow 1.6-fold. Products: (AA) %11-HETE \uparrow 4-fold, %15-HETE NC.	9,27,28
I377A	COX-2	0	0	Likely misfolded.	18
I377F	COX-2	0	0	Likely misfolded.	18
I377L	COX-2	72	72	K_{MS} : (AA) NC. k_{catS} : (AA) NC.	18
I377V	COX-2	92	86	K_{MS} : (AA) NC. k_{catS} : (AA) NC.	18
F381A	COX-1	101	4	K_{MS} : (AA) \uparrow 3-fold. Oxygenation: (EPA) \downarrow 5.8-fold; (LA) \downarrow 50-fold; (DHLLA) \downarrow 40-fold. Products: (AA) %11-HETE \uparrow 3.5-fold, %15-HETE \uparrow 1.6-fold.	9,27,28
F381L	COX-1	74	21	Oxygenation: (EPA) \downarrow 4.7-fold; (LA) \downarrow 9.2-fold; (DHLLA) \downarrow 5.8-fold. Products: (AA) %11-HETE \uparrow 2.8-fold, %15-HETE \uparrow 1.6-fold.	9,27,28
F381A	COX-2	0	0	Likely misfolded.	18
F381L	COX-2	0	0	Likely misfolded.	18
F381V	COX-2	0	0	Likely misfolded.	18
N382A	COX-2	77	94	K_{MS} : (AA) \uparrow 2-fold. Self-inactivation rate: NC. GSH Px resistance: NC.	42
N382D	COX-2	65	76	K_{MS} : (AA) NC. Self-inactivation rate: \downarrow 1.7-fold. GSH Px resistance: NC.	42
N382L	COX-2	46	103	K_{MS} : (AA) NC. Self-inactivation rate: \downarrow 2.3-fold. GSH Px resistance: \uparrow 1.6-fold.	42
T383D	COX-2	280	110	K_{MS} : (AA) NC. Self-inactivation rate: NC. GSH Px resistance: \downarrow 1.6-fold.	42
T383H	COX-2	190	120	K_{MS} : (AA) \uparrow 1.8-fold. Self-inactivation rate: NC. GSH Px resistance: \downarrow 1.7-fold.	42
L384A	COX-1	61	29	Oxygenation: (DHLLA) \downarrow 3-fold. Products: (AA) %11-HETE NC, %15-HETE \uparrow 1.5-fold.	9,28

L384F	COX-1	90	8	Oxygenation: (DHLLA) ↓9.6-fold.	9,28
L384V	COX-1	23	23	Oxygenation: (DHLLA) ↓5.4-fold. Products: (AA) %11-HETE ↓1.7-fold, %15-HETE ↓3.1-fold.	9,28
Y385F	COX-1	57	0		9,32
Y385F	COX-2	135 or 185	0	Oxygenation: (2-AG) ↓100%. Aspirin acetylation: ↓93%.	12,16, 23,25
W387A	COX-1	60	0		9
W387F	COX-1	57	44	K _{MS} : (AA) ↑12-fold. Oxygenation: (EPA) ↓2.1-fold; (LA) ↓2-fold; (DHLLA) ↓2.1-fold. Products: (AA) %11-HETE ↑14-fold, %15-HETE ↓2.5-fold.	9,27, 28
W387L	COX-1	123	7	K _{MS} : (AA) ↑4-fold. Oxygenation: (EPA) ↓71-fold; (LA) ↓12-fold; (DHLLA) ↓22-fold. Products: (AA) %11-HETE ↑16-fold, %15-HETE NC.	9,27, 28
W387R	COX-1	0	0		9
W387S	COX-1	4	0		9
W387F	COX-2	NR	15	Products: (AA) PGH ₂ ↓19-fold, 11-HETE NC; (2-AG) %HETE-Gs ↑. Potencies: Naproxen ↓; Diclofenac NC; Flurbiprofen NC; Indomethacin NC.	11,22, 43
Y404F	COX-2	79	81	K _{MS} : (AA) ↑1.7-fold. No effect on tyrosyl radical migration.	25
Y417F	COX-1	79	86		32
V434I	COX-2	NR	NR	Potencies: Meloxicam ↓9.3-fold. Reduced ability to make HETEs after acetylation.	30,44
V434I/ R513H/ V523I	COX-2	109 or 118	104	Oxygenation: (2-AG) ↓75%; (AEA) ↓62%. Products: (2-AG) %HETE-Gs ↑. Potencies: Indomethacin ↓10-fold; Meclofenamic acid ↓2.3-fold; Meloxicam ↓8.1-fold; Indomethacin esters/amides ↓; Meclofenamic acid amide NC. Unable to make HETEs after acetylation. Aspirin acetylation NC.	12,13, 21,22, 30,44
L472M	COX-2	NR	106	K _{MS} : (AA) ↓1.6-fold. k _{catS} : (AA) NC. Potencies: Indomethacin ↓1.6-fold; Naproxen NC; Flurbiprofen NC; Diclofenac NC; Celecoxib ↓1.8-fold; Indomethacin amides/esters ↓3- to 11-fold.	45
E502G	COX-2	90	70	K _{MS} : (AA) NC; (EPA) NC. No effect on activation or inactivation.	31
L503F	COX-2	NR	NR	Potencies: Indomethacin ↓2.5-fold; Lumiracoxib (AA) NC, (2-AG) ↓; Indomethacin esters/amides I; Meclofenamic acid NC; Meclofenamic amide NC.	13,46
Y504F	COX-2	240	67	K _{MS} : (AA) ↑2-fold. Blocks tyrosyl radical migration.	25,34

C512S	COX-1	92	96	K _{MS} : (AA) NC. Potencies: Flurbiprofen NC. No effect on dimer formation, glycosylation, or inactivation by maleimides.	33
H513R	COX-1	NR	136	K _{MS} : (AA) NC. Potencies: Sulindac sulfide ↓1.8-fold; Indomethacin ↑1.9-fold; Diclofenac NC; DuP697 NC; NS-398 ↑2-fold; SC-58125 NC; DFU NC; L-745,296 ↓5-fold.	47
H513F/I523V	COX-1	NR	200	K _{MS} : (AA) NC. Potencies: Sulindac sulfide NC; indomethacin ↑2.4-fold; Diclofenac ↑1.9-fold; DuP697 ↑280-fold; NS-398 ↑34-fold; SC-58125 ↑>30-fold; DFU ↑>27-fold; L-745,296 ↓13-fold.	47
R513H	COX-2	92	100	K _{MS} : (AA) ↑2.2-fold or NC; (2-AG) NC; (1-AG) NC; k _{cat} : (AA) NC; (2-AG) NC; (1-AG) NC. Oxygenation: (2-AG) ↓56% or NC; (AEA) ↓57%. Increased rate of aspirin acetylation. Reduced ability to make HETES after acetylation.	21,22, 30,48, 49
R513H/V523I	COX-2	NR	NR	Oxygenation: (2-AG) ↓62%; (AEA) ↓57%.	21,22
F518A	COX-1	23	38	K _{MS} : (AA) ↑10-fold. Products: %11-HETE ↑3.5-fold, %15-HETE NC.	9
F518L	COX-1	130	99	K _{MS} : (AA) ↑2.4-fold. Products: (AA) %11-HETE ↑1.7-fold, %15-HETE NC.	9
F518M	COX-1	55	70	Products: (AA) %11-HETE ↑2-fold, %15-HETE ↑1.8-fold.	9
F518Y	COX-1	30	44	Oxygenation: (DHLA) ↓8.1-fold. K _{MS} : (AA) ↑2-fold. Products: (AA) %11-HETE ↑1.7-fold, 15-HETE ↑2.7-fold (50% S).	9,33
M522A	COX-1	48	65	K _{MS} : (AA) NC. Oxygenation: (DHLA) ↓1.6-fold. Products: (AA) %11-HETE ↑1.5-fold, %15-HETE NC.	9,28
M522I	COX-1	105	69	Products: (AA) %11-HETE NC, %15-HETE NC.	9
M522L	COX-1	28	46	K _{MS} : (AA) ↑1.7-fold. Products: (AA) %11-HETE NC, %15-HETE ↓100%.	9
I523A	COX-1	112	64	Oxygenation: (EPA) ↓2-fold; (LA) ↓14-fold; (DHLA) NC. Products: (AA) %11-HETE ↑4.8-fold, %15-HETE NC.	9,27, 28
I523V	COX-1	57	70	Oxygenation: (LA) ↓3.7-fold. Products: (AA) %11-HETE NC, %15-HETE NC.	9,27
I523V	COX-1	NR	58	K _{MS} : (AA) NC. Potencies: Sulindac sulfide ↑13-fold; Indomethacin ↑5-fold; Diclofenac ↑1.9-fold; DuP697 ↑370-fold; NS-398 ↑4.3-fold; SC-58125 ↑>15-fold; DFU ↑>2.4-fold; L-745,296 ↑4.6-fold.	47
V523A	COX-2	NR	75	K _{MS} : (AA) NC. Potencies: NS-398 ↓1.5-fold; DuP697 ↑5-fold; SC-58125 ↑60-fold; Nimesulide ↓>25-fold.	50

V523E	COX-2	NR	211	K _{MS} : (AA) ↓1.8-fold. Potencies: NS-398 ↓>20-fold; DuP697 ↓>30-fold; SC-58125 ↓>7-fold; Nimesulide ↓>25-fold.	50
V523I	COX-2	NR	85 or ~100 or 110 or 185	K _{MS} : (AA) NC. Oxygenation: (2-AG) NC; (AEA) NC; (DHLLA) ↓1.9-fold. Potencies: Indomethacin NC or ↓2-fold; Mefenamic acid ↑3-fold; Diclofenac ↓4-fold; Flurbiprofen NC; Naproxen ↓>11-fold; DuP697 ↓10-fold; NS-398 ↓>2,000-fold; Nimesulide ↓>25-fold; SC-58125 ↓>2,500-fold; SC-236 ↓3,000-fold; Meloxicam NC; Indomethacin esters/amides ↓; Indomethacin-dansyl conjugate 1 NC; Indomethacin-dansyl conjugate 2 NC; Indomethacin-podophyllotoxin conjugate ↓3.8-fold. Reduced ability to make HETEs after acetylation.	5-6,13, 21,22, 24,28, 30,44, 50
V523K	COX-2	NR	45	K _{MS} : (AA) ↑2-fold. Potencies NS-398 ↓>20-fold; DuP697 ↓4-fold; SC-58125 ↓>7-fold; Nimesulide ↓>25-fold.	50
E524D	COX-1	85	80	K _{MS} : (AA) NC.	8
E524K	COX-1	75	85	K _{MS} : (AA) NC.	8
E524Q	COX-1	105	110	K _{MS} : (AA) ↑1.8-fold;	8
E524L	COX-2	NR	41	Oxygenation: (2-AG) ↓82%; (AEA) ↓46%. Products: (2-AG) %HETE-Gs ↑. Potencies: Indomethacin NC; Meclofenamic acid ↓3-fold; Meclofenamic acid amide ↓2.2-fold; Indomethacin esters/amides I. Binding of a fluorescent indomethacin amide: ↓100%.	13,17, 21,22
V525A	COX-2	129	150	K _{MS} : (AA) NC; (EPA) NC. No effect on activation or inactivation. Residual activities: nimesulide ↑1.6-fold; NS-398 ↑1.7-fold.	31
A527V	COX-2	NR	NR	Products: (AA) 15(R)-PGH ₂ :15(S)-PGH ₂ NC, 15(R)-HETE:15(S)-HETE ↑, 11(R)-HETE:11(S)-HETE NC.	36
F529E	COX-1	0	4	K _{MS} : (AA) NC.	51
F529K	COX-1	0	3		51
F529L	COX-1	0	0		51
F529Y	COX-1	0	0		51
S530A	COX-1	68 or 75	58 or 64	K _{MS} : (AA) NC; (EPA) ↑24-fold; (LA) ↑2.5-fold; (DHLLA) ↑2.6-fold. Oxygenation: (EPA) NC; (LA) ↓1.8-fold; (DHLLA) NC. Products: (AA) %11-HETE NC, %15-HETE NC. Potencies: Flurbiprofen NC; Flufenamic acid NC; <i>O</i> -Acetylsalicylhydroxamic acid I; Aspirin I.	9,10, 27,51, 52
S530C	COX-1	46	0.5		51

S530G	COX-1	118	3		51
S530I	COX-1	NR	0		36
S530L	COX-1	161	0		36,51
S530M	COX-1	NR	0		36
S530N	COX-1	96	0		51
S530T	COX-1	30	0 or 6 or 17	K_{MS} : (AA) \uparrow 6.5-fold or 9-fold; (EPA) \uparrow 58-fold; (LA) \uparrow 48-fold; (DHLA) \uparrow 30-fold. Oxygenation: (EPA) \downarrow 50-fold; (LA) \downarrow 6.3-fold; (DHLA) \downarrow 24-fold. Products: (AA) %11-HETE \downarrow 100%, %15-HETE \uparrow 4-fold. Human enzyme I, Ovine enzyme active. Potencies: Aspirin I.	27,36, 51
S530V	COX-1	94	0		9,36
S530A	COX-2	92	49	Oxygenation: (2-AG) \downarrow but stimulated by 13-Me-AA. Products: (2-AG) %HETE-Gs \uparrow . Potencies: Diclofenac \downarrow >650-fold; Piroxicam \downarrow >109-fold; Lumiracoxib I; Ketorolac \downarrow 23-fold; Indomethacin NC; Meclofenamic acid NC; Indomethacin esters/amides NC or \downarrow ; Meclofenamic acid amide \uparrow 3-fold; Indomethacin-dansyl conjugate 1 \downarrow 3.3-fold; Indomethacin-dansyl conjugate 2 NC; Indomethacin-podophyllotoxin conjugate \downarrow 5-fold. Aspirin acetylation \downarrow 100%; ARN-2508 NC.	5,12-14,16, 22,24, 36,38, 41
S530M	COX-2	96	NR	K_{MS} : (AA) \uparrow 2.8-fold. Products: (AA) 15(R)-PGH ₂ :15(S)-PGH ₂ \uparrow , 15(R)-HETE:15(S)-HETE \downarrow , 11(R)-HETE:11(S)-HETE NC; (2-AG) %15-HETE-G \uparrow ; (AEA) %15-HETE-EA \uparrow . Potencies: L-745,337 \downarrow 4.5-fold; SC-57666 \downarrow 6-fold; NS-398 \downarrow 7.5-fold; DuP697 NC; Flurbiprofen \downarrow 20-fold; Ketoprofen \downarrow 17-fold; Sulindac sulfide \downarrow 19-fold; Indomethacin \uparrow 1.9-fold; Meclofenamic acid \downarrow >4800-fold; Diclofenac \downarrow >3400-fold.	21,22, 36,53
S530T	COX-2	NR	24	Products: (AA) 15(R)-PGH ₂ :15(S)-PGH ₂ \uparrow , 15(R)-HETE:15(S)-HETE NC, 11(R)-HETE:11(S)-HETE NC. Potencies: ARN-2508 \downarrow 7.5-fold	36,41, 54
S530V	COX-2	NR	NR	Products: (AA) 15(R)-PGH ₂ :15(S)-PGH ₂ \uparrow , 15(R)-HETE:15(S)-HETE \uparrow , 11(R)-HETE:11(S)-HETE NC.	36
S530T/G533V	CPX-2	NR	0		54
L531A	COX-1	100	4.6	K_{MS} : (AA) \uparrow 27-fold. Oxygenation: (DHLA) \downarrow 12-fold. Products: (AA) %11-HETE NC, %15-HETE NC.	9,28

L531D	COX-1	26	13	K _{MS} : (AA) NC or ↓2.5-fold. Products: (AA) %11-HETE NC, %15-HETE NC. Potencies: Aspirin NC.	9,51
L531I	COX-1	74	19	K _{MS} : (AA) ↓5-fold or 12-fold. Potencies: Aspirin NC.	9,51
L531K	COX-1	0	0		9,51
L531N	COX-1	9	7	K _{MS} : (AA) ↑1.5-fold or ↓1.7-fold. Products: (AA) %11-HETE NC, %15-HETE NC. Potencies: Aspirin NC.	9,51
L531V	COX-1	75	8	K _{MS} : (AA) NC; (DHLLA) ↑2.5-fold. Oxygenation: (DHLLA) ↓5.1-fold. Products: (AA) %11-HETE NC, %15-HETE NC.	9,28
L531A	COX-2	~100 or 89	58 or 1.5	K _{MS} : (AA) NC; (2-AG) ↓1.9-fold. k _{catS} : (AA) ↓1.9-fold; (2-AG) ↓1.6-fold. Oxygenation: (2-AG) ↓1.6-fold and not stimulated by 13-Me-AA; (AEA) ↓ but <AA. Products: (2-AG) %HETE-Gs ↑.	14,21, 22,40, 48,49
L531F	COX-2	~100 or 82	89	K _{MS} : (AA) ↑2.9-fold or NC; (2-AG) NC; (1-AG) NC. k _{catS} : (AA) NC or ↓1.5-fold; (2-AG) NC; (1-AG) NC. Oxygenation: (2-AG) NC. Potencies: Aspirin I; celecoxib ↓9-fold. Eliminates inverted binding conformation of AA, but binding in one subunit is still suboptimal.	40,48, 49
L531I	COX-2	NR	NR	Oxygenation: (AA) ↓; (2-AG) ↓ but stimulated by 13-Me-AA; AEA ↓. Products: (AA) 15(R)-PGH ₂ :15(S)-PGH ₂ ↑.	14,21, 22,36
L531N	COX-2	106	38	K _{MS} : (AA) ↑2.3-fold. k _{catS} : (AA) ↓2.6-fold. Potencies: Aspirin ↓; celecoxib ↓3.4-fold.	49
L531P	COX-2	~100	64	K _{MS} : (AA) ↓1.8-fold; (2-AG) NC. k _{catS} : (AA) ↓1.8-fold; (2-AG) ↓1.4-fold. Oxygenation: (2-AG) ↓1.5-fold.	39,48
L531 T	COX-2	~100	56	Oxygenation: (2-AG) ↓1.8-fold.	48
L531V	COX-2	NR	NR	Oxygenation: (AA) ↓; (2-AG) ↓ but <AA and not stimulated by 13-Me-AA; (AEA) ↓ but <AA. Products: (2-AG) HETE-Gs ↑.	14,21, 22
L531W	COX-2	37	22		49
K532E	COX-1	0	0		51
K532L	COX-1	1	15	K _{MS} : (AA) NC. Potencies: Aspirin I.	51
K532R	COX-1	55	55	K _{MS} : (AA) NC. Potencies: Aspirin NC.	51
G533A	COX-1	54 or 85	0		9,51
G533A/I523V	COX-1	54	0		9
G533A	COX-2	99 or 104	8	K _{MS} : (αLA) NC; (SA) NC; (EPA) NC; k _{catS} : (αLA) NC; (SA) NC; (EPA) ↓2.1-fold. Oxygenation: (LA) ↓3.2-fold or 100%;(αLA) NC; (SA) NC; (EPA) ↓2.2-fold. Unable to make HETEs after acetylation.	18,30, 55

G533L	COX-2	107	0	Oxygenation: (LA) ↓100%; (αLA) ↓5-fold or 100%; (SA) ↓5.5-fold. Activity with αLA and SA increased with added H ₂ O ₂ . Unable to make HETEs after acetylation. Potencies: ARN-2508 ↓.	18,30, 41,55
G533V	COX-2	93 or 97	0	Oxygenation: (LA) 100%; (αLA) ↓1.7-fold or 6-fold or >95%; (SA) ↓2.4-fold or >95%; (EPA) ↓>95%; (2-AG) ↓100%. Activity with αLA and SA increased with added H ₂ O ₂ . Unable to make HETEs after acetylation.	18,23, 30,55
L534A	COX-1	72	59	K _{MS} : (AA) ↑4-fold. Oxygenation: (EPA) ↓2-fold; (LA) ↓2.4-fold; (DHLLA) ↓1.9-fold. Products: (AA) %11-HETE NC, %15-HETE ↑22-fold (95% S).	9,27, 28
L534V	COX-1	102	98	Oxygenation: (EPA) ↓10-fold; (LA) ↓100%; (DHLLA) ↓2.4-fold. Products: (AA) %11-HETE ↑3.2-fold, %15-HETE ↑19-fold (96% S).	9,27, 28
C540S	COX-1	44	11	K _{MS} : (AA) ↓7-fold. Potencies: Flurbiprofen NC. No effect on dimer formation, glycosylation, or inactivation by maleimides.	33
S541C/ΔC	COX-2	NR	100 or 110	Dimer not cross-linked upon oxidation	1,2
A543C/ΔC	COX-2	NR	81 or 88	Dimer not cross-linked upon oxidation	1,2
A543E	COX-2	NR	110		1
A543E/H122N	COX-2	NR	120		1
N594A	COX-2	NR	NR	Improves crystallization by elimination of glycosylation site.	40,48
G601R	COX-2	86	80	K _{MS} : (AA) NC; (EPA) NC. No effect on activation or inactivation.	31

^aPercent of wild-type peroxidase activity, if reported. NR – not reported.

^bPercent of wild-type peroxidase activity, if reported. NR – not reported.

^cAA – arachidonic acid; 2-AG – 2-arachidonoylglycerol; AEA – arachidonylethanolamide; LA – linoleic acid; (αLA) – α-linolenic acid; EPA – eicosapentaenoic acid; DHLLA – dihomo-γ-linolenic acid; SA – stearidonic acid; 13-Me-AA – 13(S)-methyl-arachidonic acid; GSH Px – glutathione peroxidase; NC – no change or difference from wild-type < 1.5-fold; ↑ – increased; ↓ – decreased; I – inactive. All changes are relative to behavior with wild-type enzyme.

References

- (1) Dong, L.; Yuan, C.; Orlando, B. J.; Malkowski, M. G.; Smith, W. L. *J Biol Chem* **2016**, *291*, 25641.
- (2) Yuan, C.; Sidhu, R. S.; Kuklev, D. V.; Kado, Y.; Wada, M.; Song, I.; Smith, W. L. *J Biol Chem* **2009**, *284*, 10046.
- (3) MirAfzali, Z.; Leipprandt, J. R.; McCracken, J. L.; DeWitt, D. L. *J Biol Chem* **2006**, *281*, 28354.
- (4) Blobaum, A. L.; Xu, S.; Rowlinson, S. W.; Duggan, K. C.; Banerjee, S.; Kudalkar, S. N.; Birmingham, W. R.; Ghebreselasie, K.; Marnett, L. J. *J Biol Chem* **2015**, *290*, 12793.

- (5) Xu, S.; Uddin, M. J.; Banerjee, S.; Duggan, K.; Musee, J.; Kiefer, J. R.; Ghebreselasie, K.; Rouzer, C. A.; Marnett, L. J. *J Biol Chem* **2019**, *294*, 8690.
- (6) Gierse, J. K.; McDonald, J. J.; Hauser, S. D.; Rangwala, S. H.; Koboldt, C. M.; Seibert, K. *J Biol Chem* **1996**, *271*, 15810.
- (7) Mancini, J. A.; Riendeau, D.; Falguyret, J. P.; Vickers, P. J.; O'Neill, G. P. *J Biol Chem* **1995**, *270*, 29372.
- (8) Bhattacharyya, D. K.; Lecomte, M.; Rieke, C. J.; Garavito, M.; Smith, W. L. *J Biol Chem* **1996**, *271*, 2179.
- (9) Thuresson, E. D.; Lakkides, K. M.; Rieke, C. J.; Sun, Y.; Wingerd, B. A.; Micielli, R.; Mulichak, A. M.; Malkowski, M. G.; Garavito, R. M.; Smith, W. L. *J Biol Chem* **2001**, *276*, 10347.
- (10) Loll, P. J.; Sharkey, C. T.; O'Connor, S. J.; Dooley, C. M.; O'Brien, E.; Devocelle, M.; Nolan, K. B.; Selinsky, B. S.; Fitzgerald, D. J. *Mol Pharmacol* **2001**, *60*, 1407.
- (11) Duggan, K. C.; Walters, M. J.; Musee, J.; Harp, J. M.; Kiefer, J. R.; Oates, J. A.; Marnett, L. J. *J Biol Chem* **2010**, *285*, 34950.
- (12) Hochgesang, G. P., Jr.; Rowlinson, S. W.; Marnett, L. J. *J Am Chem Soc* **2000**, *122*.
- (13) Kalgutkar, A. S.; Crews, B. C.; Rowlinson, S. W.; Marnett, A. B.; Kozak, K. R.; Remmel, R. P.; Marnett, L. J. *Proc Natl Acad Sci U S A* **2000**, *97*, 925.
- (14) Kudalkar, S. N.; Nikas, S. P.; Kingsley, P. J.; Xu, S.; Galligan, J. J.; Rouzer, C. A.; Banerjee, S.; Ji, L.; Eno, M. R.; Makriyannis, A.; Marnett, L. J. *J Biol Chem* **2015**, *290*, 7897.
- (15) Orlando, B. J.; Lucido, M. J.; Malkowski, M. G. *J Struct Biol* **2015**, *189*, 62.
- (16) Rowlinson, S. W.; Kiefer, J. R.; Prusakiewicz, J. J.; Pawlitz, J. L.; Kozak, K. R.; Kalgutkar, A. S.; Stallings, W. C.; Kurumbail, R. G.; Marnett, L. J. *J Biol Chem* **2003**, *278*, 45763.
- (17) Timofeevski, S. L.; Prusakiewicz, J. J.; Rouzer, C. A.; Marnett, L. J. *Biochemistry* **2002**, *41*, 9654.
- (18) Vecchio, A. J.; Orlando, B. J.; Nandagiri, R.; Malkowski, M. G. *J Biol Chem* **2012**, *287*, 24619.
- (19) Greig, G. M.; Francis, D. A.; Falguyret, J. P.; Ouellet, M.; Percival, M. D.; Roy, P.; Bayly, C.; Mancini, J. A.; O'Neill, G. P. *Mol Pharmacol* **1997**, *52*, 829.
- (20) Rieke, C. J.; Mulichak, A. M.; Garavito, R. M.; Smith, W. L. *J Biol Chem* **1999**, *274*, 17109.
- (21) Kozak, K. R.; Prusakiewicz, J. J.; Rowlinson, S. W.; Prudhomme, D. R.; Marnett, L. J. *Biochemistry* **2003**, *42*, 9041.
- (22) Kozak, K. R.; Prusakiewicz, J. J.; Rowlinson, S. W.; Schneider, C.; Marnett, L. J. *J Biol Chem* **2001**, *276*, 30072.
- (23) Kozak, K. R.; Rowlinson, S. W.; Marnett, L. J. *J Biol Chem* **2000**, *275*, 33744.
- (24) Uddin, M. J.; Crews, B. C.; Xu, S.; Ghebreselasie, K.; Daniel, C. K.; Kingsley, P. J.; Banerjee, S.; Marnett, L. J. *ACS Chem Biol* **2016**, *11*, 3052.
- (25) Rogge, C. E.; Liu, W.; Wu, G.; Wang, L. H.; Kulmacz, R. J.; Tsai, A. L. *Biochemistry* **2004**, *43*, 1560.
- (26) Landino, L. M.; Crews, B. C.; Gierse, J. K.; Hauser, S. D.; Marnett, L. J. *J Biol Chem* **1997**, *272*, 21565.
- (27) Malkowski, M. G.; Thuresson, E. D.; Lakkides, K. M.; Rieke, C. J.; Micielli, R.; Smith, W. L.; Garavito, R. M. *J Biol Chem* **2001**, *276*, 37547.
- (28) Thuresson, E. D.; Malkowski, M. G.; Lakkides, K. M.; Rieke, C. J.; Mulichak, A. M.; Ginell, S. L.; Garavito, R. M.; Smith, W. L. *J Biol Chem* **2001**, *276*, 10358.
- (29) Chubb, A. J.; Fitzgerald, D. J.; Nolan, K. B.; Moman, E. *Biochemistry* **2006**, *45*, 811.
- (30) Rowlinson, S. W.; Crews, B. C.; Goodwin, D. C.; Schneider, C.; Gierse, J. K.; Marnett, L. J. *J Biol Chem* **2000**, *275*, 6586.
- (31) Liu, W.; Poole, E. M.; Ulrich, C. M.; Kulmacz, R. J. *Pharmacogenomics J* **2011**, *11*, 337.
- (32) Shimokawa, T.; Kulmacz, R. J.; DeWitt, D. L.; Smith, W. L. *J Biol Chem* **1990**, *265*, 20073.
- (33) Smith, C. J.; Marnett, L. J. *Arch Biochem Biophys* **1996**, *335*, 342.
- (34) Rogge, C. E.; Ho, B.; Liu, W.; Kulmacz, R. J.; Tsai, A. L. *Biochemistry* **2006**, *45*, 523.
- (35) Harman, C. A.; Rieke, C. J.; Garavito, R. M.; Smith, W. L. *J Biol Chem* **2004**, *279*, 42929.

- (36) Schneider, C.; Boeglin, W. E.; Prusakiewicz, J. J.; Rowlinson, S. W.; Marnett, L. J.; Samel, N.; Brash, A. R. *J Biol Chem* **2002**, *277*, 478.
- (37) Prusakiewicz, J. J.; Felts, A. S.; Mackenzie, B. S.; Marnett, L. J. *Biochemistry* **2004**, *43*, 15439.
- (38) Blobaum, A. L.; Marnett, L. J. *J Biol Chem* **2007**, *282*, 16379.
- (39) Swinney, D. C.; Mak, A. Y.; Barnett, J.; Ramesha, C. S. *J Biol Chem* **1997**, *272*, 12393.
- (40) Vecchio, A. J.; Malkowski, M. G. *J Biol Chem* **2011**, *286*, 20736.
- (41) Goodman, M. C.; Xu, S.; Rouzer, C. A.; Banerjee, S.; Ghebreselasie, K.; Migliore, M.; Piomelli, D.; Marnett, L. J. *J Biol Chem* **2018**.
- (42) Bambai, B.; Rogge, C. E.; Stec, B.; Kulmacz, R. J. *J Biol Chem* **2004**, *279*, 4084.
- (43) Kiefer, J. R.; Pawlitz, J. L.; Moreland, K. T.; Stegeman, R. A.; Hood, W. F.; Gierse, J. K.; Stevens, A. M.; Goodwin, D. C.; Rowlinson, S. W.; Marnett, L. J.; Stallings, W. C.; Kurumbail, R. G. *Nature* **2000**, *405*, 97.
- (44) Xu, S.; Hermanson, D. J.; Banerjee, S.; Ghebreselasie, K.; Clayton, G. M.; Garavito, R. M.; Marnett, L. J. *J Biol Chem* **2014**, *289*, 6799.
- (45) Konkle, M. E.; Blobaum, A. L.; Moth, C. W.; Prusakiewicz, J. J.; Xu, S.; Ghebreselasie, K.; Akingbade, D.; Jacobs, A. T.; Rouzer, C. A.; Lybrand, T. P.; Marnett, L. J. *Biochemistry* **2016**, *55*, 348.
- (46) Windsor, M. A.; Valk, P. L.; Xu, S.; Banerjee, S.; Marnett, L. J. *Bioorg Med Chem Lett* **2013**, *23*, 5860.
- (47) Wong, E.; Bayly, C.; Waterman, H. L.; Riendeau, D.; Mancini, J. A. *J Biol Chem* **1997**, *272*, 9280.
- (48) Vecchio, A. J.; Simmons, D. M.; Malkowski, M. G. *J Biol Chem* **2010**, *285*, 22152.
- (49) Dong, L.; Anderson, A. J.; Malkowski, M. G. *Biochemistry* **2019**, *58*, 3990.
- (50) Guo, Q.; Wang, L. H.; Ruan, K. H.; Kulmacz, R. J. *J Biol Chem* **1996**, *271*, 19134.
- (51) Shimokawa, T.; Smith, W. L. *J Biol Chem* **1992**, *267*, 12387.
- (52) DeWitt, D. L.; el-Harith, E. A.; Kraemer, S. A.; Andrews, M. J.; Yao, E. F.; Armstrong, R. L.; Smith, W. L. *J Biol Chem* **1990**, *265*, 5192.
- (53) Mancini, J. A.; Vickers, P. J.; O'Neill, G. P.; Boily, C.; Falgueyret, J. P.; Riendeau, D. *Mol Pharmacol* **1997**, *51*, 52.
- (54) Lucido, M. J.; Orlando, B. J.; Vecchio, A. J.; Malkowski, M. G. *Biochemistry* **2016**, *55*, 1226.
- (55) Rowlinson, S. W.; Crews, B. C.; Lanzo, C. A.; Marnett, L. J. *J Biol Chem* **1999**, *274*, 23305.

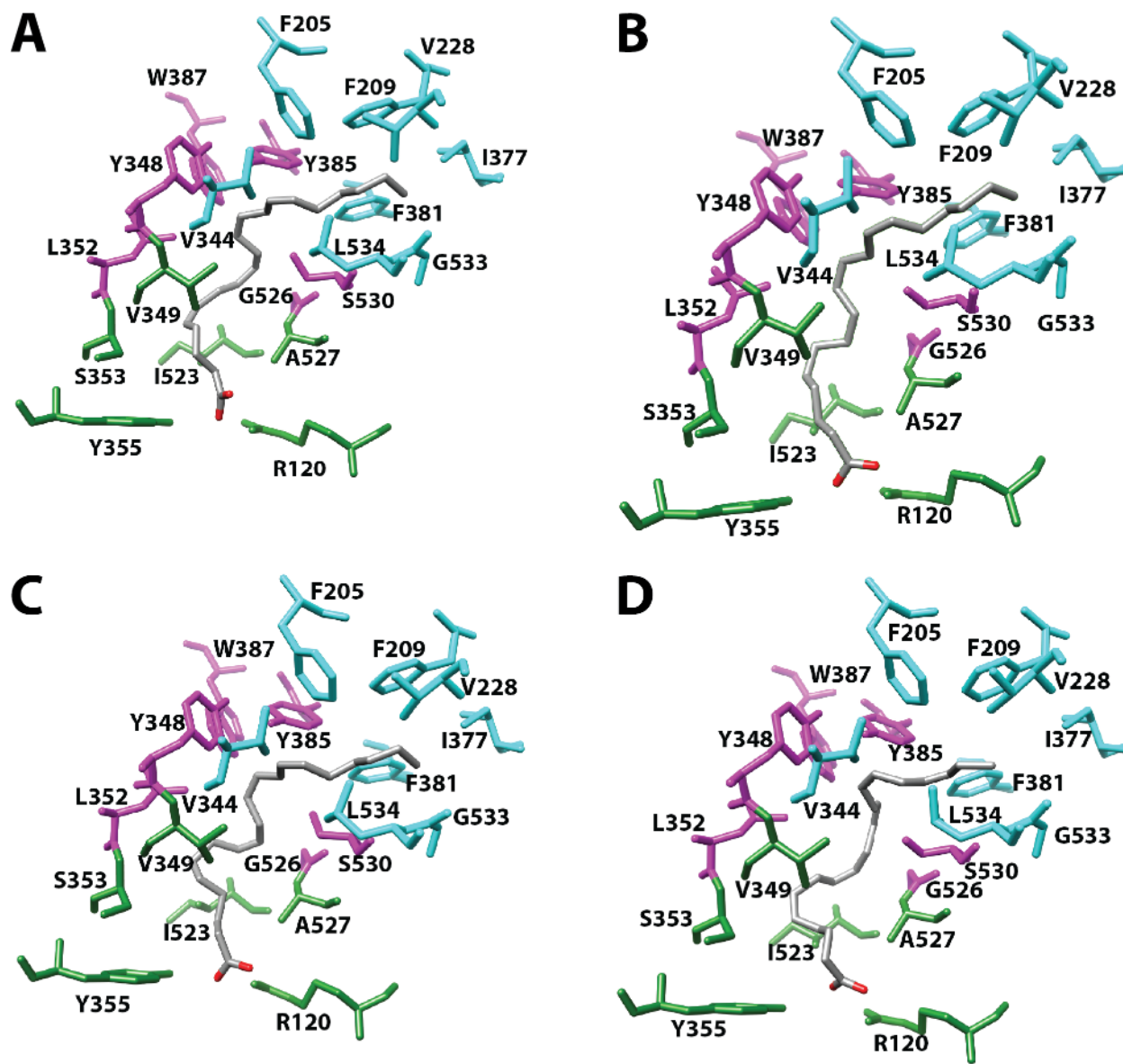


Figure S1. Structure of (A) AA, (B) LA, (C) DHLA, and (D) EPA, bound in the cyclooxygenase active site of COX-1 and the side chains that make up the proximal binding pocket (green), the central binding pocket (magenta), and the distal binding pocket (cyan). An overlay of these structures in stereoscopic view is provided in Figure 5B. From PDB #1DIY, #1IGZ, #1FE2, and #1IGX.

proximal binding pocket (green), the central binding pocket (magenta), and the distal binding pocket (cyan). An overlay of these structures is provided in Figure S3. From PDB #3HS5 (chain B), #4E1G, #3HS6 (chain B), #3HS7, and #3QH0.

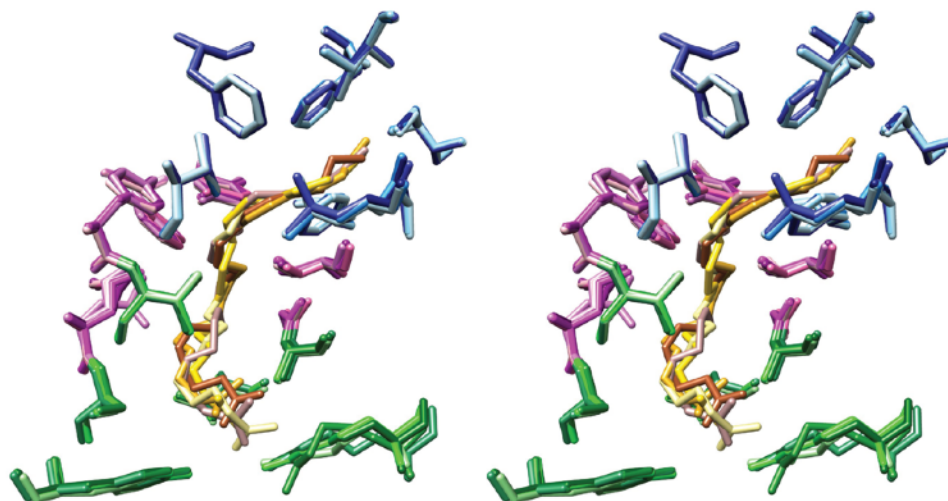


Figure S3. Wall-eyed stereo view of an overlay of the structures of five fatty acids in the cyclooxygenase active site of COX-2 and the side chains that make up the proximal binding pocket (green), the central binding pocket (magenta), and the distal binding pocket (blue). Fatty acids and amino acid side chains are colored from lightest to darkest in the order PA, α LA, EPA, DHA, and AA. Notable is the minimal movement of active site residues to accommodate the structural differences among the various fatty acids. Monoscopic views of the individual structures are provided in Figure S2. From PDB #3HS5 (chain B), #4E1G, #3HS6 (chain B), #3HS7, and #3QH0 (chain A).

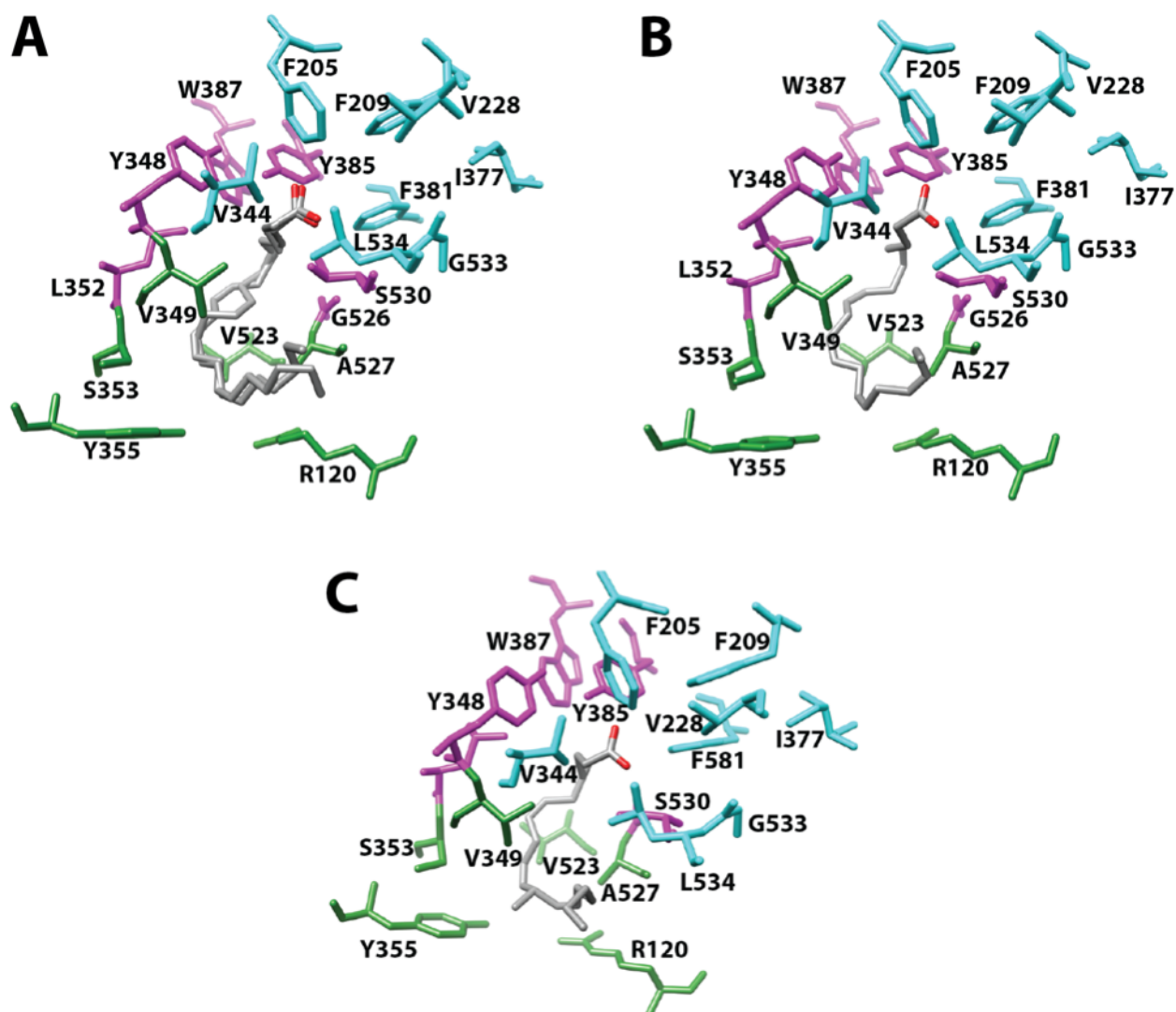


Figure S4. Structure of (A) AA (nonproductive conformation), (B) EPA (nonproductive conformation), and (C) 13-Me-AA bound in the cyclooxygenase active site of COX-2 and the side chains that make up the proximal binding pocket (green), the central binding pocket (magenta), and the distal binding pocket (cyan). Note that AA is observed in two slightly different conformations. From PDB #3HS5 (chain A), #3HS6 (chain A), and #4RUT.

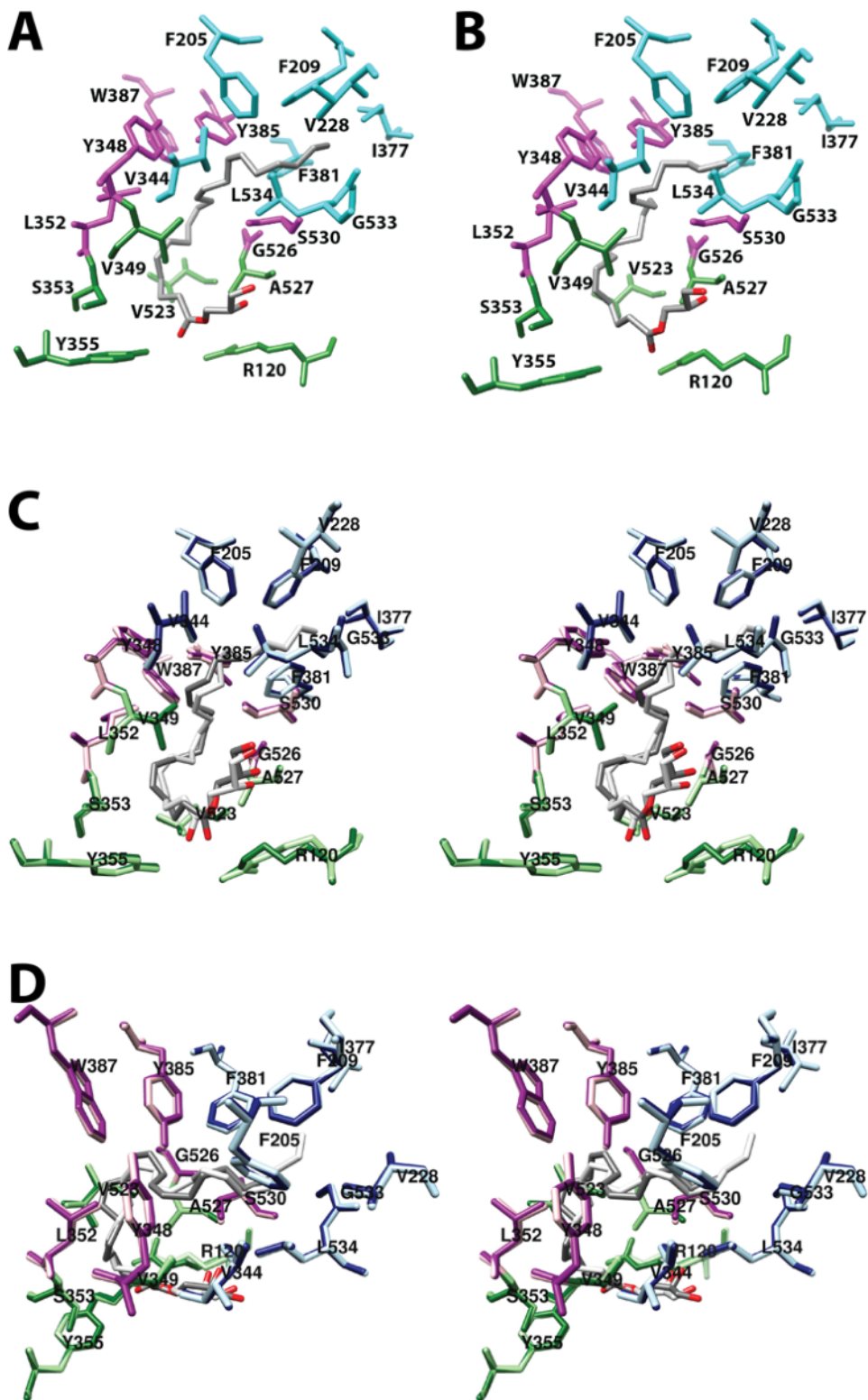


Figure S5. Structure of 1-AG in the (A) productive conformation and (B) nonproductive conformation bound in the active site of COX-2 and the side chains that make up the proximal binding pocket (green), the central binding pocket (magenta), and the distal binding pocket (cyan). (C) and (D) Two different wall-eyed stereo views of the overlay of the structures of the nonproductive (dark gray) and productive (light

gray) conformations of 1-AG bound in the cyclooxygenase active site. Residues in the surrounding binding pockets are colored similarly to those in (A) and (B) with the lighter and darker colors corresponding to the productive and nonproductive conformations, respectively. From PDB #3MDL.

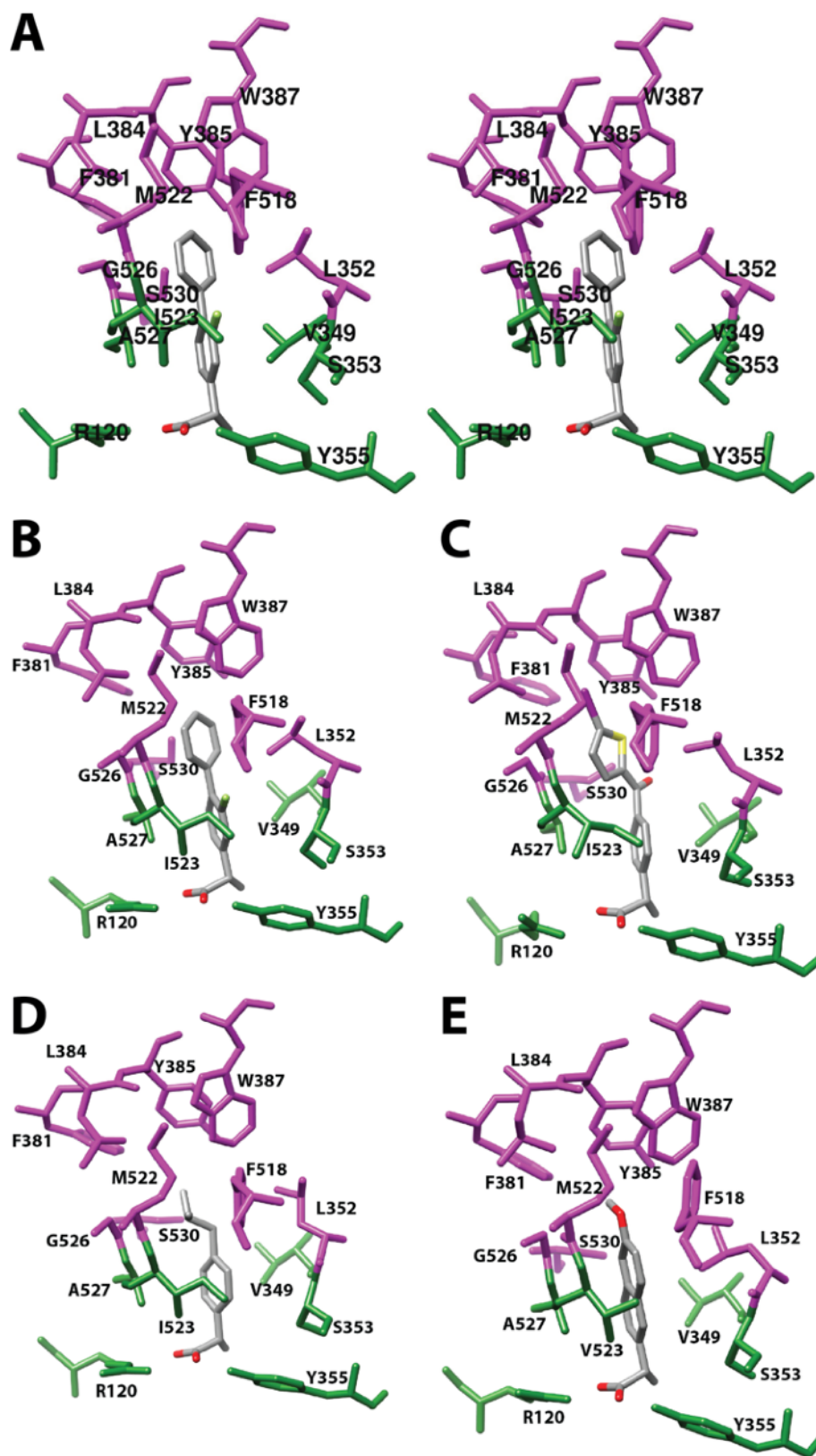


Figure S6. Wall-eyed stereo view of the structure of (S)-flurbiprofen bound in the cyclooxygenase active

site of COX-1. Structures of (B) (*S*)-flurbiprofen, (C) (*S*)-iodosuprofen, (D) (*S*)-ibuprofen, and (E) (*S*)-naproxen, bound in the cyclooxygenase active site of COX-1 (B, C, and D) or COX-2 (E). The side chains that make up the proximal binding pocket (green) and the central binding pocket (magenta) are shown. From PDB #1EQH (A and B), #1PGE, #1EQG, and #3NT1.

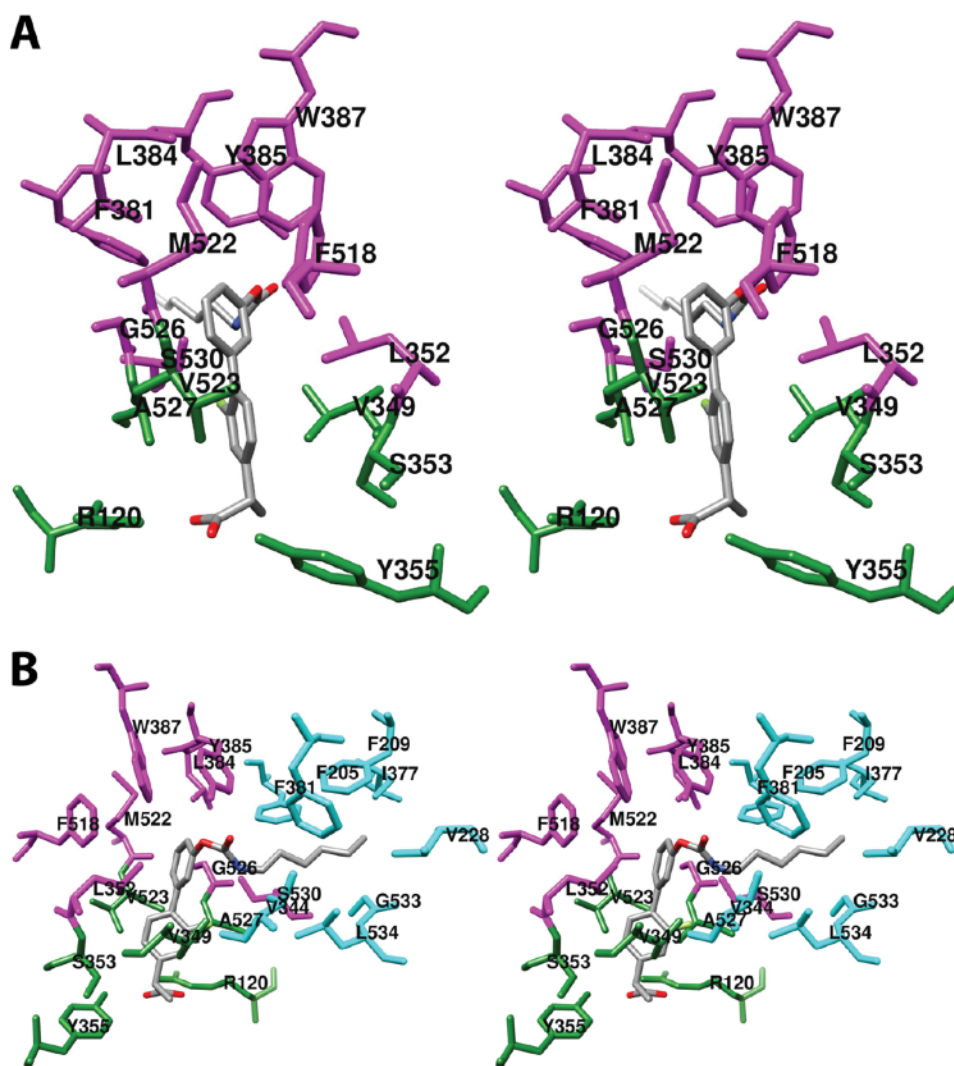


Figure S7. (A) Wall-eyed stereo view of the structure of ARN-2508 bound in the cyclooxygenase active site of COX-2 and the side chains that make up the proximal binding pocket (green) and the central binding pocket (magenta). (B) Same as (A) from a different perspective. Residues belonging to the distal AA binding pocket have been added and highlighted in cyan to reveal the localization of the hydrocarbon tail of ARN-2508 in this pocket. From PDB #5W58.

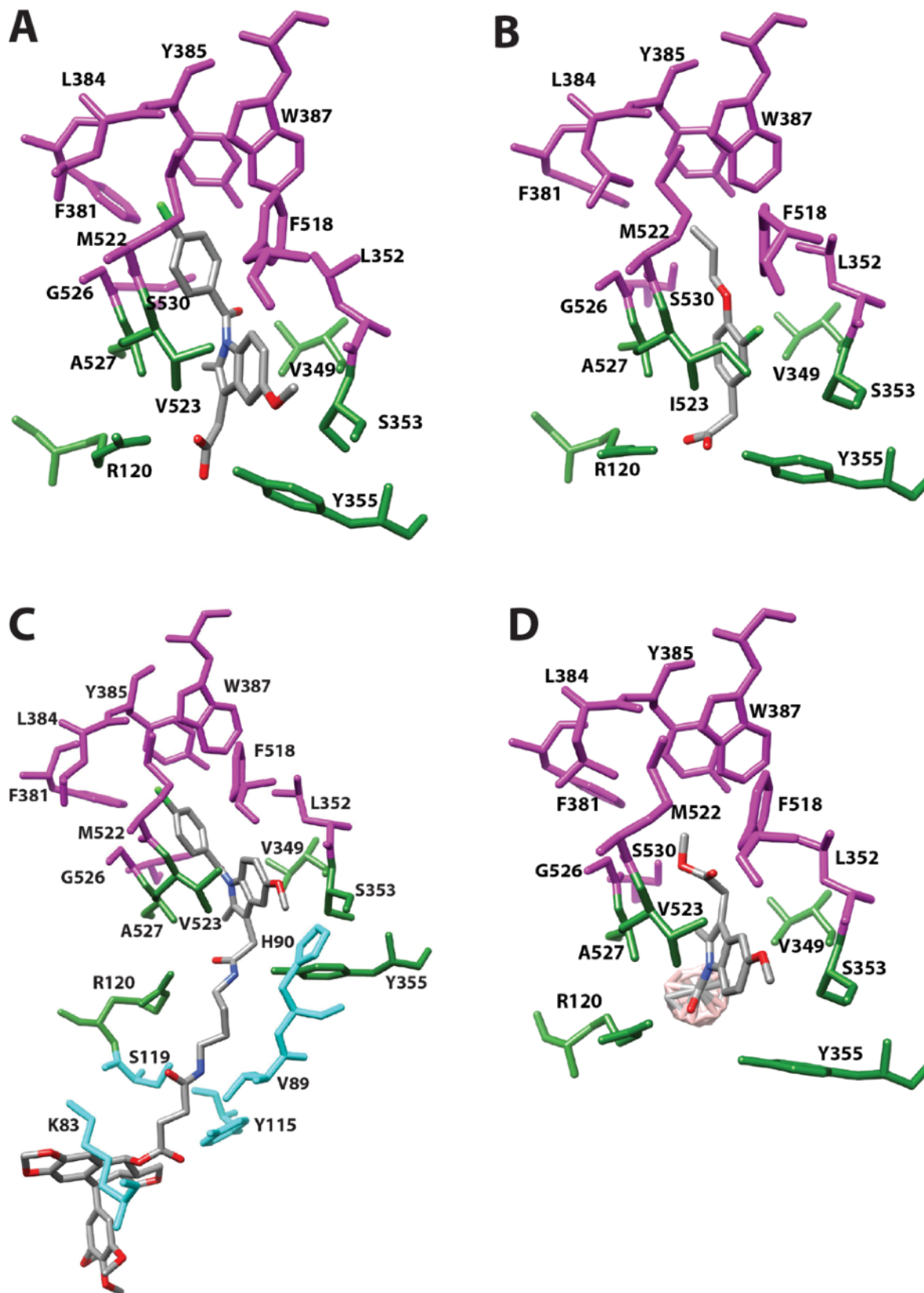


Figure S8. Structure of (A) indomethacin, (B) alclofenac, (C) an indomethacin-podophyllotoxin conjugate,

and (D) a *nido*-dicarbaborate derivative of indomethacin bound in the cyclooxygenase active site of COX-2 (A, C, & D) or COX-1 (B). The side chains that make up the proximal binding pocket (green), the central binding pocket (magenta), and membrane-binding domain residues that are predicted by molecular modeling to interact with the podophyllotoxin moiety (cyan) (C) are shown. From PDB #4COX, #1HT8, #4OTJ, and #4Z0L.

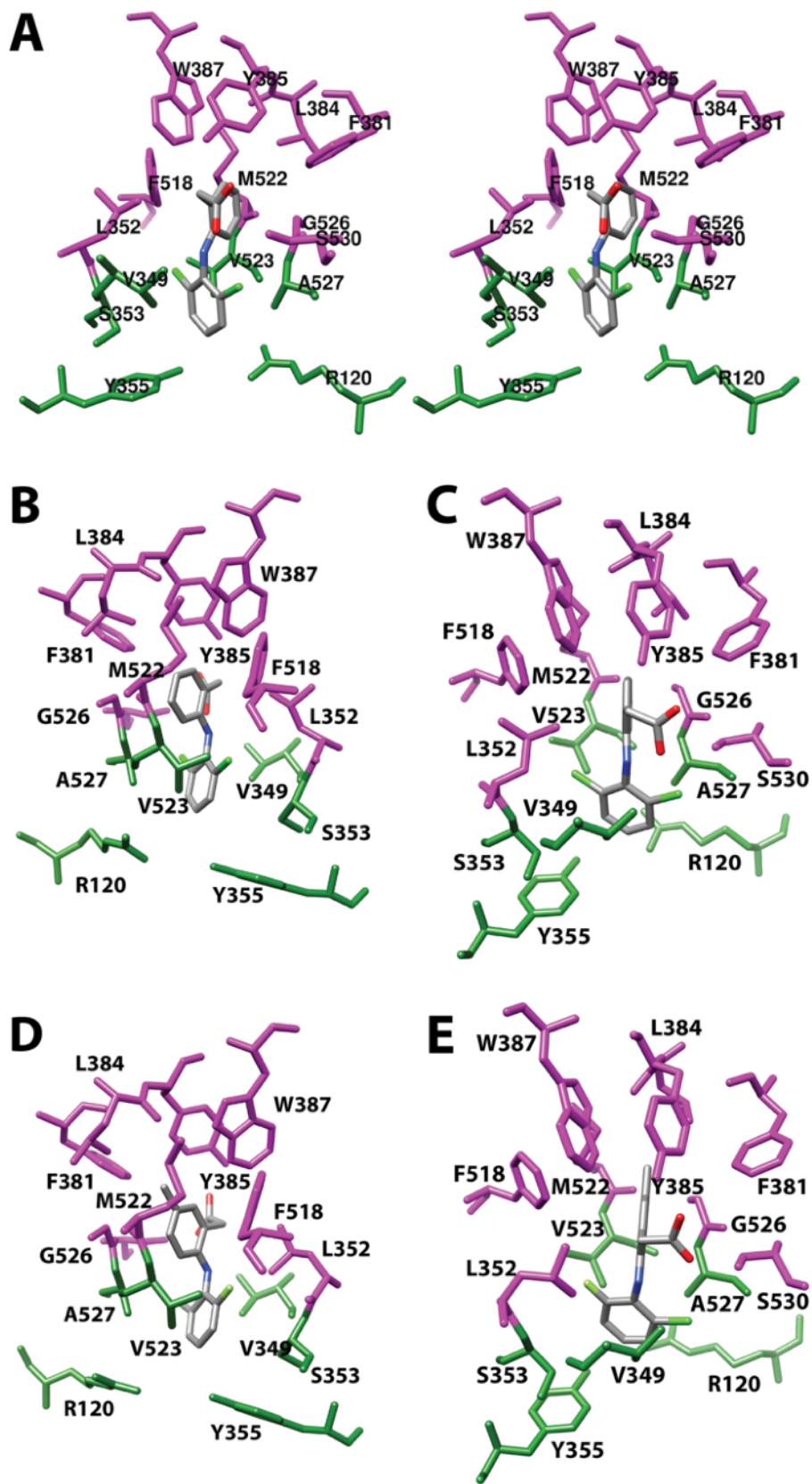


Figure S9. (A) Wall-eyed stereo view of diclofenac bound in the cyclooxygenase active site of COX-2.

Structures of (B & C) diclofenac and (D & E) lumiracoxib bound in the cyclooxygenase active site of COX-2. The side chains that make up the proximal binding pocket (green) and the central binding pocket (magenta) are shown. In each case, two views of the inhibitor are provided. Both are from the side (i.e., parallel to the plane of the membrane). Views (A, C, and E) highlight the proximity of the carboxylate of the inhibitor to the side chains of Ser-530 and Tyr-385. From PDB #1PXX and #4OTY.

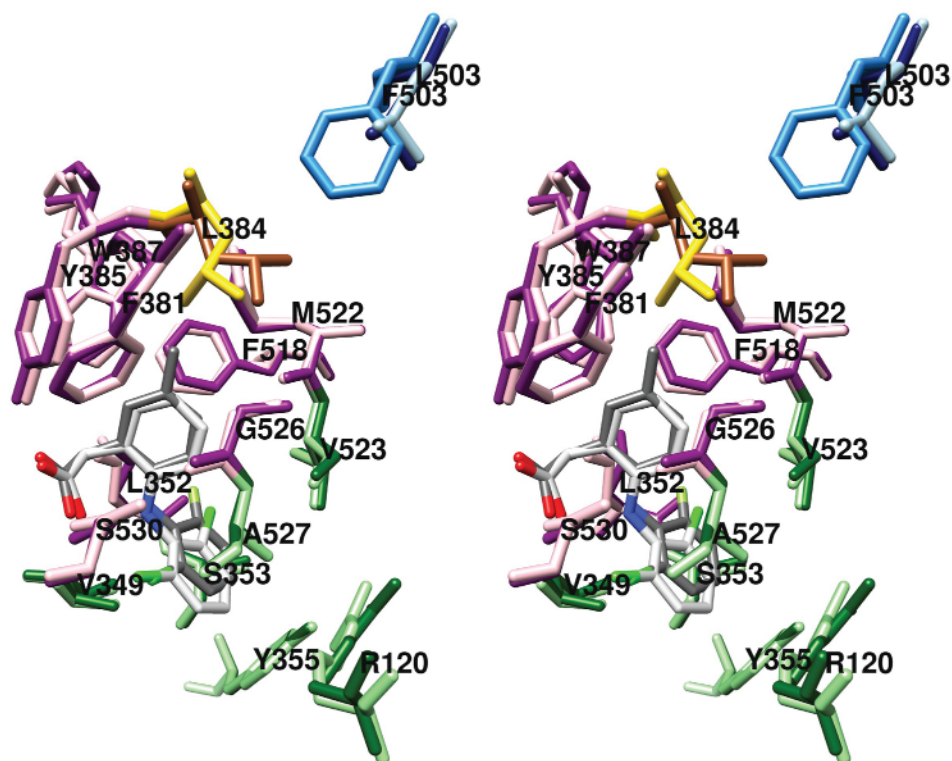


Figure S10. Wall-eyed stereo view of the overlay of the structures of diclofenac and lumiracoxib, bound in the cyclooxygenase active site of COX-2 and the side chains that make up the proximal binding pocket (light/dark green) and the central binding pocket (pink/magenta). Leu-384 is highlighted in gold/sienna, and Leu-503 is shown in light blue/navy blue. Also shown is the position that Phe-503 (dodger blue) occupies in the structure of diclofenac bound in the cyclooxygenase active site of COX-1. In each case, structures related to diclofenac (light gray) are shown in the lighter color and those related to lumiracoxib (dark gray) are shown in the darker color. From PDB #1PXX, #4OTY, and #3N8Y.

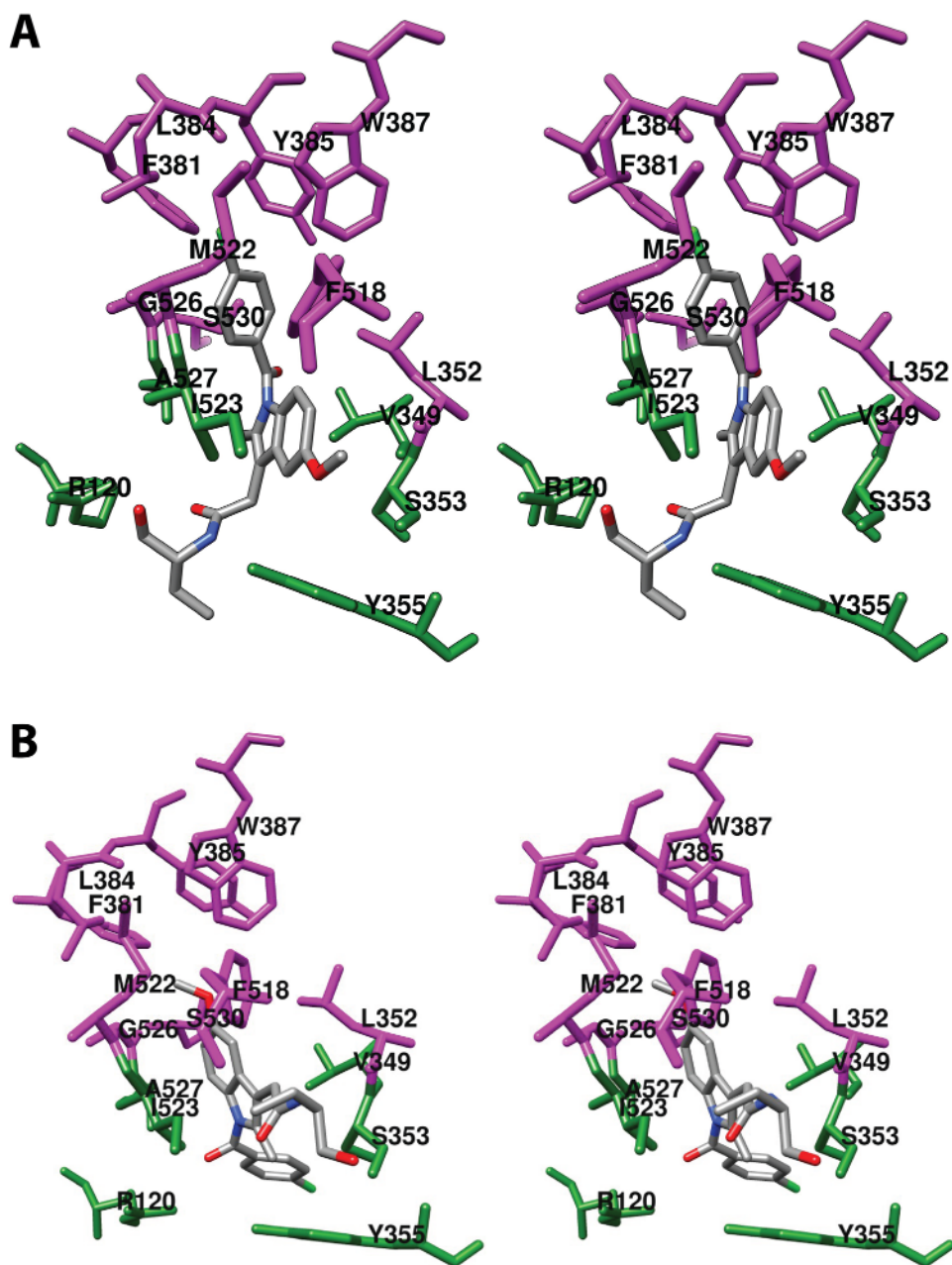


Figure S11. Wall-eyed stereo view of the structure of (A) indomethacin-(*R*)- α -ethyl-ethanolamide and (B) indomethacin-(*S*)- α -ethyl-ethanolamide bound in the cyclooxygenase active site of COX-2 and the side chains that make up the proximal binding pocket (green) and the central binding pocket (magenta). From PDB #2OYE and #2OYU.

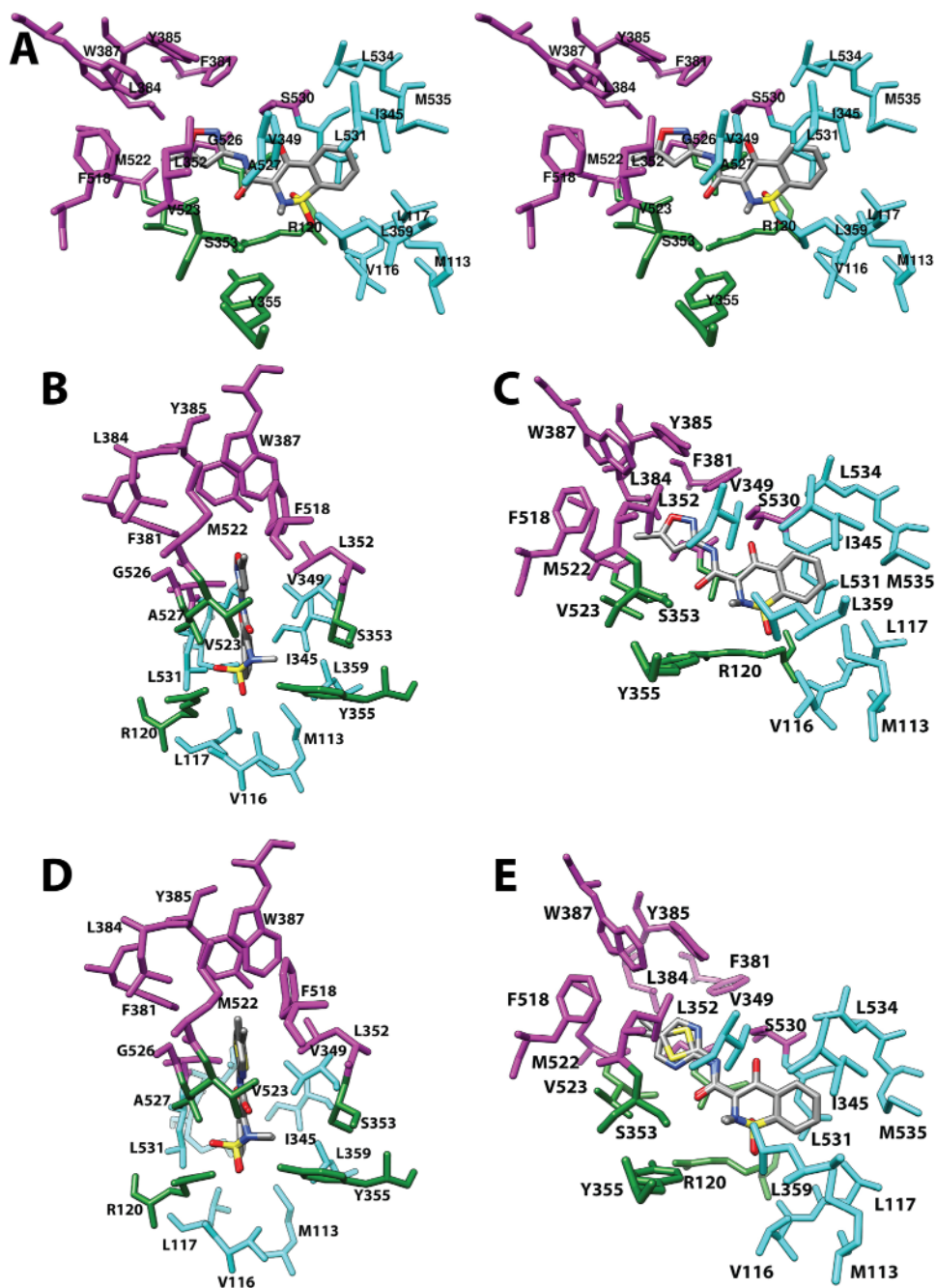


Figure S12. (A) Wall-eyed stereo view of isoxicam bound in the cyclooxygenase active site of COX-2. Structure of (B & C) isoxicam and (D & E) meloxicam bound in the cyclooxygenase active site of COX-2. The side chains that make up the proximal binding pocket (green), the central binding pocket (magenta), and the oxamic pocket (cyan) are shown. Note that Val-349 is part of both the proximal pocket and the oxamic pocket. It is colored in cyan. The exact conformation of the thiazole ring of meloxicam could not be determined. From PDB #4M10 and #4M11.

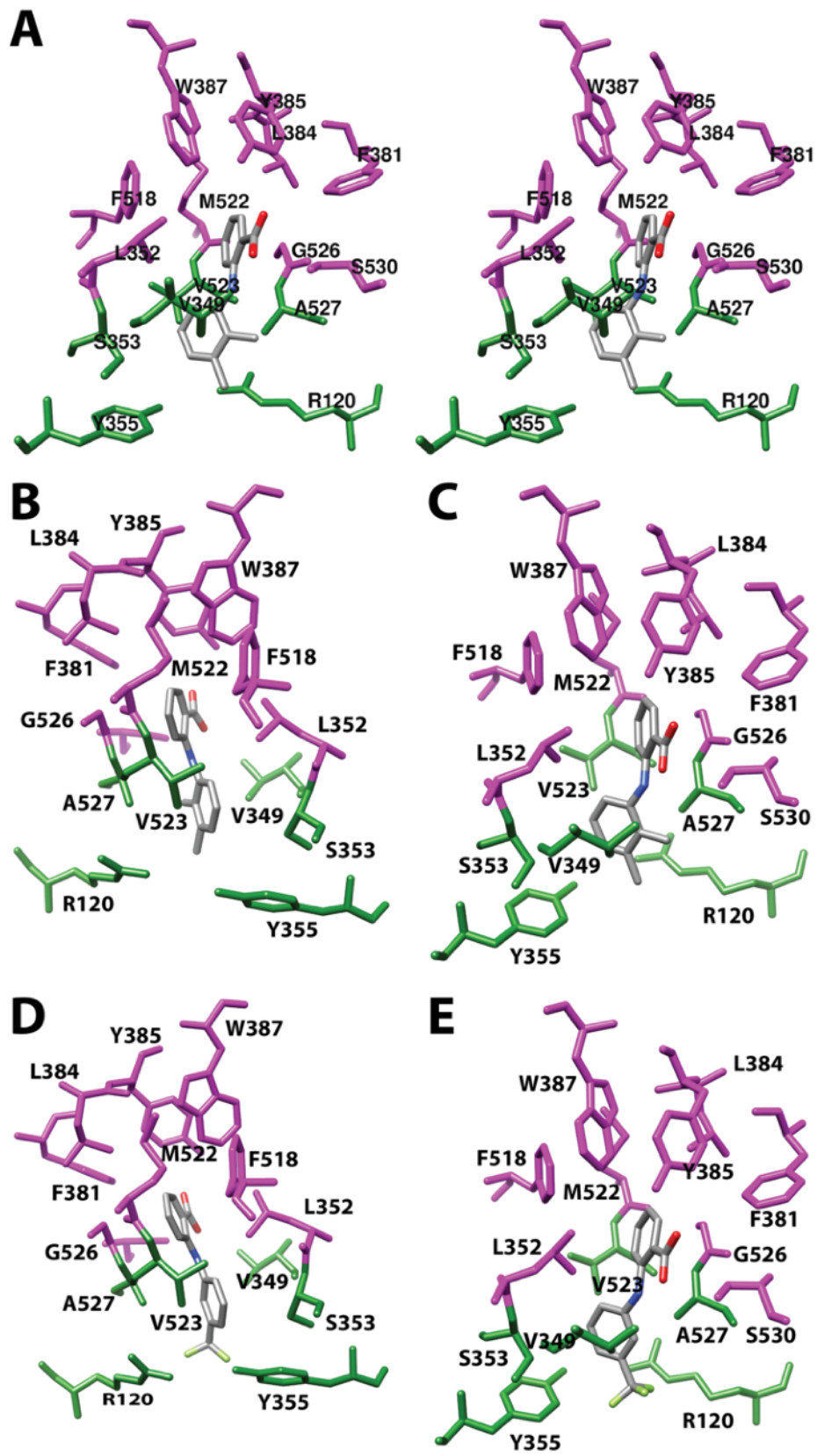


Figure S13. (A) Wall-eyed stereo view of mefenamic acid bound in the cyclooxygenase active site of

COX-2. Structures of (B & C) mefenamic acid and (D & E) flufenamic acid bound in the cyclooxygenase active site of COX-2. The side chains that make up the proximal binding pocket (green) and the central binding pocket (magenta) are shown. In each case, two views of the inhibitor are provided. Both are from the side (i.e., parallel to the plane of the membrane). Views (A), (C), and (E) highlight the proximity of the carboxylate of the inhibitor to the side chains of Ser-530 and Tyr-385. From PDB #5IKR and #5IKV.

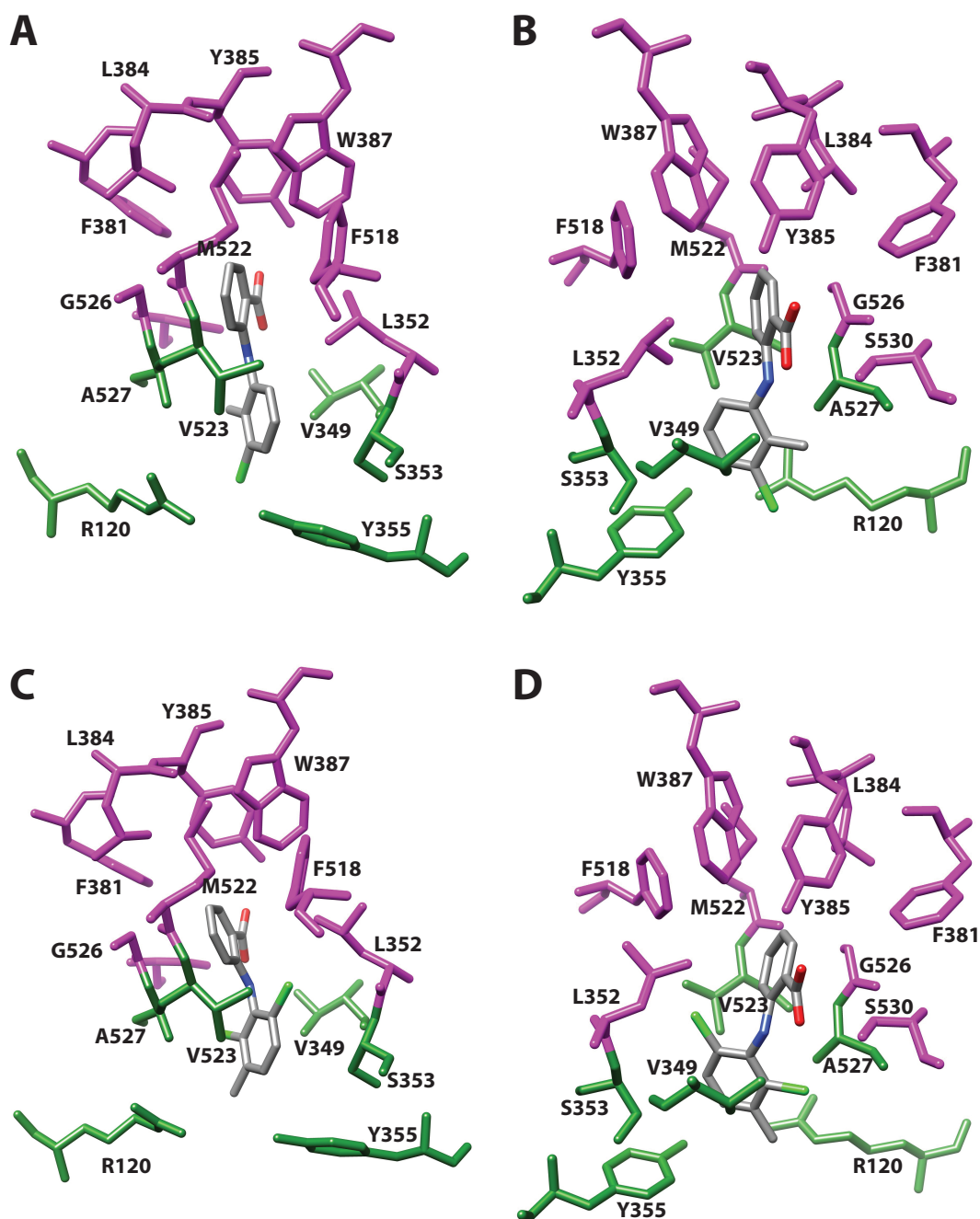


Figure S14. Structure of (A & B) tolfenamic acid and (C & D) meclofenamic acid bound in the cyclooxygenase active site of COX-2 and the side chains that make up the proximal binding pocket (green) and the central binding pocket (magenta). In each case, two views of the inhibitor are shown. Both are from the side (i.e., parallel to the plane of the membrane). Views (B) and (D) highlight the proximity of the carboxylate of the inhibitor to the side chains of Ser-530 and Tyr-385. From PDB #5IKT and #5IKQ.

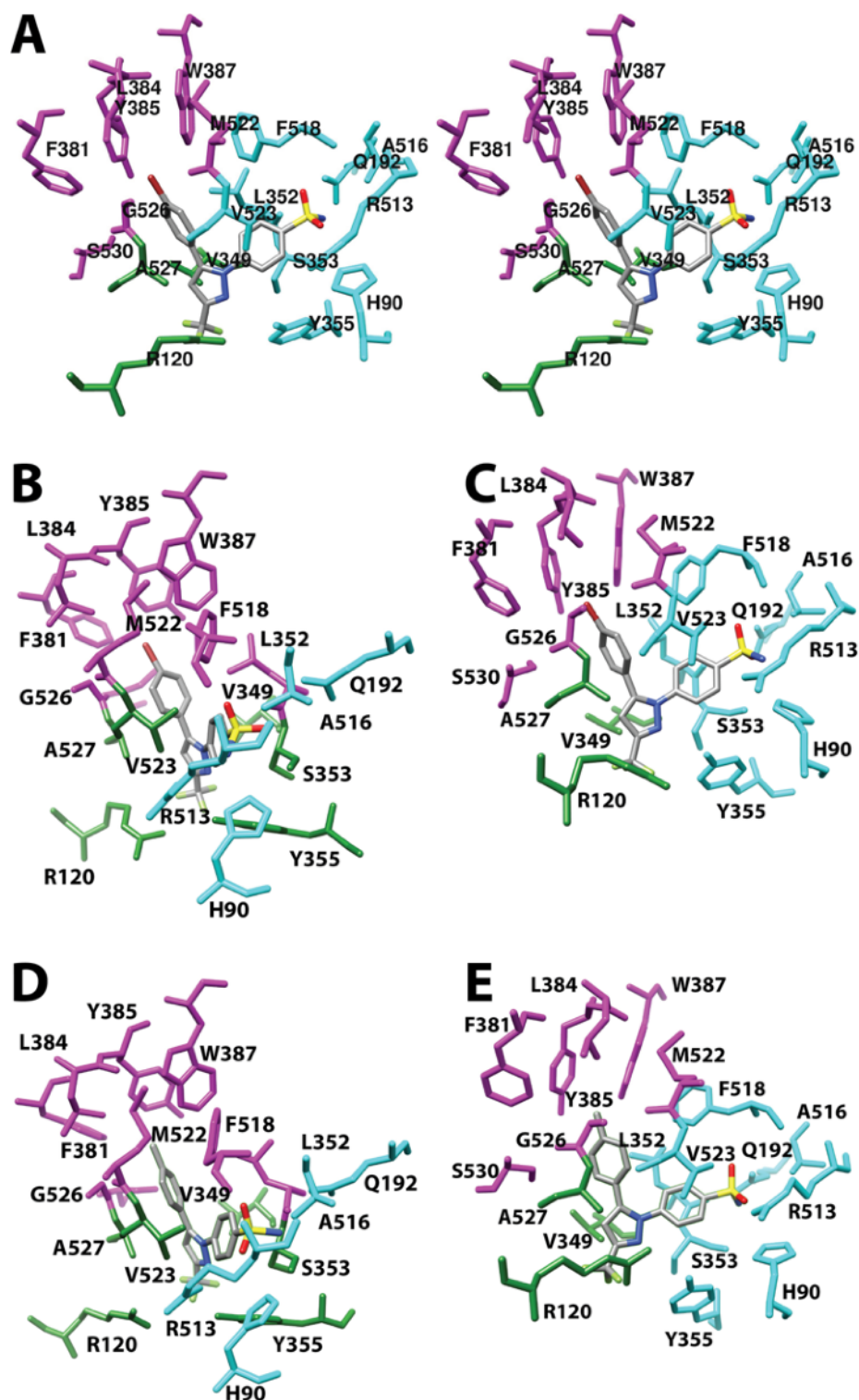


Figure S15. (A) Wall-eyed stereo view of SC-558 bound in the cyclooxygenase active site of COX-2. Structures of SC-558 (B & C) and celecoxib (D & E) bound in the cyclooxygenase active site of COX-2. The side chains that make up the proximal binding pocket (green), the central binding pocket (magenta), and the COX-2 side pocket (cyan) are shown. In (B) and (D), the residues are colored as in most previous figures. In (A), (C), and (E), some residues in the proximal and central binding pockets that are shared

with the COX-2 side pocket are colored cyan to highlight the interaction with the phenylsulfonamide group of each inhibitor. From PDB #6COX and #3LN1.

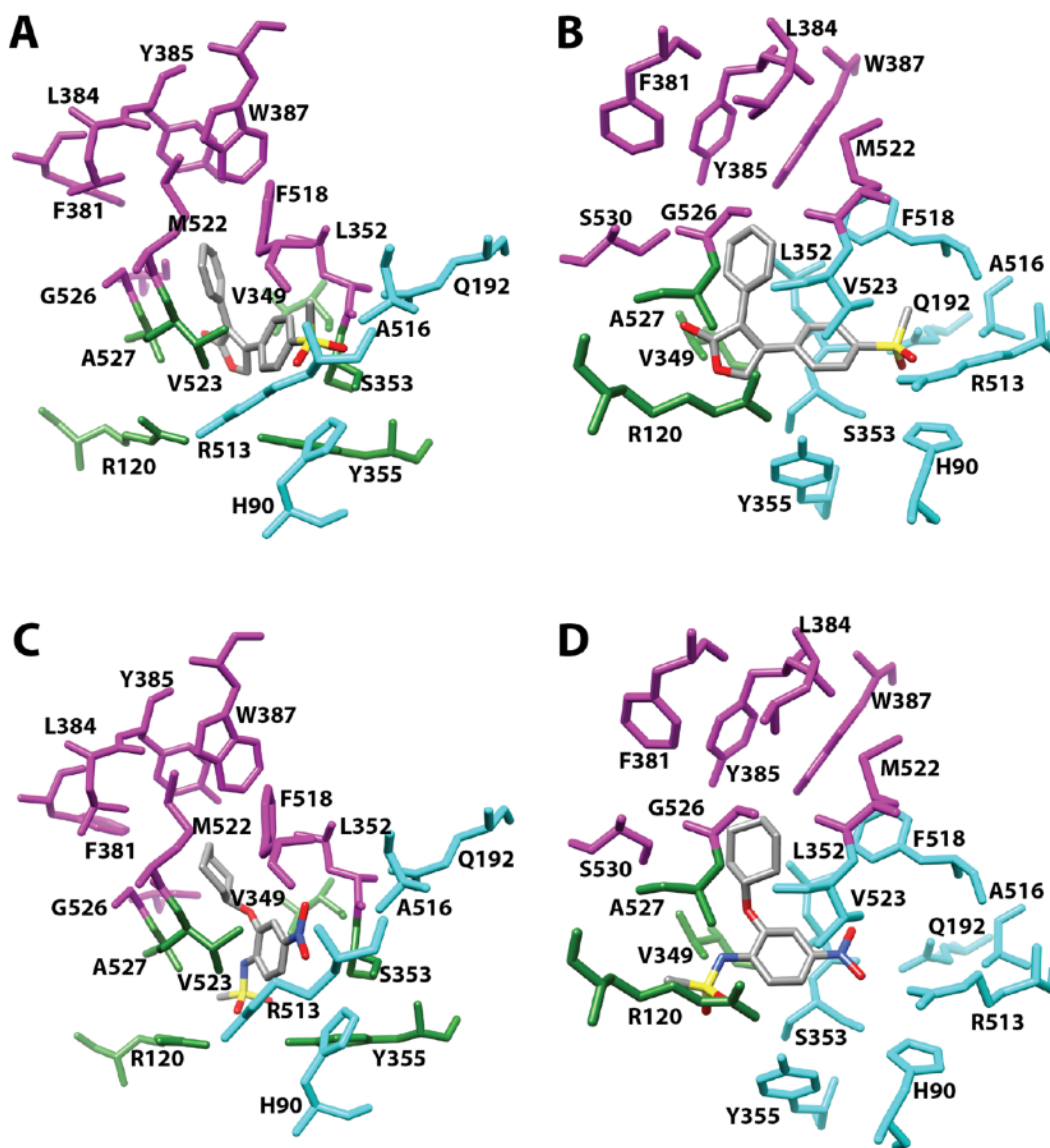


Figure S16. Structure of (A & B) rofecoxib and (C & D) NS-398 bound in the cyclooxygenase active site of COX-2 and the side chains that make up the proximal binding pocket (green), the central binding pocket (magenta), and the COX-2 side pocket (cyan). In (A) and (C), the residues are colored as in most previous figures. In (B) and (D), some residues in the proximal and central binding pockets that are shared with the COX-2 side pocket are colored cyan to highlight the interaction with the phenylmethylsulfone group of rofecoxib and the absence of an interaction with the side pocket in the case of NS-398. From PDB #5KIR and #3QMO.

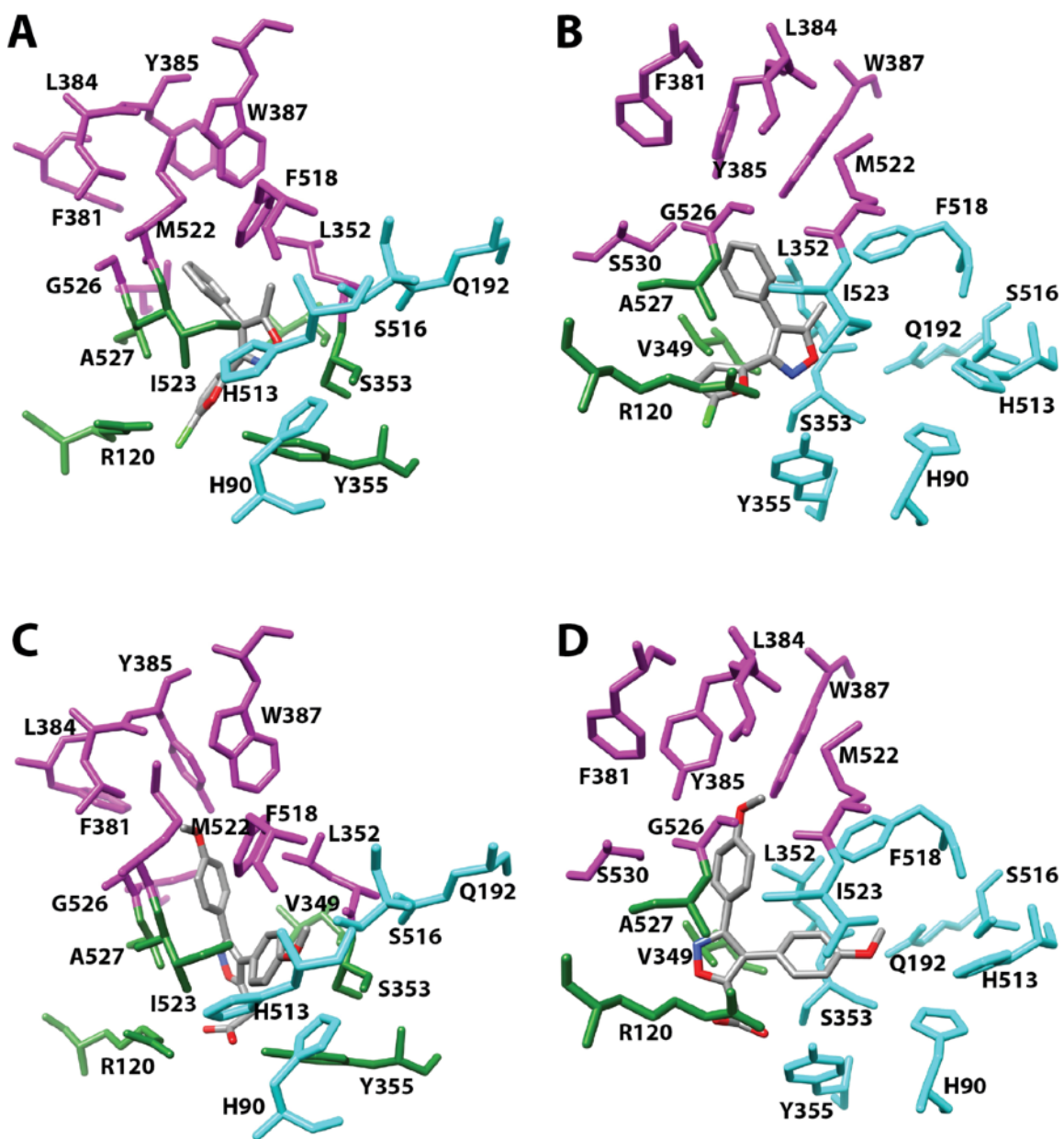


Figure S17. Structure of (A & B) P6 and (C & D) mofezolac bound in the cyclooxygenase active site of COX-1 and the side chains that make up the proximal binding pocket (green), the central binding pocket (magenta), and residues corresponding to the COX-2 side pocket (cyan). In (A) and (C), the residues are colored as in most previous figures. In (B) and (D), some residues in the proximal and central binding pockets that are shared with the COX-2 side pocket are colored cyan to highlight the interaction with the methoxybenzyl group of mofezolac and the absence of a significant interaction with the side pocket in the case of P6. From PDB #5U6X and #5WBE.

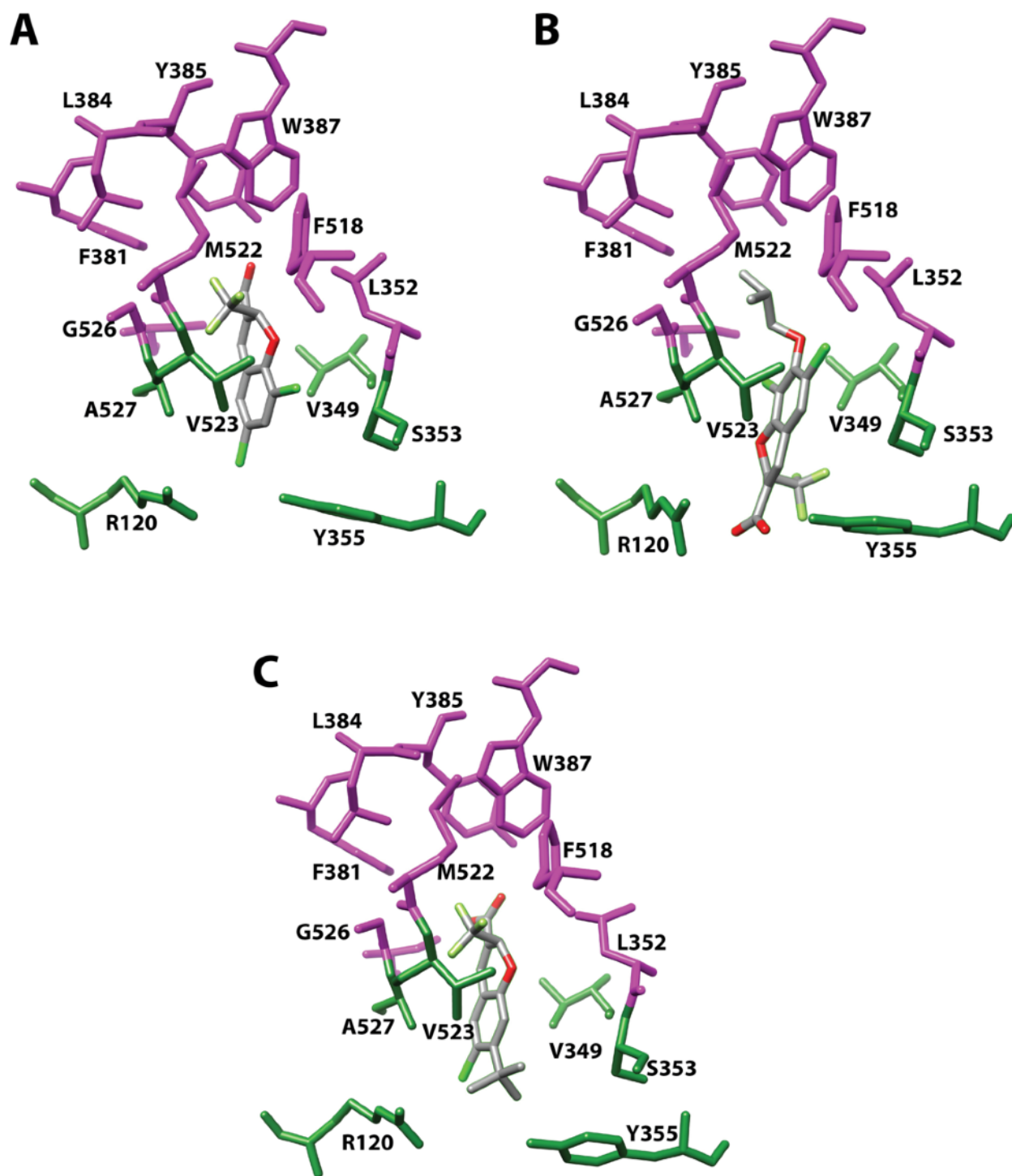


Figure S18. Structure of (A) (*S*)-5c, (B) (*R*)-23d, and (C) (*S*)-SC-75416 bound in the cyclooxygenase active site of COX-2 and the side chains that make up the proximal binding pocket (green) and the central binding pocket (magenta). From PDB #3LN0, #3NTG, and 3MQE.

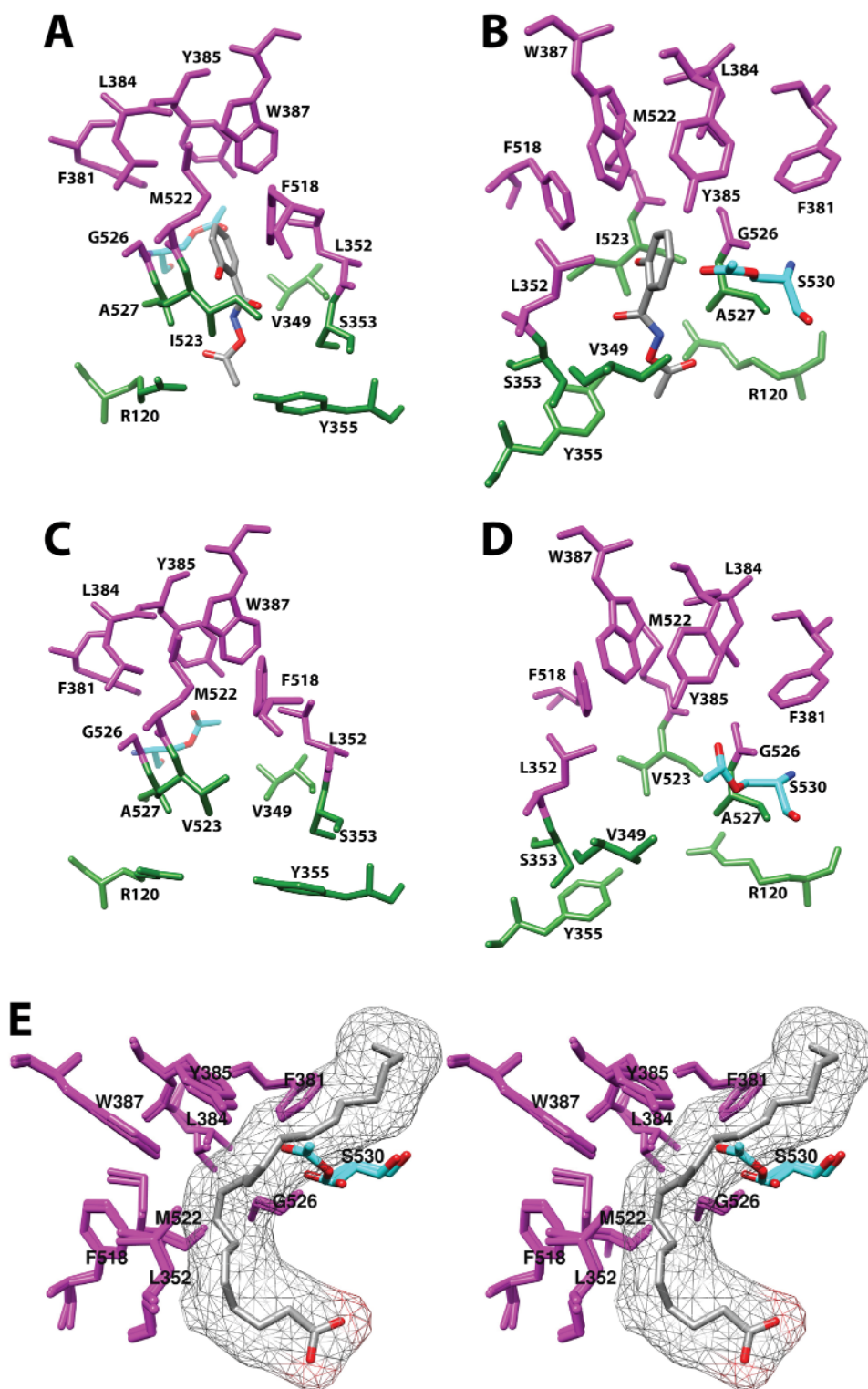


Figure S19. Structure of (A & B) acetylated COX-1 containing *O*-acetylsalicylhydroxamic acid bound in the cyclooxygenase active site and (C & D) acetylated COX-2. (E) Wall-eyed stereo view of the structure of acetylated COX-2 superimposed over the structure of the productive conformation of AA complexed with COX-2. AA is colored by atom, with its surface shown in mesh. The steric clash between AA and the acetyl group on Ser-530 can be readily seen. The side chains that make up the proximal binding pocket

(green, A-D) and the central binding pocket (magenta, A-E) are shown. The acetylated Ser-530 residue is colored by element on a cyan background. From PDB #1EBV and #5F19.

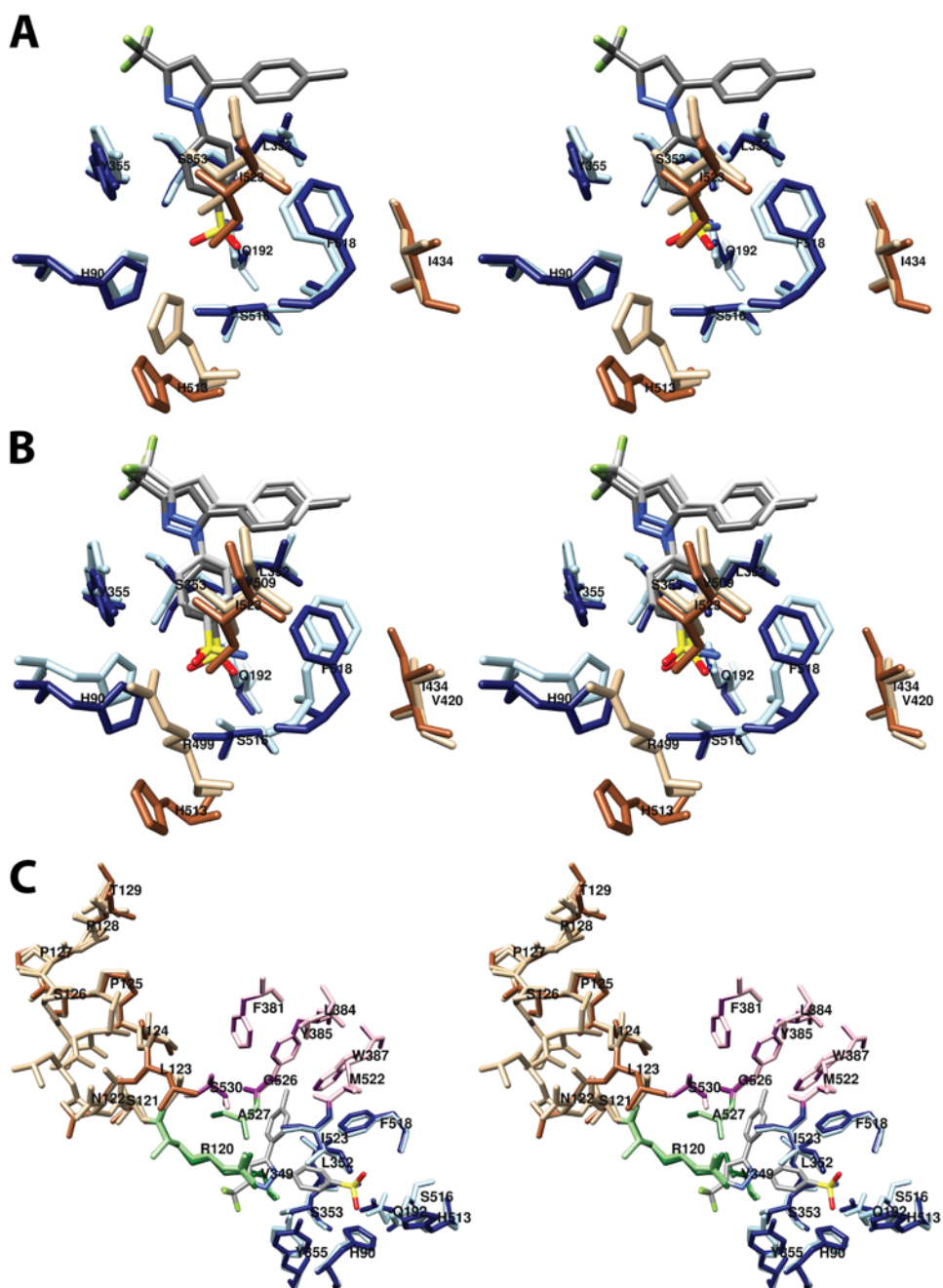


Figure S20. Wall-eyed stereo views of the structure of COX-1 complexed with celecoxib overlaid with (A) the structure of COX-1 complexed with (*S*)-flurbiprofen or (B) the structure of COX-2 complexed with celecoxib. Key residues making up the side pocket are shown in dark blue (COX-1-celecoxib complex) or light blue (alternative complexes). The residues that differ between COX-1 and COX-2 (Ile/Val-434, His/Arg-513, Ile/Val-523) are shown in sienna (COX-1-celecoxib complex) or tan (alternative complexes). Celecoxib is colored by heteroatom on a dark gray (COX-1-celecoxib complex) or light gray (COX-2-celecoxib complex) background. (*S*)-Flurbiprofen is not shown. Note that the numbering in the COX-2-celecoxib complex, for residues Val-434, His-513, and Val-523 use the actual COX-2 residue numbers of 420, 499, and 509, respectively, reflecting the numbers in the PDB file. (C) Wall-eyed stereo view of COX-1 complexed with celecoxib. The side chains that make up the proximal binding pocket (green), the central binding pocket (magenta), and the side pocket (blue) are shown. The structures of the two

subunits are overlaid with subunit A (containing celecoxib) shown in the darker colors. Also shown are residues 121-129, which exist in two conformations in subunit B depending on the presence or absence of bound celecoxib. Subunits containing inhibitor exhibit the same conformation as is observed in subunit A (sienna), whereas those lacking inhibitor diverge between Ser-121 and Pro-125. From PDB #3KK6, #1EHQ, and #3LN1.

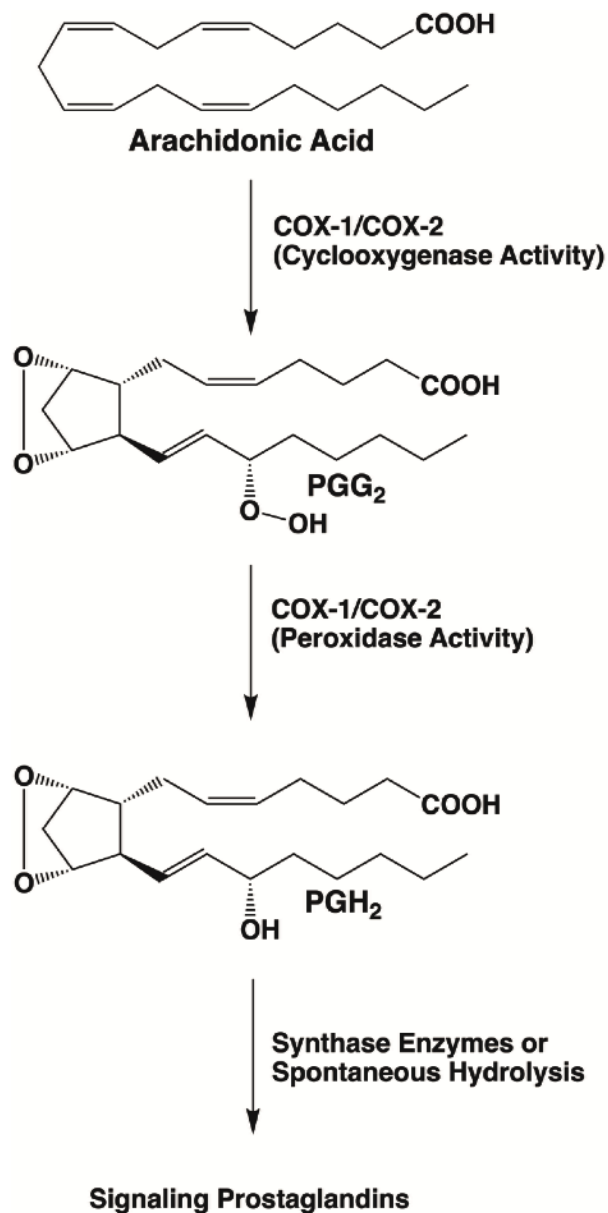


Figure 1. Prostaglandin (PG) biosynthetic pathway. *Bis*-dioxygenation and cyclization of arachidonic acid at the cyclooxygenase active site of COX-1 or COX-2 yields PGG₂. Reduction of the 15-hydroperoxyl group of PGG₂ at the peroxidase active site of COX-1 or COX-2 yields PGH₂. PGH₂ serves as substrate for five different synthases, producing four signaling PG products (PGE₂, PGI₂, PGF_{2α}, PGD₂) or thromboxane A₂ (TXA₂). PGH₂ is chemically unstable under physiological conditions, and in the absence of the synthase enzymes, it is hydrolyzed to a mixture of PGE₂ and PGD₂.

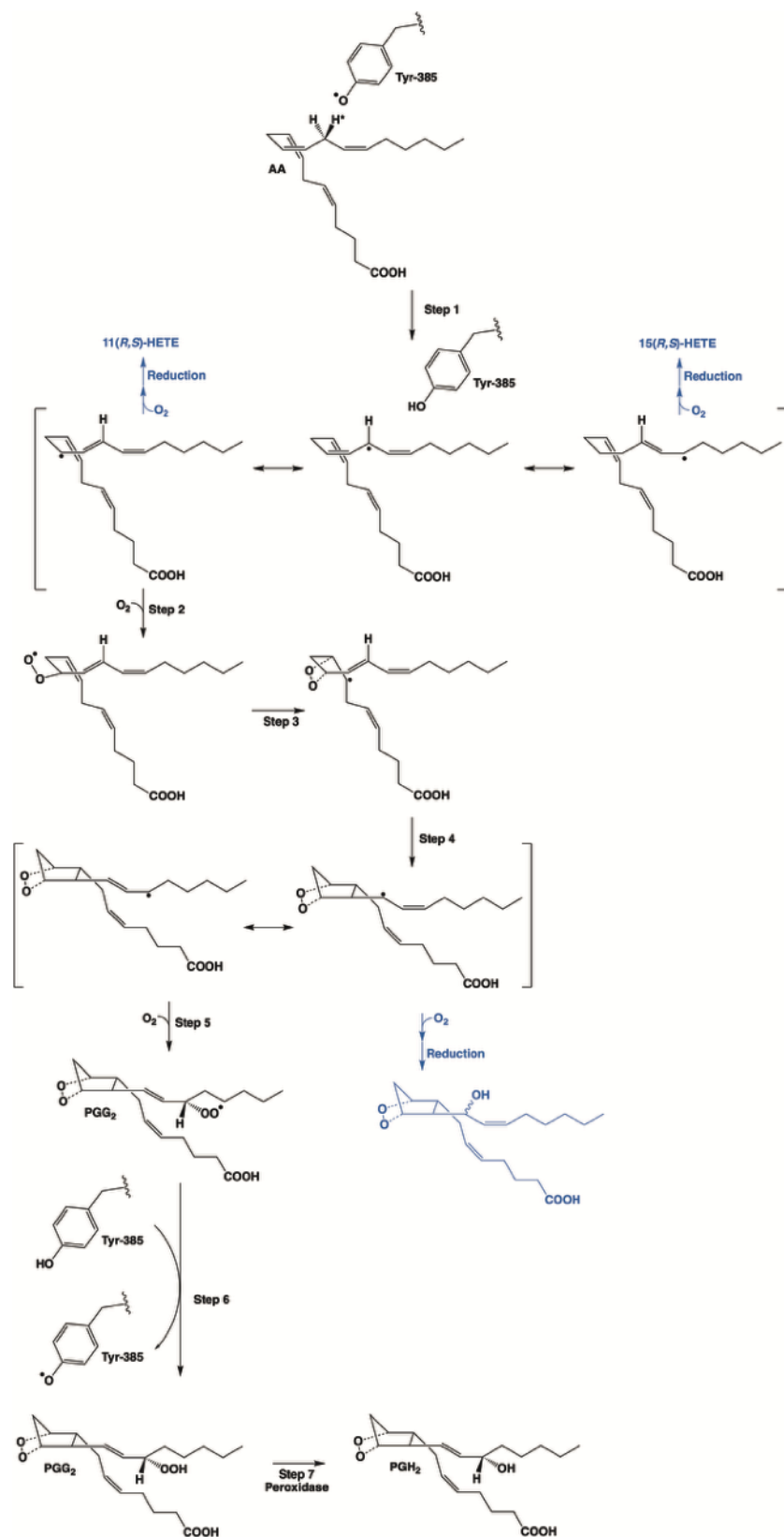


Figure 2. Proposed mechanism of the cyclooxygenase reaction. Activation of the COX enzymes occurs through oxidation of the heme prosthetic group during reduction of a peroxide substrate at the peroxidase

active site. Transfer of an electron from Tyr-385 in the cyclooxygenase active site to the heme then generates the catalytic tyrosyl radical. Step 1: The tyrosyl radical abstracts the 13-(*pro*)-*S*-hydrogen atom (indicated by an asterisk) from AA. Resonance places the unpaired electron at carbon-13, carbon-11, or carbon-15. Addition of oxygen at the carbon-11 or carbon-15 radical, followed by enzymatic or nonenzymatic reduction results in the 11(*R,S*)-HETE or 15(*R,S*)-HETE minor products (indicated in blue), respectively. Step 2: Antarafacial oxygen addition occurs at carbon-11. Step 3: The peroxy group then attacks carbon-9, forming the endoperoxide ring and placing the unpaired electron at carbon-8. Step 4: Bond formation between carbon-8 and carbon-12 generates the five-membered ring of PGG₂ and places the unpaired electron on carbon-13. Resonance enables migration of the unpaired electron to carbon-15. Step 5: Attack of oxygen at carbon-15 follows, generating a peroxy radical at that position. Step 6: Transfer of a hydrogen atom from Tyr-385 reduces the peroxy radical to a hydroperoxide, yielding PGG₂, and regenerates the tyrosyl radical for a new round of catalysis. Step 7: Reduction of PGG₂ at the peroxidase active site yields PGH₂. Alternatively, attack of oxygen at carbon-13 rather than carbon-15 in step 5 followed by enzymatic or nonenzymatic reduction leads to a PGH₂ analog with the hydroxyl group at carbon-13 (shown in blue). Note that the overall mechanism requires a peroxidase turnover to produce the catalytic tyrosyl radical, but once this has occurred, the cyclooxygenase reaction is self-perpetuating.

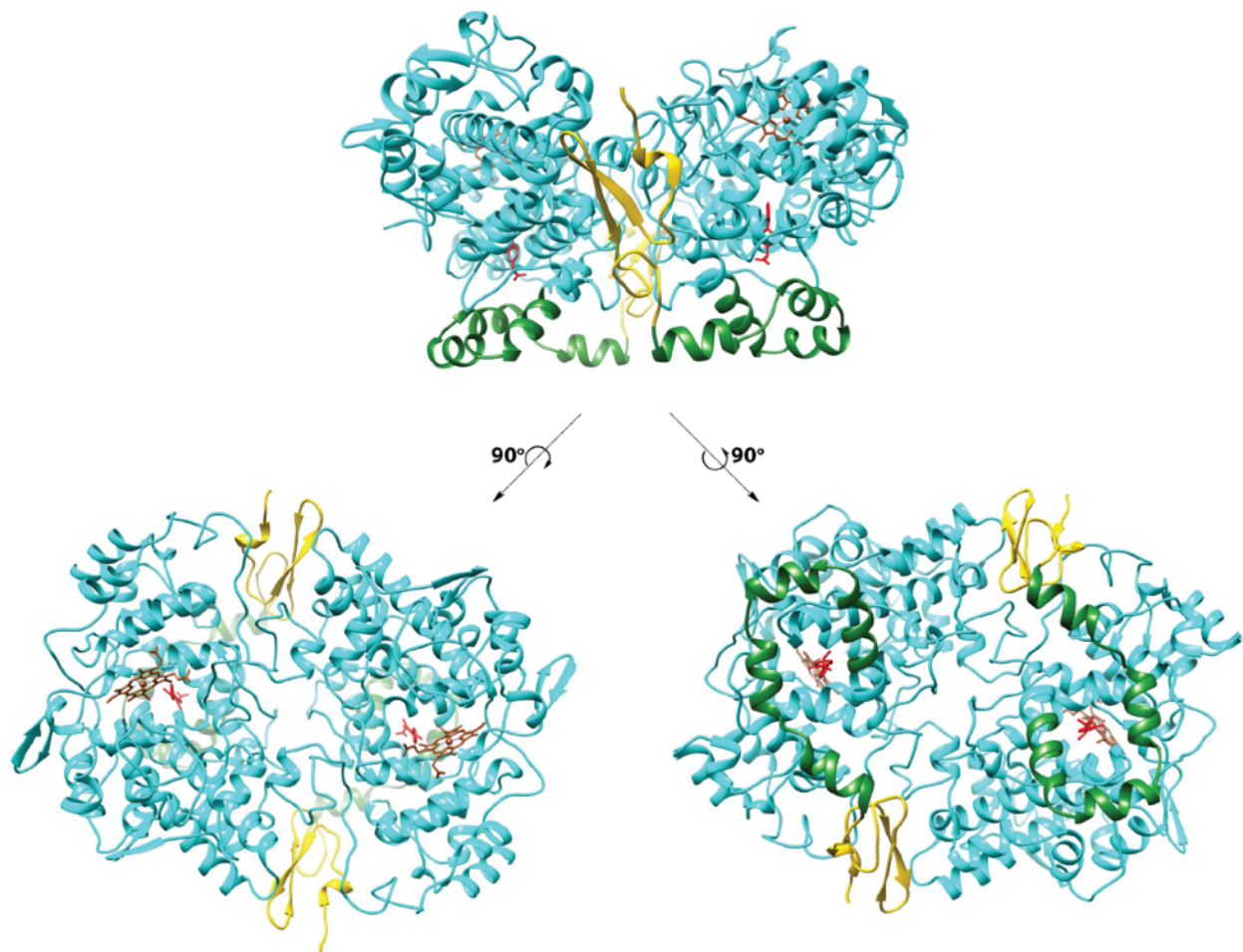


Figure 3. Domain structure of the cyclooxygenases. The top view shows the dimeric protein (COX-1) as observed from the side (i.e., parallel to the plane of the membrane). Each of the bottom views follows rotation of the top view by 90°. To the left, the protein is viewed looking down on the enzyme from above. To the right, the protein is viewed looking up from below. In all cases, the epidermal growth factor domain is gold, the membrane-binding domain is green, the catalytic domain is cyan, heme is sienna, and the flurbiprofen ligand is red. The membrane-binding domain inserts into the top leaflet of the underlying membrane bilayer. From PDB #1CQE.

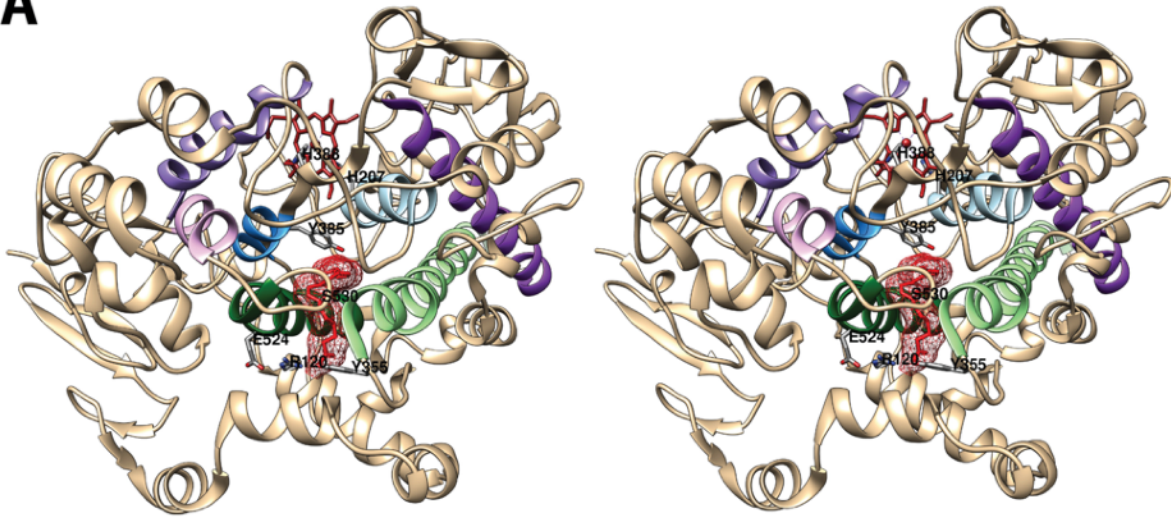
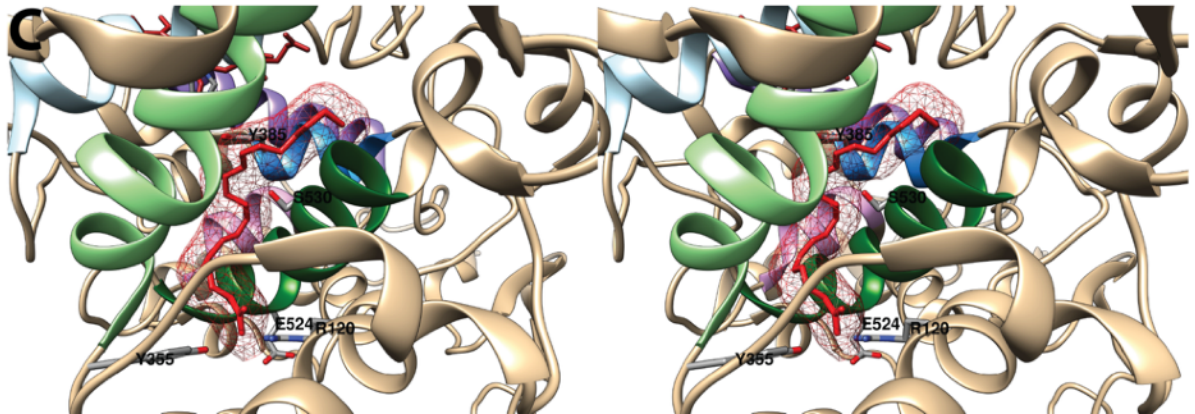
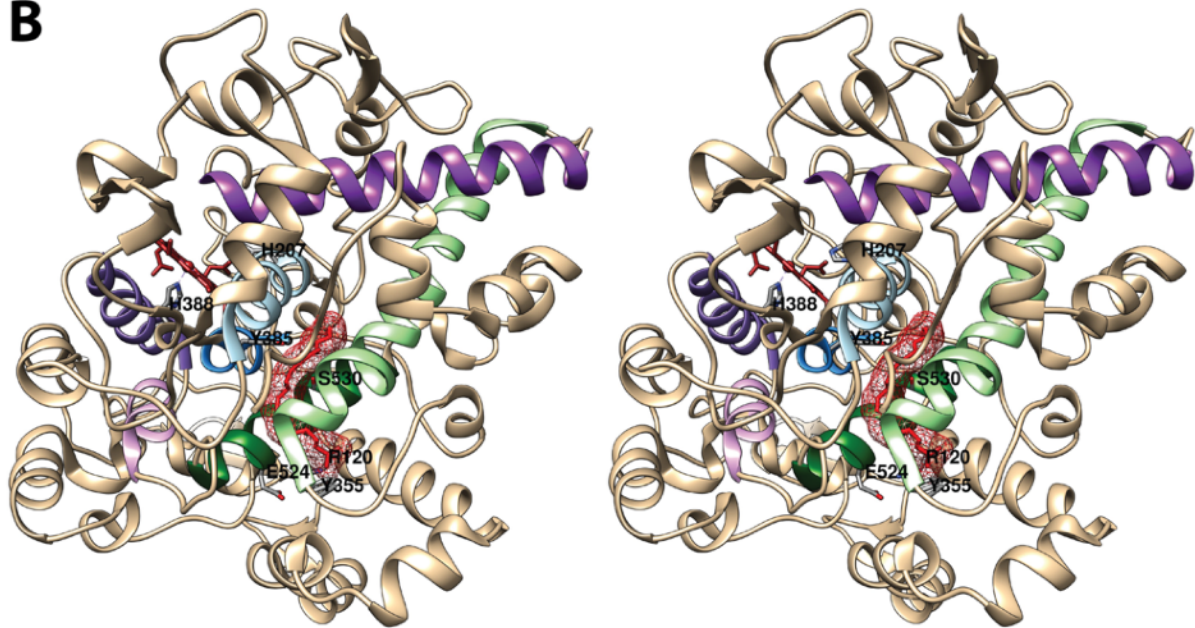
A**B**

Figure 4. Structure of the cyclooxygenase active site. Two Cross-eyed stereo views of the COX-1 monomer (A and B) and a close-up view of the cyclooxygenase active site (C) are shown as observed

from the side (i.e., parallel to the plane of the membrane). In all cases, Co³⁺-protoporphyrin IX (an inactive heme analog) is dark brown, and AA is red mesh. The side chains of the constriction residues (Arg-120, Tyr-355, and Glu-524) are displayed and labeled, as are the catalytic residue (Tyr-385) and the target of aspirin-mediated inactivation (Ser-530), which are located at the bend of the L-shaped channel. In A and B, His-388, the proximal heme ligand, and His-207, which serves as the distal heme ligand through a coordinating water molecule, are visible. Helices 2 (residues 195-207, light blue), 8 (residues 378-385, medium blue), 6 (residues 324-354, light green), and 17 (residues 519-535, dark green), which surround the active site, along with helices 5 (residues 295-320, dark purple), 11/12 (residues 444-459, medium purple), and 16 (residues 503-510, light purple) form a bundle that is conserved among a number of peroxidases, with helices 2, 5, 6, 8, and 11/12 involved in binding the heme prosthetic group. From PDB #1DIY.

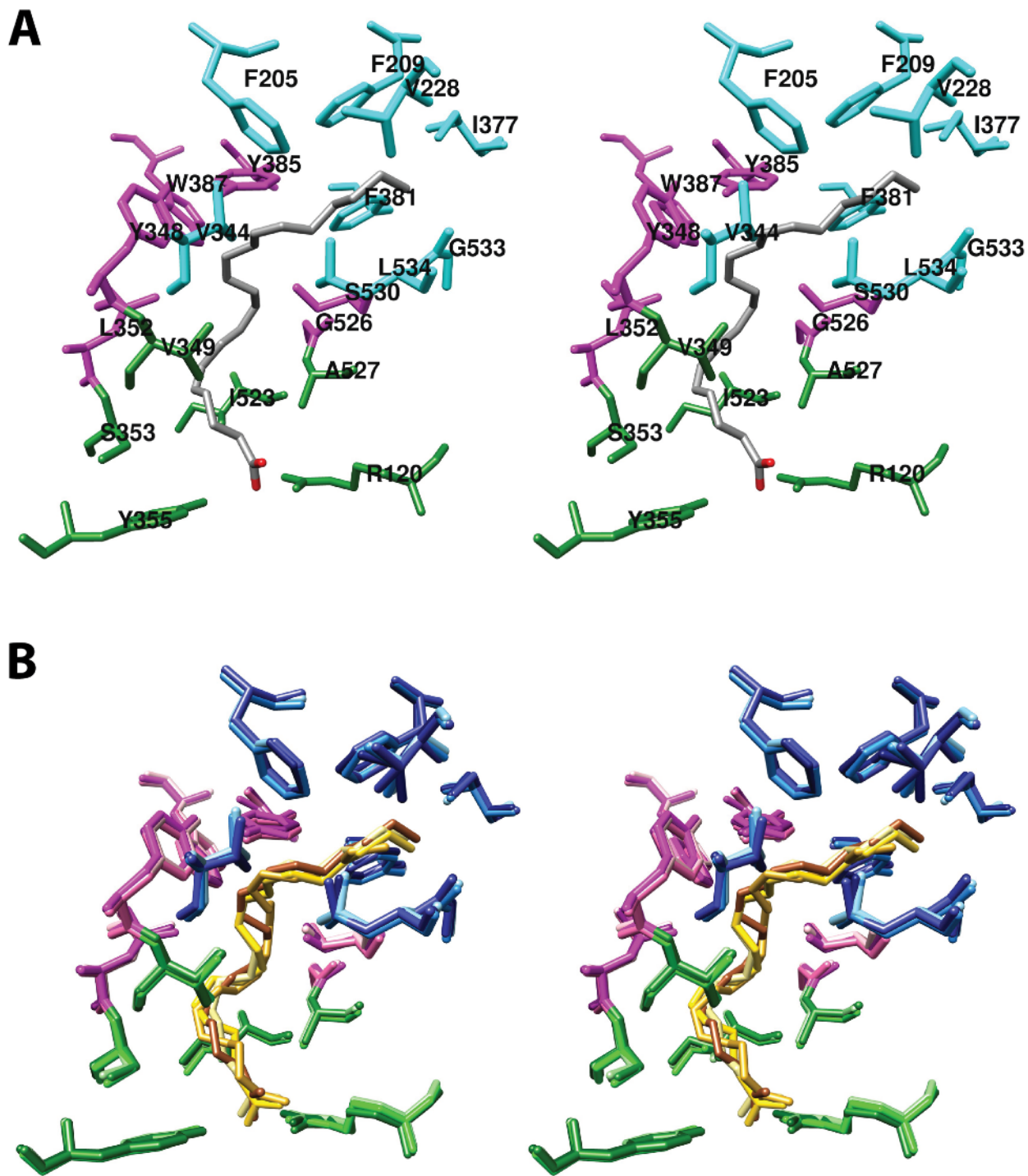


Figure 5. (A) Cross-eyed stereo view of AA bound in the cyclooxygenase active site of COX-1 and the side chains that make up the proximal binding pocket (green), the central binding pocket (magenta), and the distal binding pocket (cyan). This view is similar to that used to depict most structures of fatty acids in complex with COX-1 or COX-2 throughout the review. (B) Cross-eyed stereo view of an overlay of the structures of four fatty acids in the active site of COX-1. Fatty acids and amino acid side chains are colored from lightest to darkest in the order LA, DHLA, EPA, and AA. Notable is the minimal movement of active site residues to accommodate the structural differences among the various fatty acids. Monoscopic

views of the individual structures are provided in Figure S1. From PDB #1DIY (A & B) and #1IGZ, #1FE2, and #1IGX (B only).

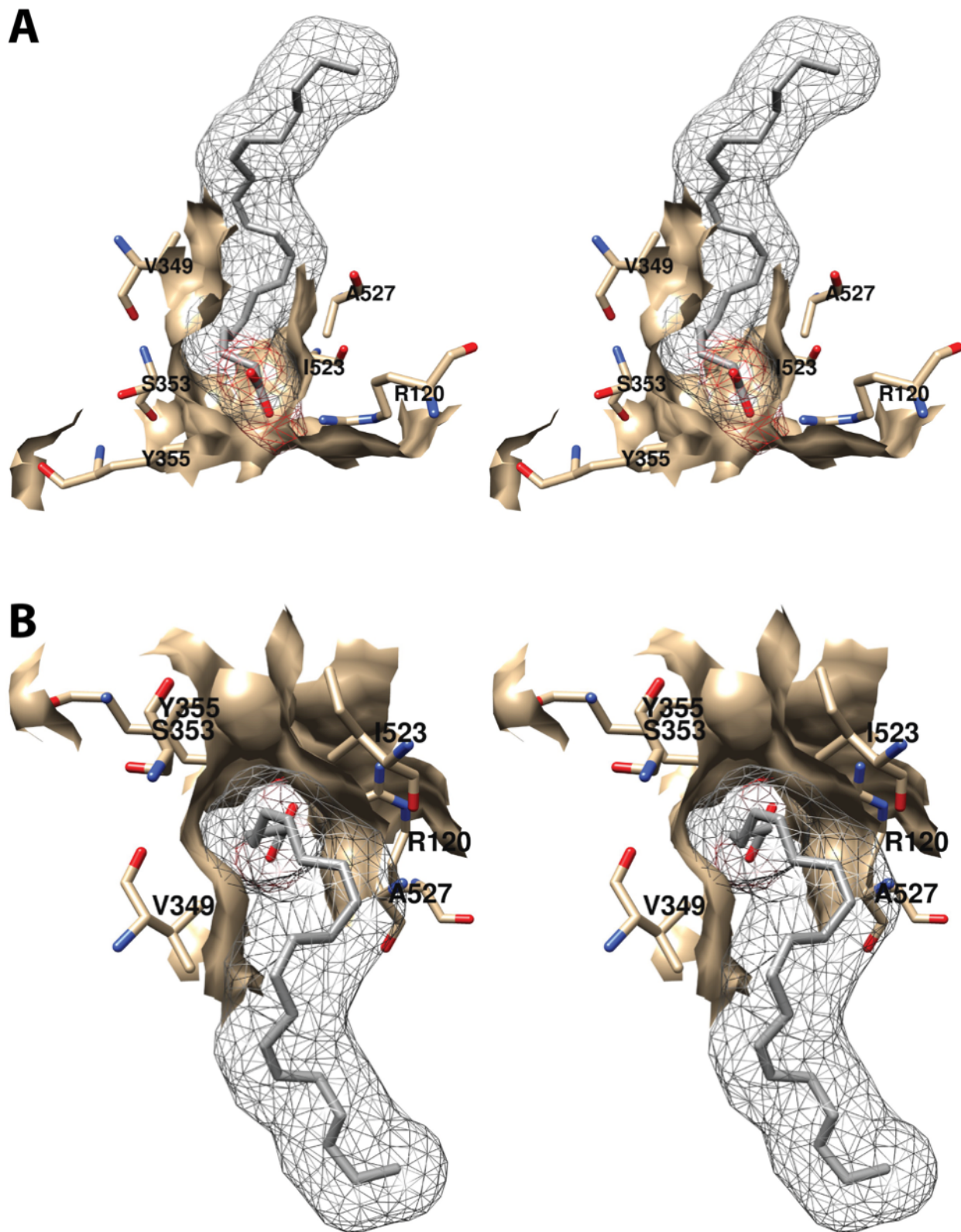


Figure 6. Cross-eyed stereo view of the proximal AA binding pocket as observed from the side (i.e., parallel to the plane of the membrane) (A) or looking downward toward the membrane from above (B). AA

is colored by element, and its surface is shown as a mesh. Side chains of the residues comprising the pocket are displayed, and their surface is shown in solid tan. From PDB #1DIY.

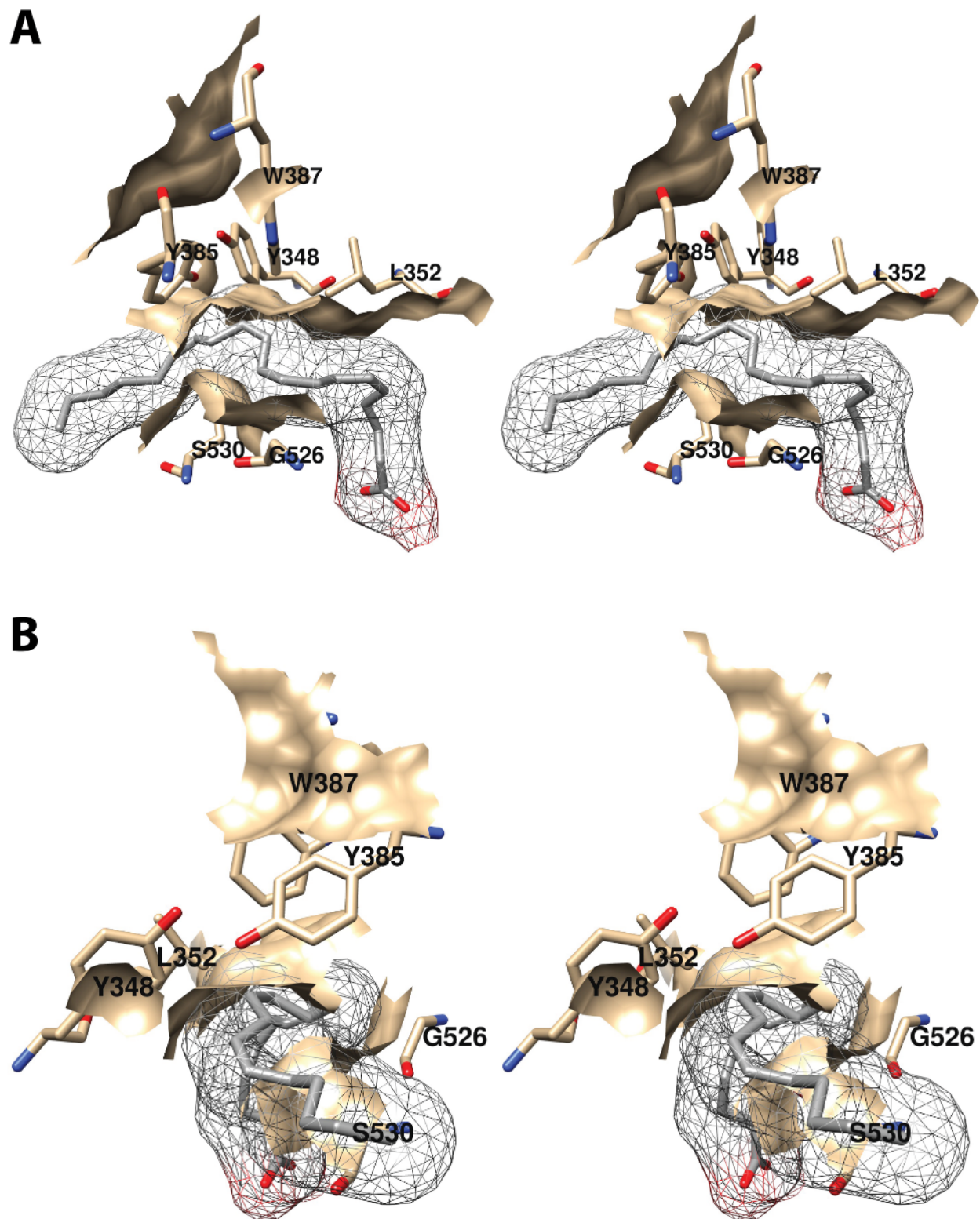


Figure 7. Cross-eyed stereo view of the central AA binding pocket as observed from the side (i.e., parallel to the plane of the membrane) (A) or looking along the axis of the pocket (B). AA is colored by element,

and its surface is shown as a mesh. Side chains of the residues comprising the pocket are displayed, and their surface is shown in solid tan. From PDB #1DIY.

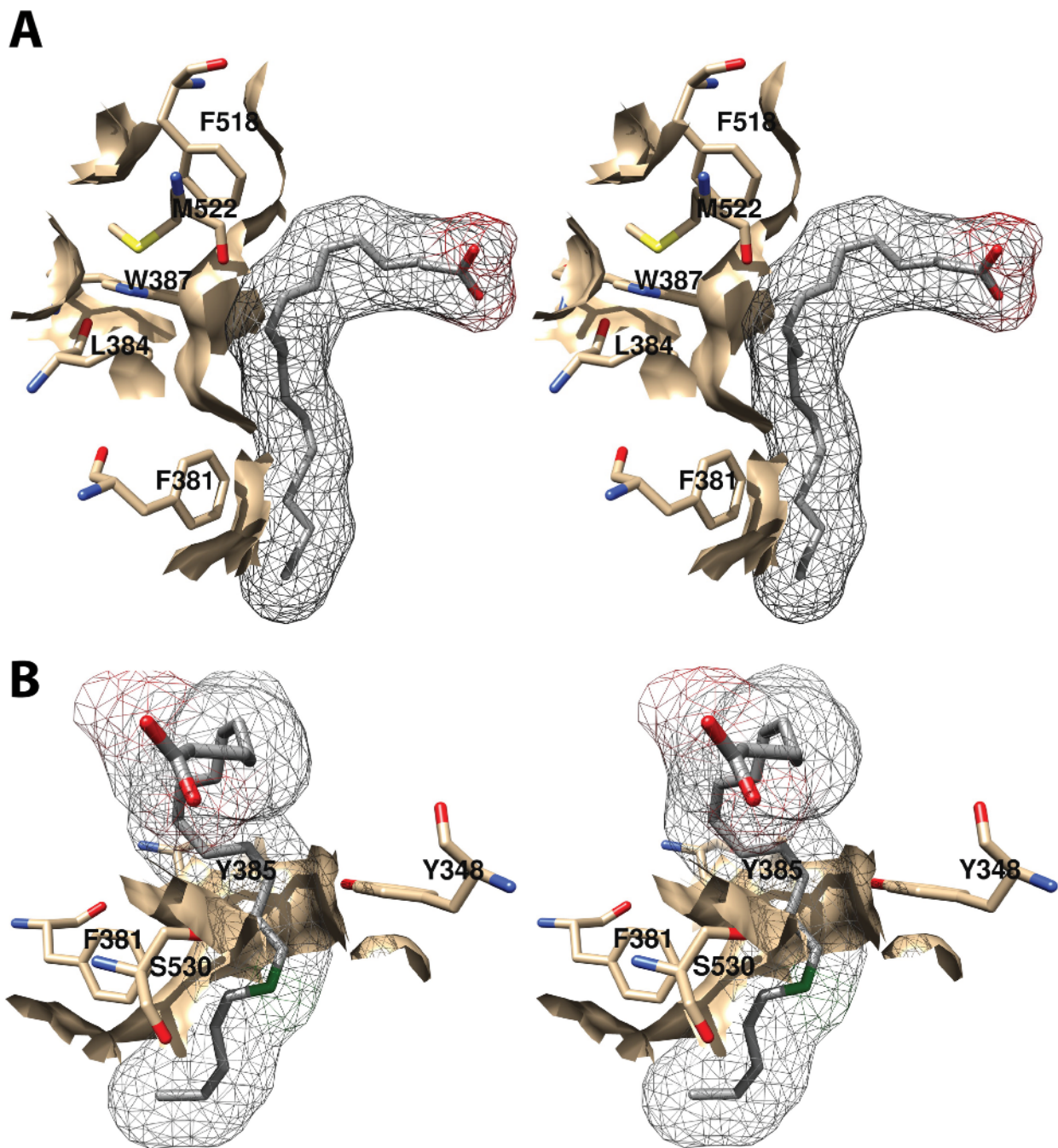


Figure 8. Cross-eyed stereo view of AA bound to the active site of COX-1. (A) A pocket formed by Phe-381, Leu-384, Trp-387, Phe-518, and Met-522 provides space for formation of the endoperoxide ring. (B) Tyr-348, Phe-381, Tyr-385, and Ser-530 surround carbon-15 of AA (green) dictating the orientation of oxygen addition at this site. AA is colored by element (with the exception of carbon-15 in B), and its surface is shown as a mesh. Side chains of the residues indicated are displayed, and their surface is shown in solid tan. From PDB #1DIY.

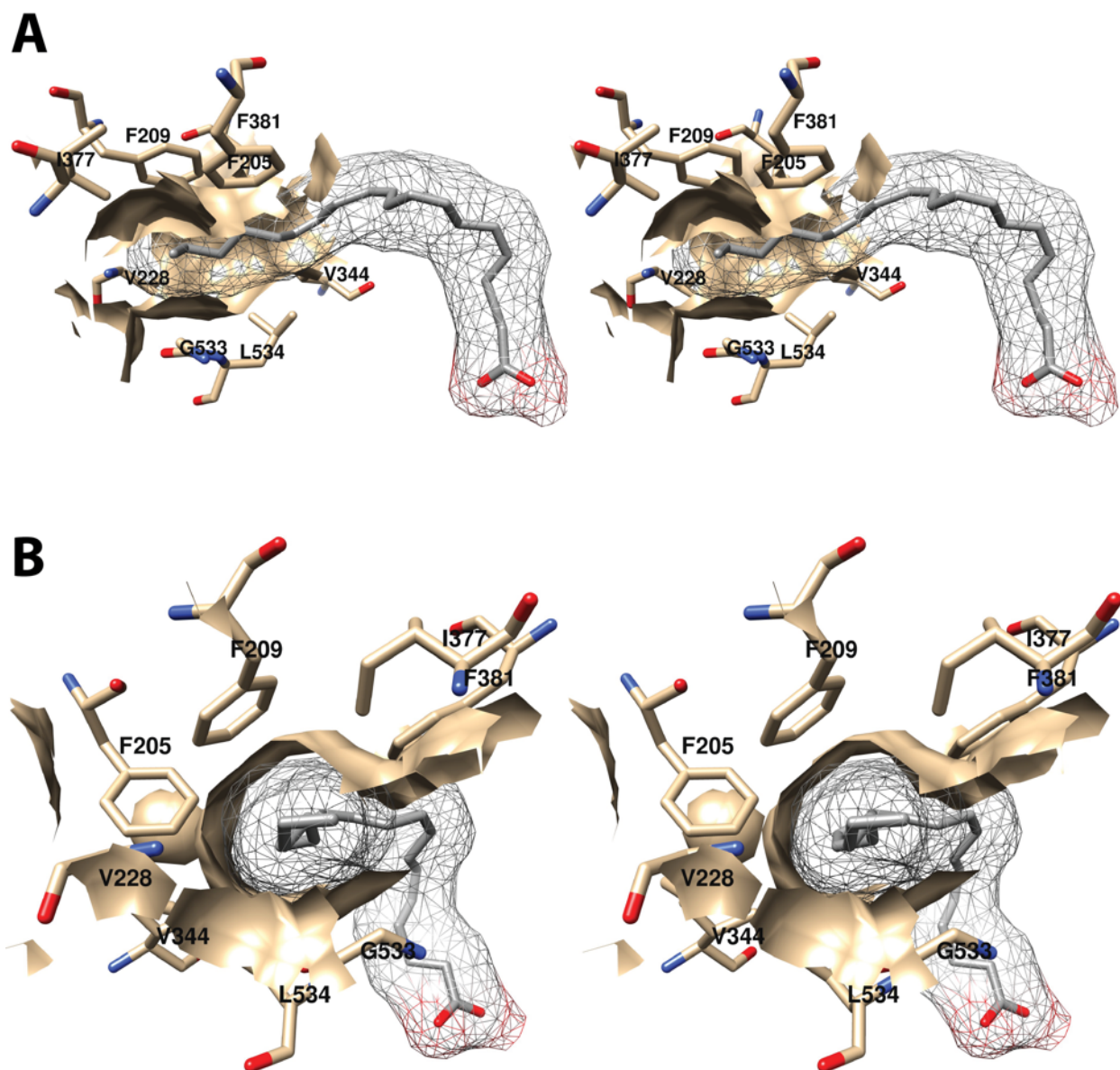


Figure 9. Cross-eyed stereo view of the distal AA binding pocket as observed from the side (i.e., parallel to the plane of the membrane) (A) or looking along the axis of the pocket (B). AA is colored by element, and its surface is shown as a mesh. Side chains of the residues comprising the pocket are displayed, and their surface is shown in solid tan. From PDB #1DIY.

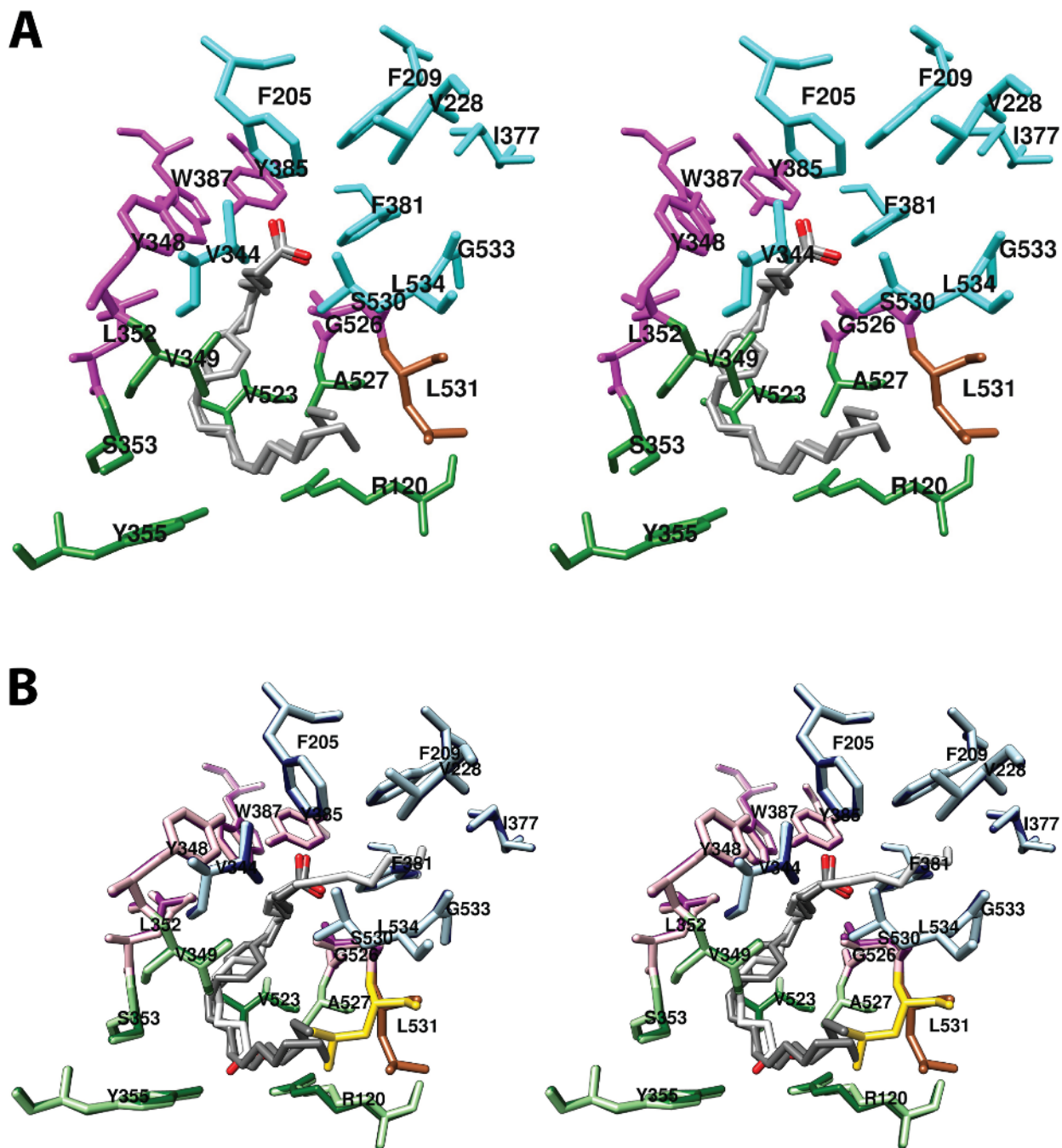


Figure 10. (A) Cross-eyed stereo view of the structure of AA (nonproductive conformation) bound in the cyclooxygenase active site of COX-2 and the side chains that make up the proximal binding pocket (green), the central binding pocket (magenta), and the distal binding pocket (cyan). Note that AA is observed in two slightly different conformations. (B) Wall-eyed stereo view of an overlay of the structures of the nonproductive (dark gray) and productive (light gray) conformations of AA bound in the cyclooxygenase active site. Residues in the surrounding binding pockets are colored similarly to those in (A) with the lighter and darker colors corresponding to the productive and nonproductive conformations, respectively. Also shown is the marked difference in the position of Leu-531 between the productive conformation (gold) and the nonproductive conformation (sienna). From PDB #3HS5. Figure 10. Cross-

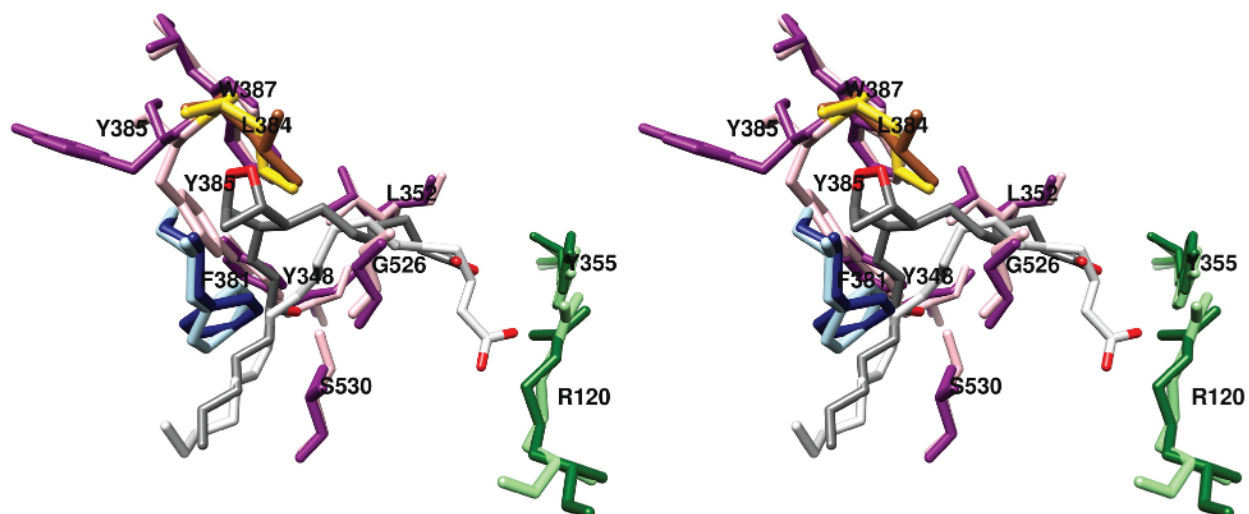


Figure 11. Wall-eyed stereo view of the structure of PGG₂/H₂ overlaid with that of AA (productive conformation) bound in the active site of COX-2. Side chains that make up the central binding pocket are shown (light and dark magenta), as are Leu-384 (gold and sienna), proximal binding pocket residues Arg-120 and Tyr-355 (light and dark green), and distal binding pocket residue Phe-381 (dark and light blue). PGG₂ (dark gray) and AA (light gray) are colored by heteroatom. In the case of residue side chains, the darker and lighter colors denote positions in the complexes containing PGG₂/H₂ and AA, respectively. The major shift in the position of Tyr-385 is readily apparent, as is the upward shift in the position of the carboxyl group of PGG₂ relative to that of AA. These displacements are enabled by the absence of heme and likely would not occur in the holoenzyme. From PDB #3HS5 (chain B) and #1DDX.

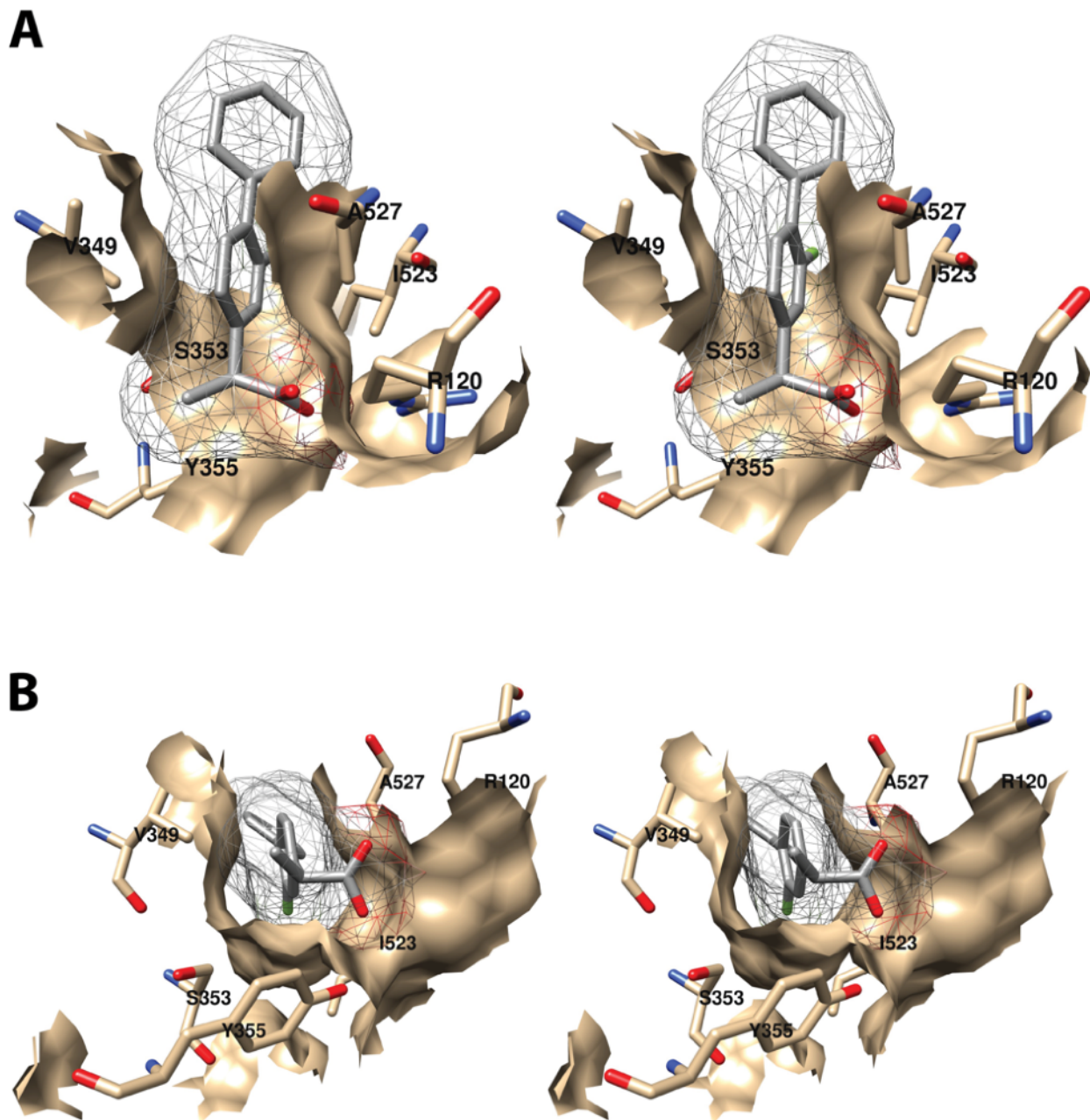


Figure 12. Cross-eyed stereo view of the interaction of the proximal inhibitor binding pocket with (*S*)-flurbiprofen as observed from the side (i.e., parallel to the plane of the membrane) (A) or looking upward from the membrane (B). (*S*)-Flurbiprofen is colored by element, and its surface is shown as a mesh. Side chains of the residues comprising the pocket are displayed, and their surface is shown in solid tan. From PDB #1EQH.

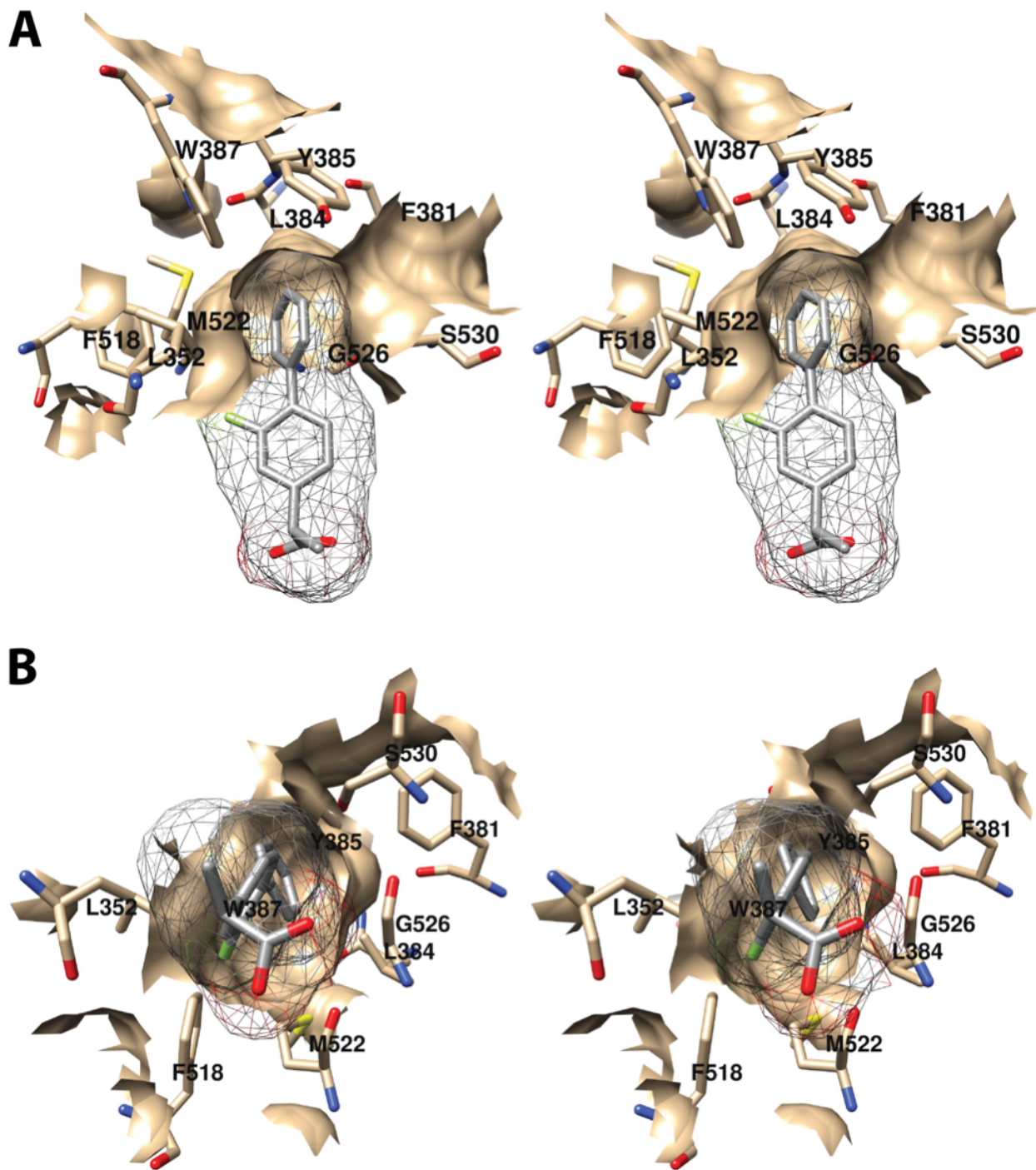


Figure 13. Wall-eyed stereo view of the interaction of the central inhibitor binding pocket with (*S*)-flurbiprofen as observed from the side (i.e., parallel to the plane of the membrane) (A) or looking upward from the membrane (B). (*S*)-Flurbiprofen is colored by element, and its surface is shown as a mesh. Side chains of the residues comprising the pocket are displayed, and their surface is shown in solid tan. From PDB #1EQH.

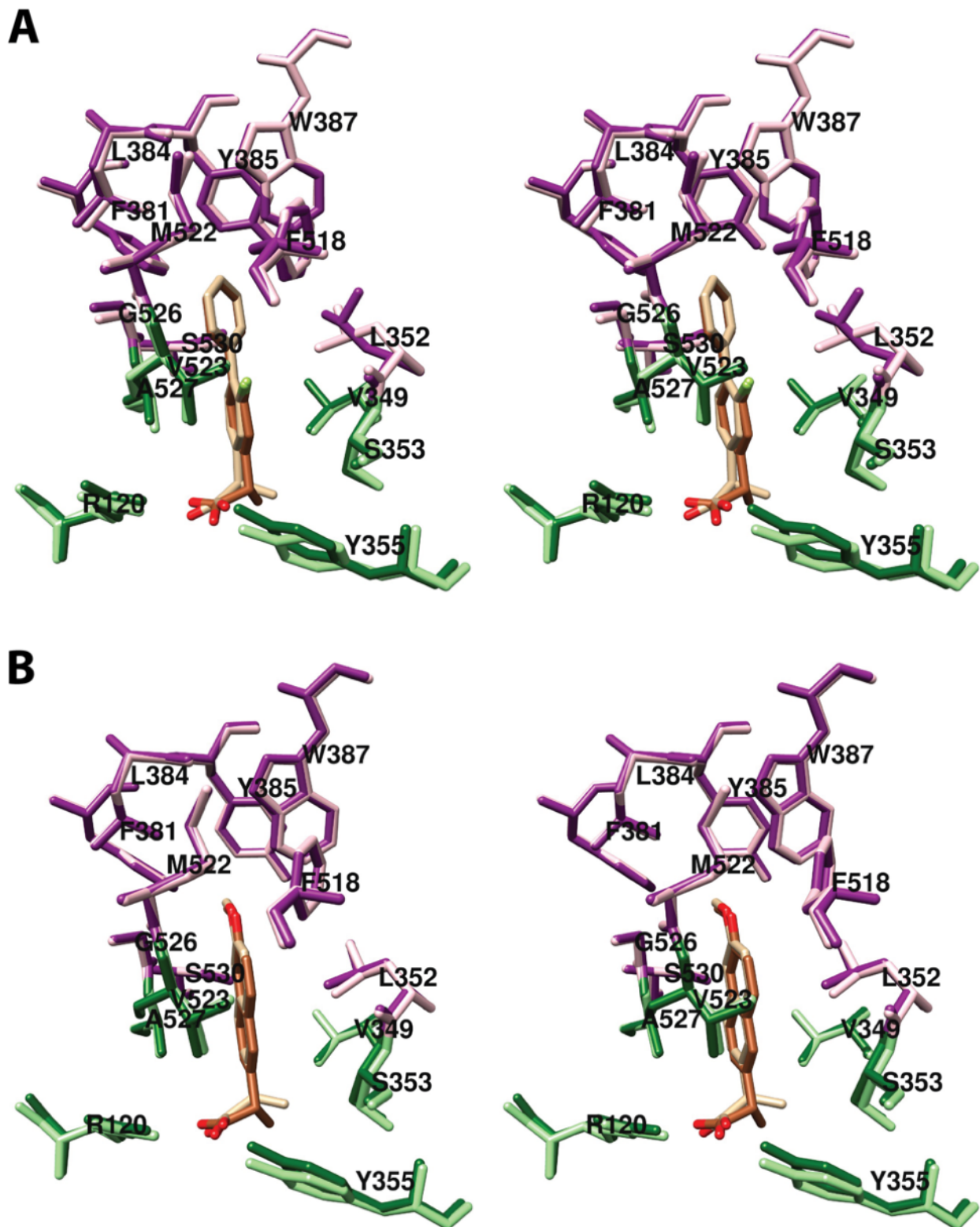


Figure 14. Cross-eyed stereo views of overlays of the structures of (A) (*R*)- and (*S*)-flurbiprofen and (B) (*R*)- and (*S*)-naproxen, bound in the cyclooxygenase active site of COX-2 and the side chains that make up the proximal binding pocket (light/dark green) and the central binding pocket (pink/magenta). In each case, structures related to the (*R*)-enantiomer (tan) are shown in the lighter color and those related to the

(S)-enantiomer (sienna) are shown in the darker color. From PDB #3PGH and #3RR3 (A) and PDB #3NT1 and #3Q7D (B).

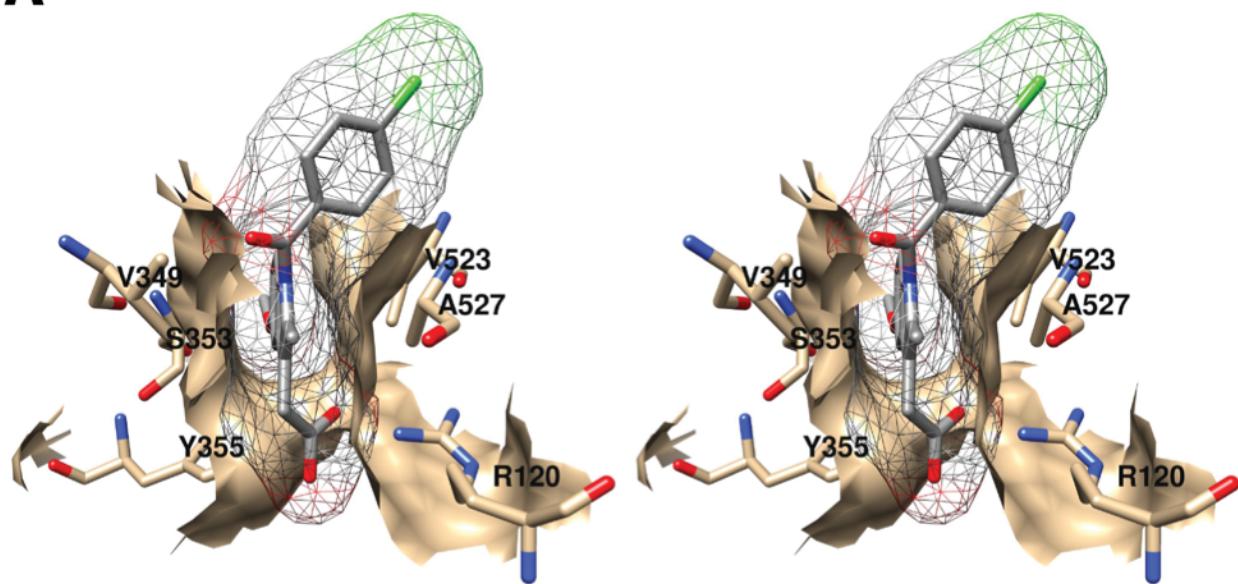
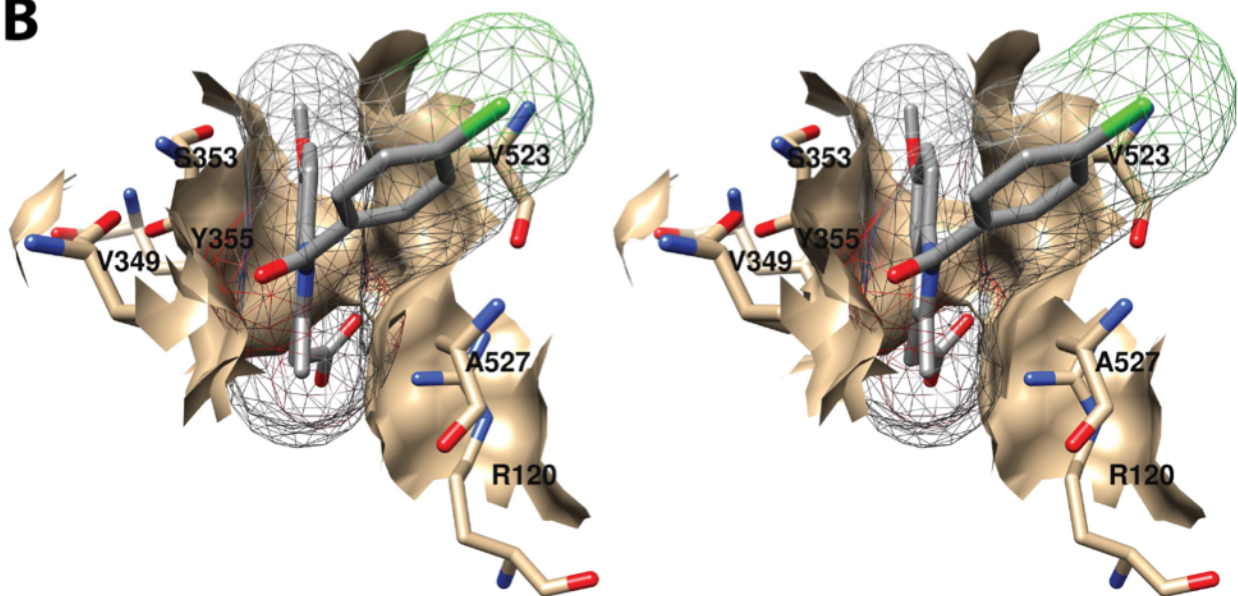
A**B**

Figure 15. Cross-eyed stereo view of the interaction of the proximal inhibitor binding pocket with indomethacin as observed from the side (i.e., parallel to the plane of the membrane) (A) or from above (B). Indomethacin is colored by element, and its surface is shown as a mesh. Side chains of the residues comprising the pocket are displayed, and their surface is shown in solid tan. From PDB #4COX.

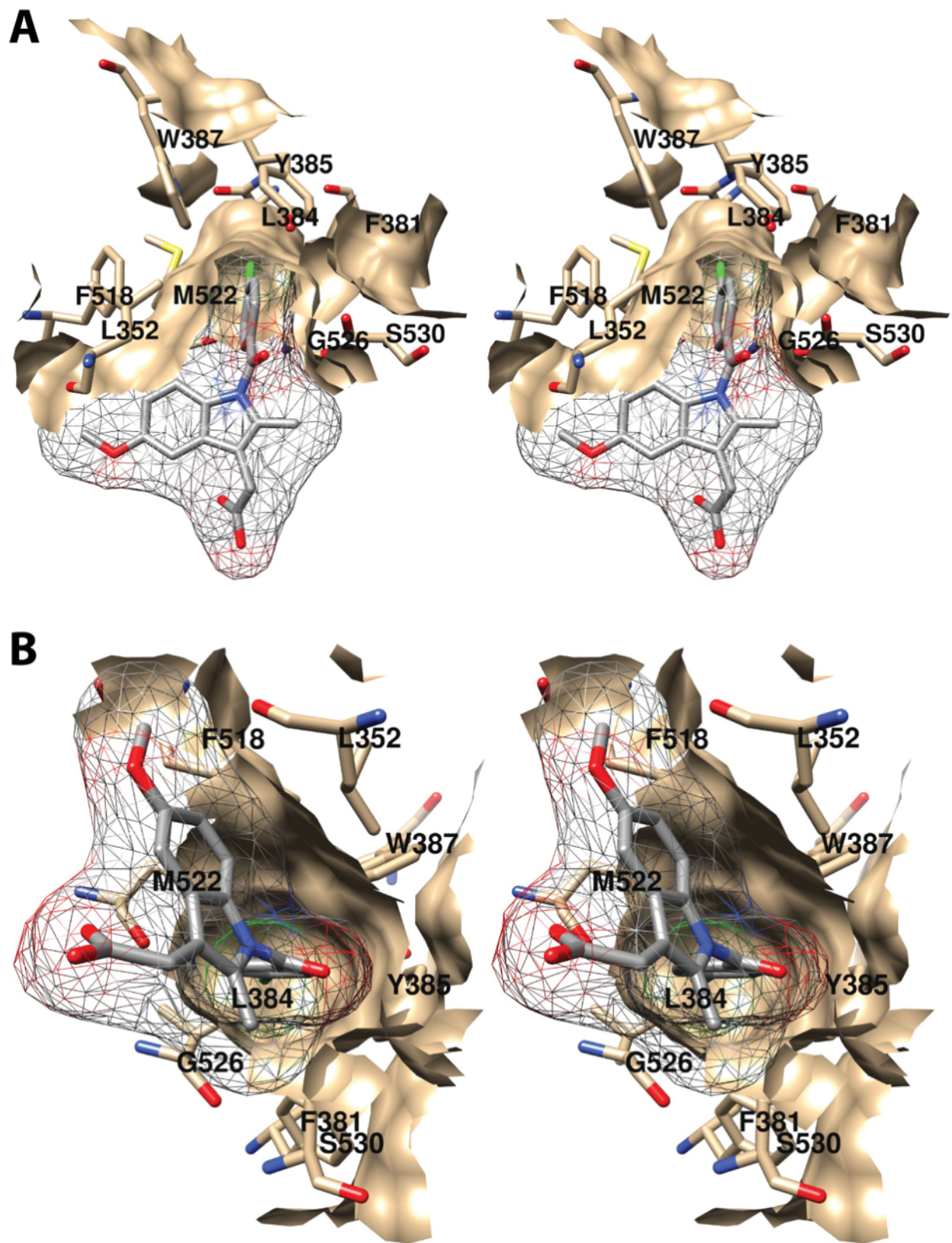


Figure 16. Cross-eyed stereo view of the interaction of the central inhibitor binding pocket with indomethacin as observed from the side (i.e., parallel to the plane of the membrane) (A) or looking

upward from the membrane (B). Indomethacin is colored by element, and its surface is shown as a mesh. Side chains of the residues comprising the pocket are displayed, and their surface is shown in solid tan. From PDB #4COX.

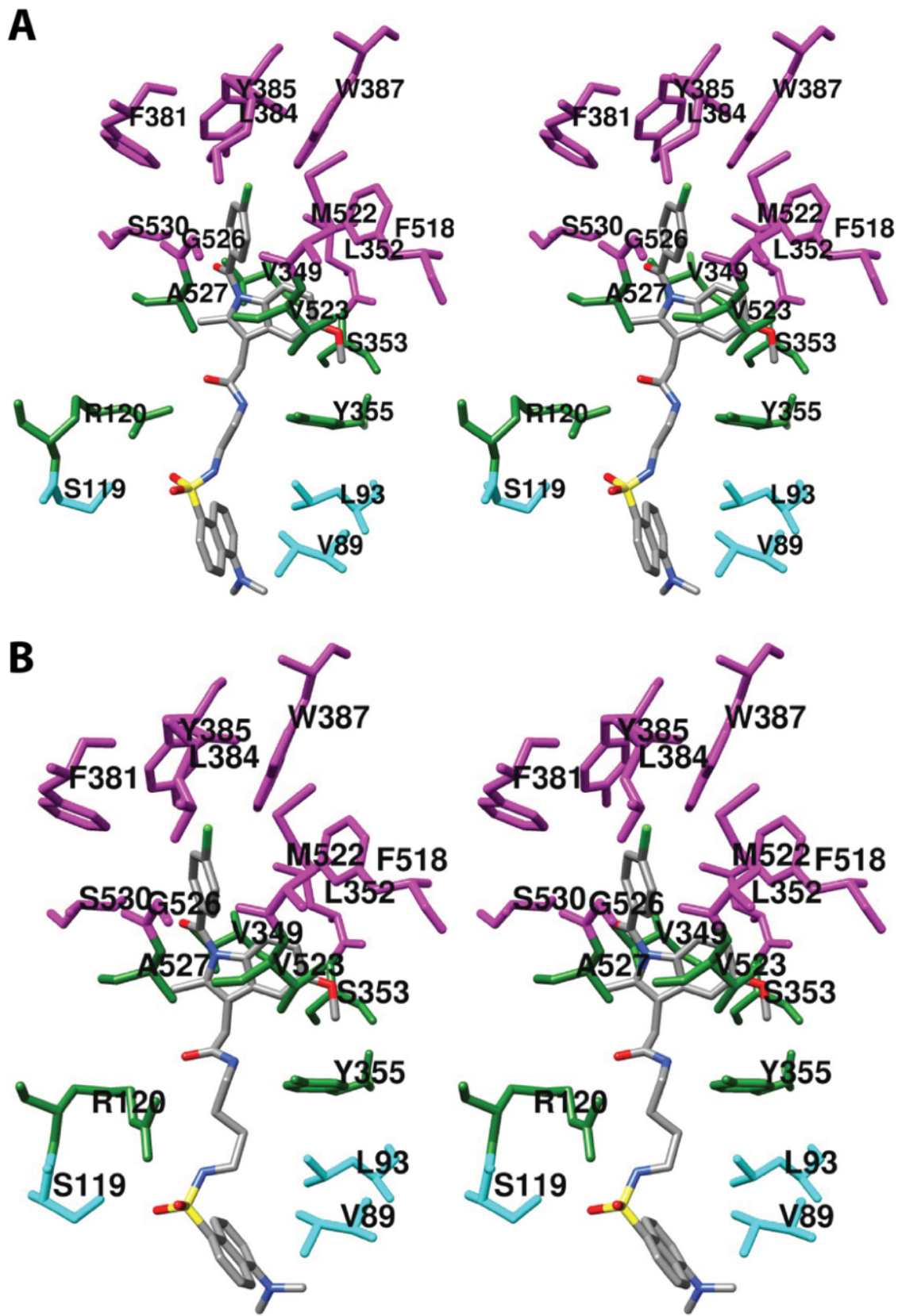


Figure 17. Cross-eyed stereo views of the structure of (A) indomethacin-dansyl conjugate 1 and (B)

indomethacin-dansyl conjugate 2 bound in the cyclooxygenase active site of COX-2. The side chains that make up the proximal binding pocket (green), the central binding pocket (magenta), and membrane-binding domain residues that interact with the dansyl moiety (cyan) are shown. From PDB #6BL4 (A) and #6BL3 (B).

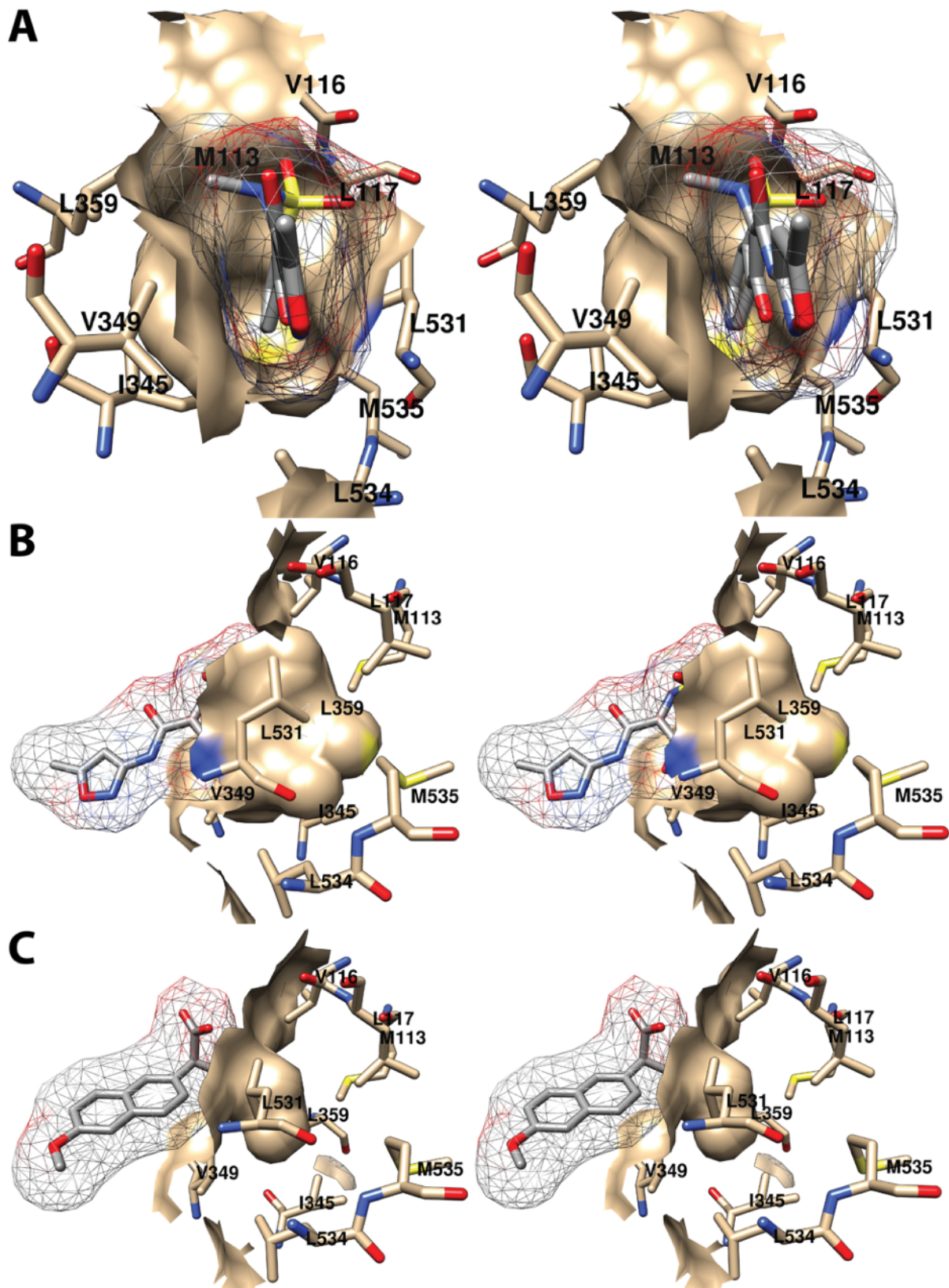


Figure 19. (A) Cross-eyed stereo view of the interaction of the oxycam binding pocket with isoxicam as observed from the side (i.e., parallel to the plane of the membrane), and comparison of the size of the

oxicam binding pocket (B) with the comparable region in the structure of COX-2 complexed to naproxen (C). The difference in the position of Leu-531 is clearly visible, as is the marked difference in the size of the pockets between the two complexes. Isoxicam and naproxen are colored by element, and their surface is shown as a mesh. Side chains of the residues comprising the pocket are displayed, and their surface is shown in solid tan. From PDB #4M10 and #3NT1.

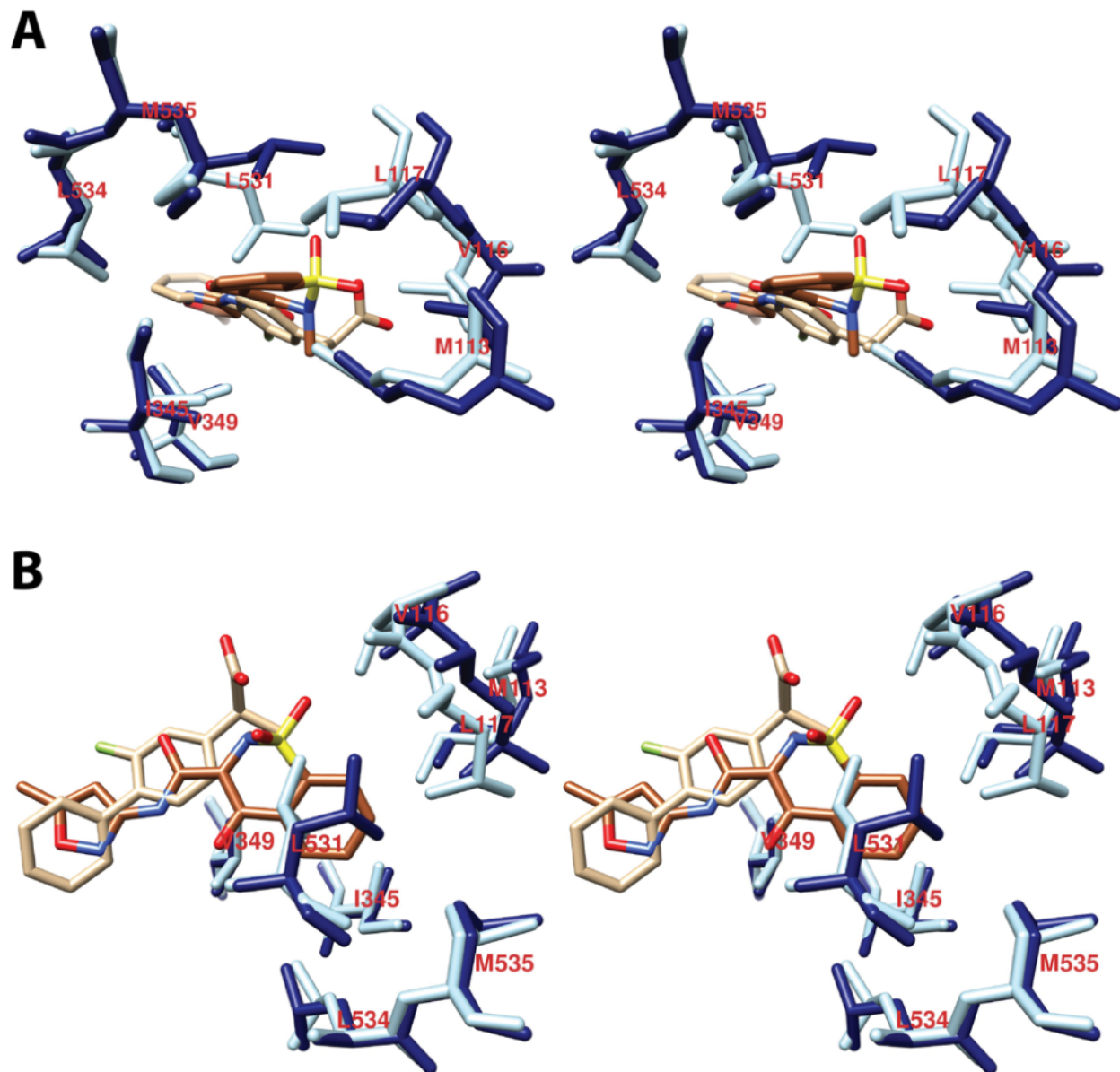


Figure 19. (A) and (B) Cross-eyed stereo views of the structure of isoxicam overlaid with that of (*S*)-flurbiprofen bound in the COX-2 active site along with the residues that form the oxicam pocket. Isoxicam is shown in sienna, and the associated amino acid residues are in dark blue. (*S*)-Flurbiprofen is in tan, and the associated amino acids are in light blue. Note the large difference in the conformation of Leu-531 between the two structures. This rotation is necessary to provide access to the oxicam pocket. Note also the difference in the positions of Met-113, Val-116, and Leu-117 that results from the movement of helix D. From PDB #4M10 and #3PGH.

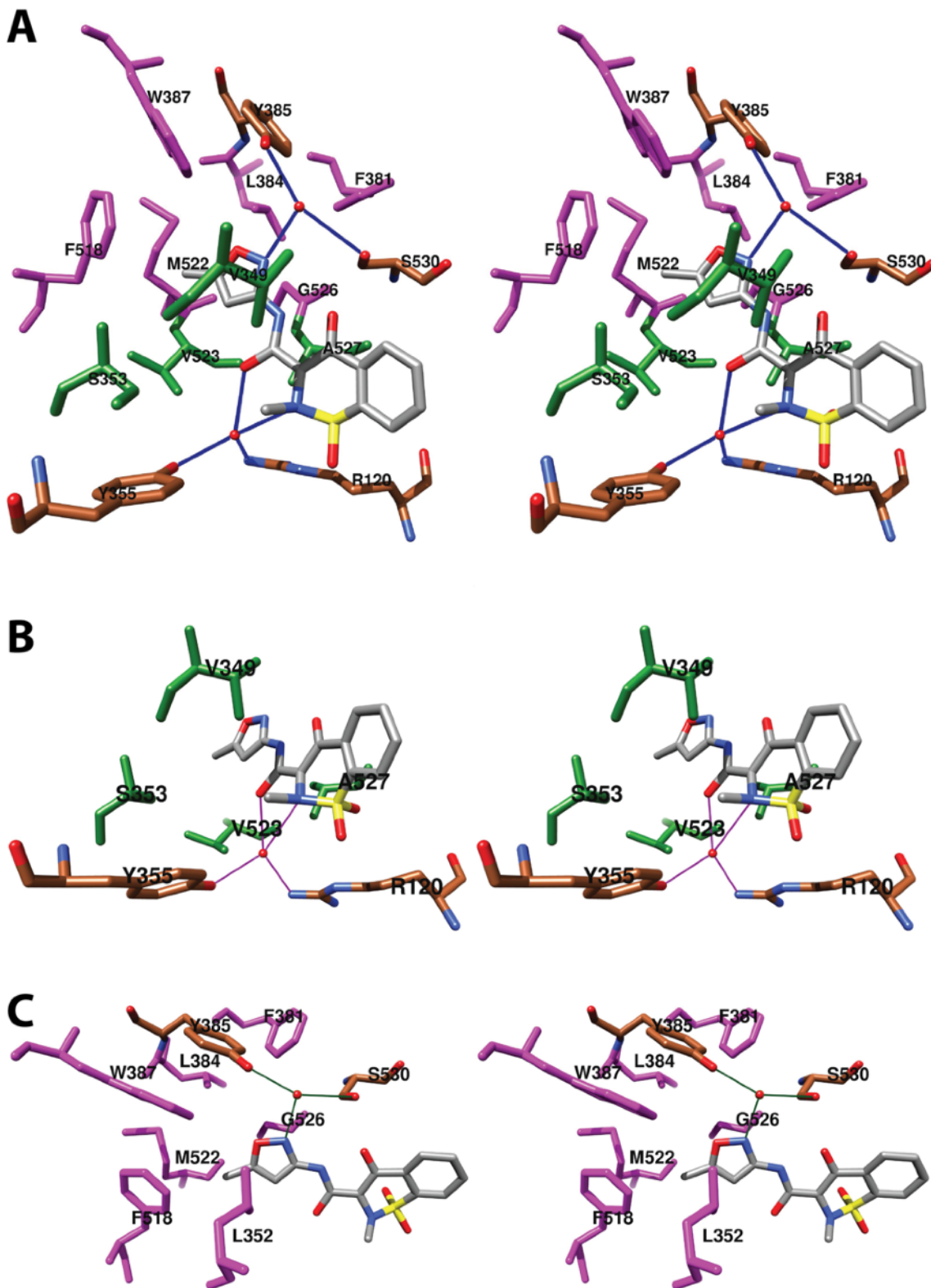


Figure 20. Cross-eyed stereo view of isoxicam bound in the cyclooxygenase active site of COX-2 and the hydrogen bonded water molecules through which the inhibitor establishes polar contacts with the side chains of residues in the proximal binding pocket (A & C) and the central binding pocket (B & C). Side chains are colored in green (proximal

binding pocket) or magenta (central binding pocket) with the exception of Arg-120, Tyr-355, Tyr-385, and Ser-530, which are colored by heteroatom on a sienna background. Isoxicam is colored by atom. The coordinated water molecule is shown as a red sphere. From PDB #4M10

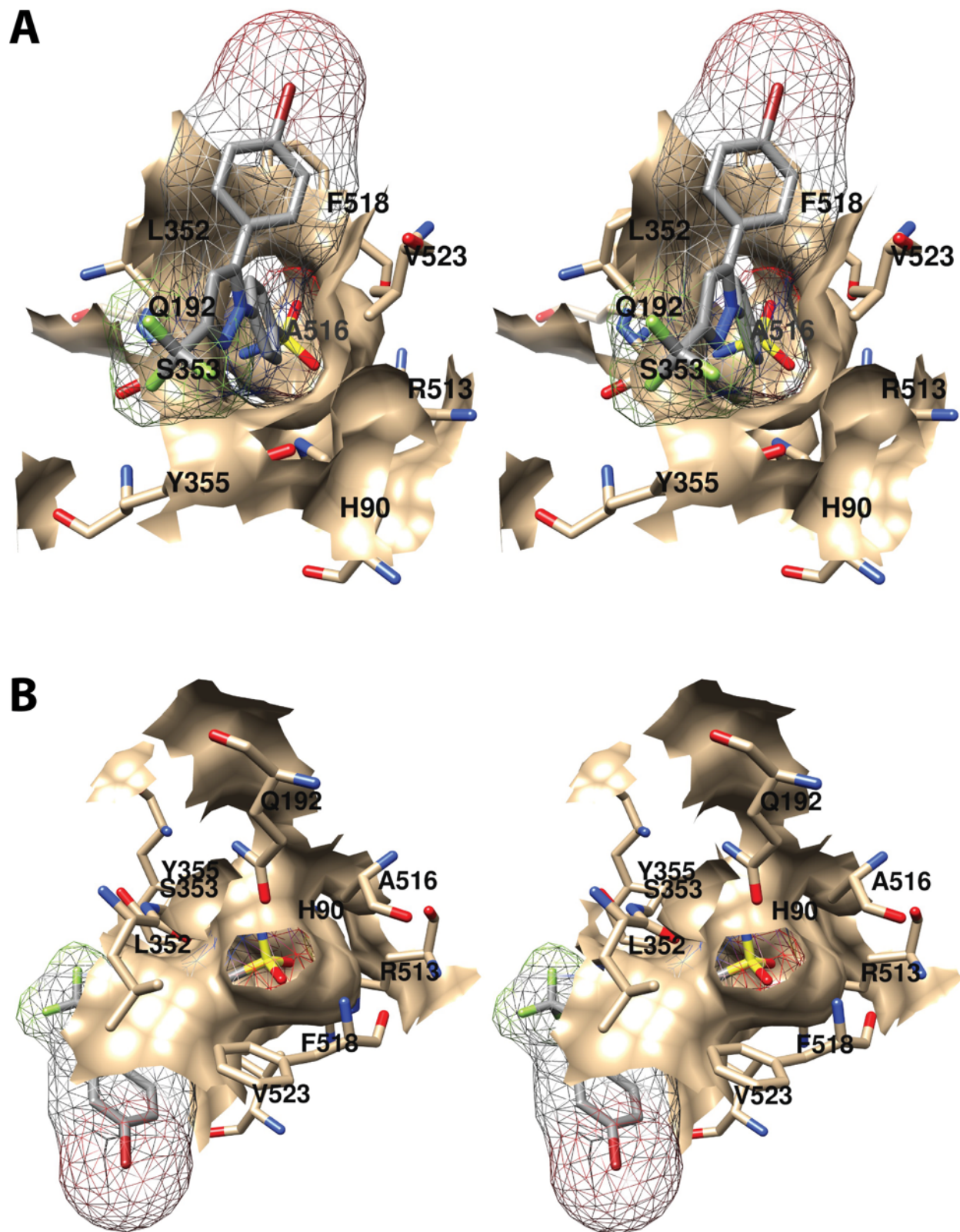


Figure 21. Cross-eyed stereo view of the interaction of the COX-2 side pocket with the phenylsulfonamide group of SC-558 as seen from two different views. SC-558 is colored by element, and

its surface is shown as a mesh. Side chains of the residues comprising the pocket are displayed, and their surface is shown in solid tan. In (B), the phenylsulfonamide group of SC-558 is completely surrounded by the pocket, so that only the sulfonamide can be seen. From PDB #6COX.

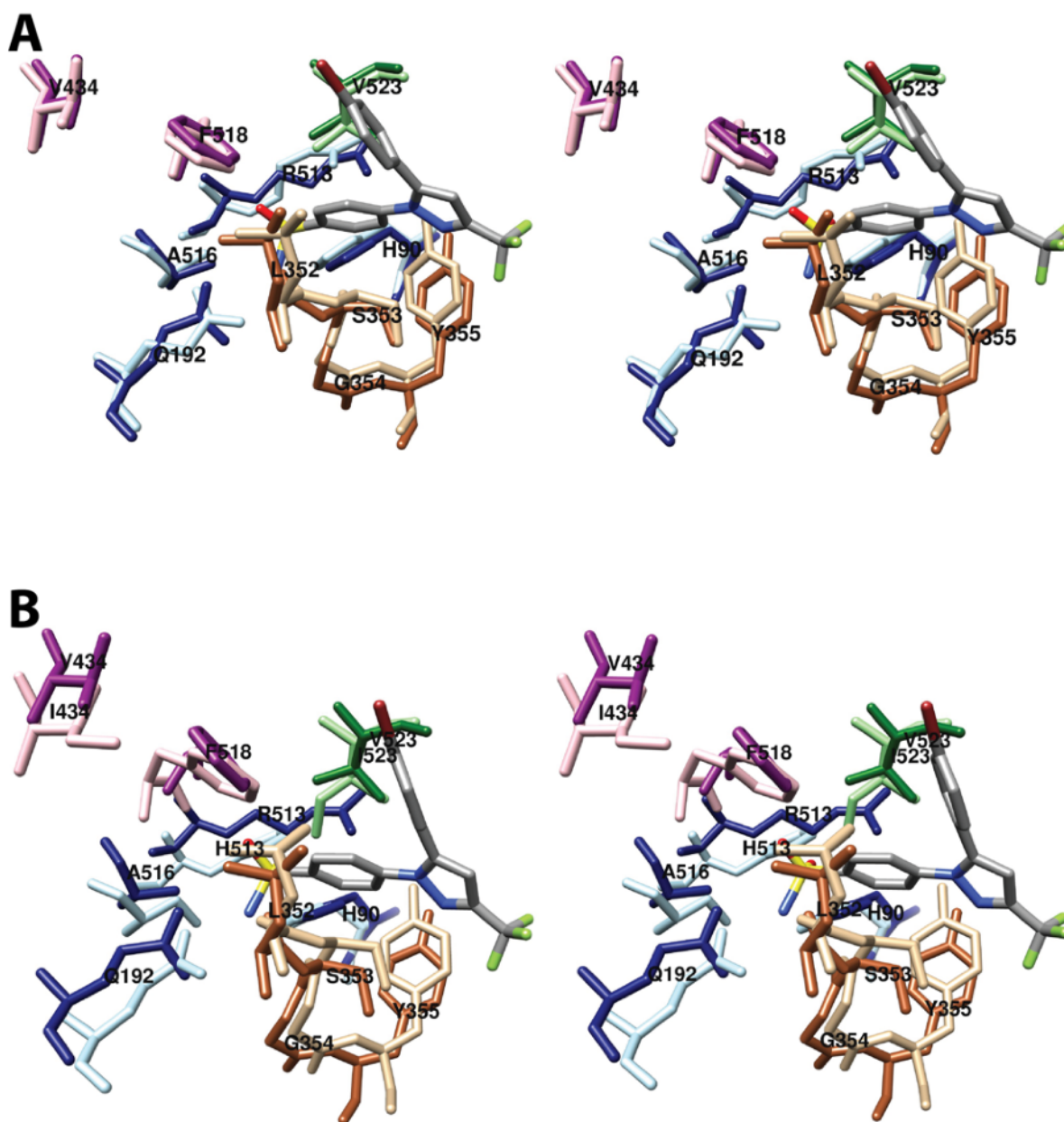


Figure 22. (A) Cross-eyed stereo view of the structure of SC-558 bound in the cyclooxygenase active site of COX-2 highlighting residues involved in side pocket formation and interactions. Overlaid are the same residues as observed in the structure of (*S*)-flurbiprofen bound in the cyclooxygenase active site of COX-2. Highlighted are Phe-518, which packs against Val-434 (pink/magenta) to open the side pocket, residues 352-355 (tan/sienna), which move to enlarge the side pocket upon diarylheterocycle binding, Val-523 (light/dark green), which is Ile-523 in COX-1, and other side pocket residues (light/navy blue). In each case, the darker colors correspond to residues in the SC-558-COX-2 structure whereas the lighter colors correspond to the (*S*)-flurbiprofen-COX-2 structure. (B) Same as (A) except that the structure of the SC-558-COX-2 complex (dark colors) is overlaid with the corresponding residues from the structure of (*S*)-flurbiprofen bound in the cyclooxygenase active site of COX-1 (light colors). Note the three key residues at positions, 434, 513, and 523 that are different between the two isoforms. In particular, Ile-523

in COX-1 encroaches on the side pocket, and Ile-434 in COX-1 prevents the movement of Phe-518 that provides access into the pocket. From PDB #6COX, #1EQH, and #3PGH.

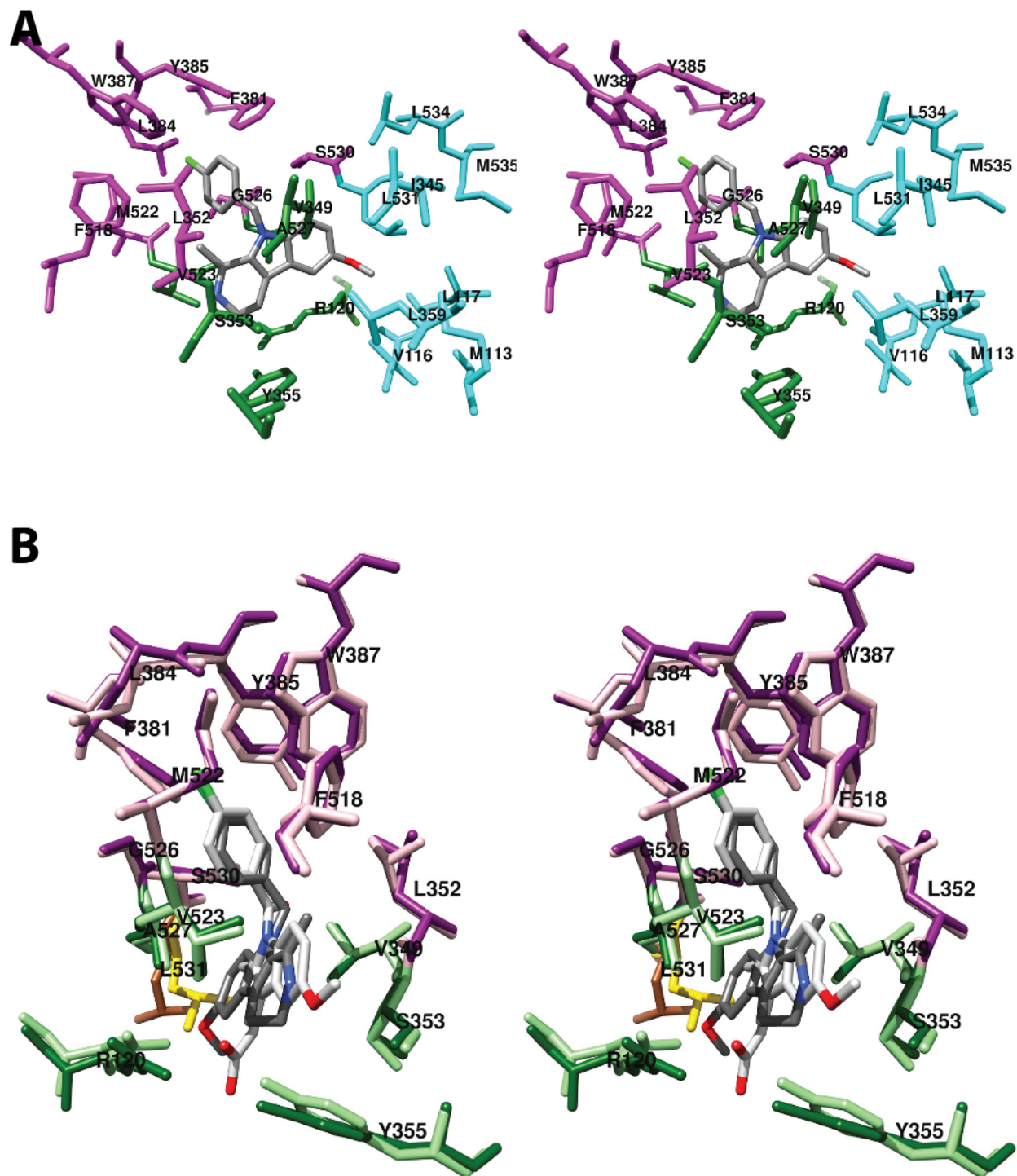


Figure 23. (A) Cross-eyed stereo view of the structure of harmaline compound 3 bound in the cyclooxygenase active site of COX-2. The side chains that make up the proximal binding pocket (green), the central binding pocket (magenta), and the oxicam pocket (cyan) are shown. Note that Val-349 is part of both the proximal pocket and the oxicam pocket. It is colored in cyan. (B) Wall-eyed stereo view of an overlay of the structures of harmaline compound 3 and indomethacin bound in the active site of COX-2, including residues that make up the proximal (light/dark green) and central (pink/magenta) binding pockets. Indomethacin and compound 3 are shown in light and dark gray, respectively, and the lighter

residue colors correspond to those in the indomethacin-COX-2 complex. Also shown is Leu-531 (yellow/sienna) which moves away from the constriction to accommodate the tricyclic harmaline nucleus. From PDB #63VR.

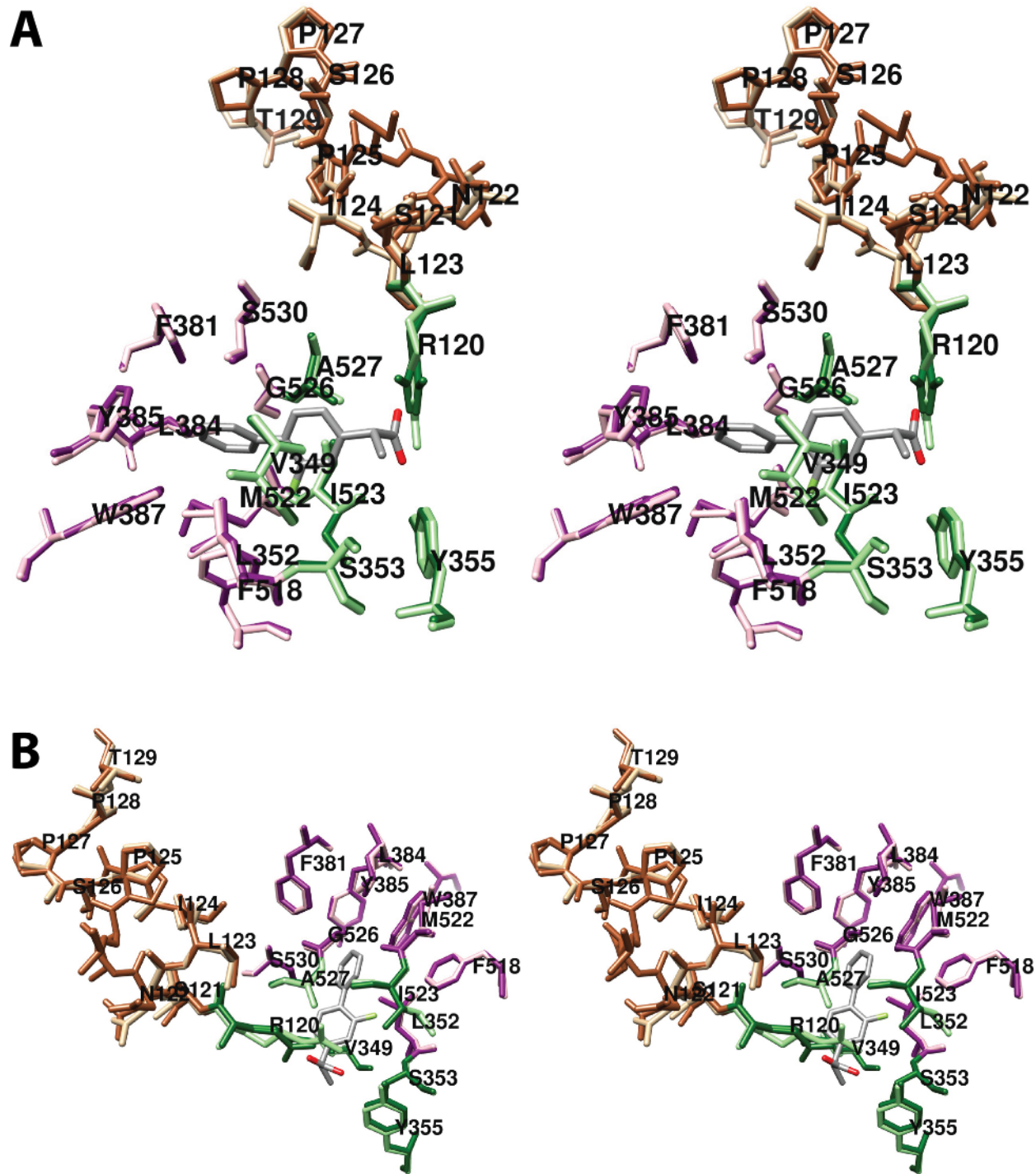


Figure 24. (A) and (B) Wall-eyed stereo views of the structure of (*S*)-flurbiprofen bound in the cyclooxygenase active site of a wild-type/R12Q COX-1 heterodimer and the side chains that make up the proximal binding pocket (green) and the central binding pocket (magenta). The structures of the two subunits are overlaid, with the wild-type subunit (containing flurbiprofen) shown in the lighter colors. Also shown are residues 121-129, which exist in two conformations in the R120Q subunit (sienna) depending on the presence or absence of bound flurbiprofen. Subunits containing inhibitor exhibit the same conformation as is observed in the wild-type subunit (tan), whereas those lacking inhibitor diverge between Ser-121 and Pro-125. From PDB #3N8W.

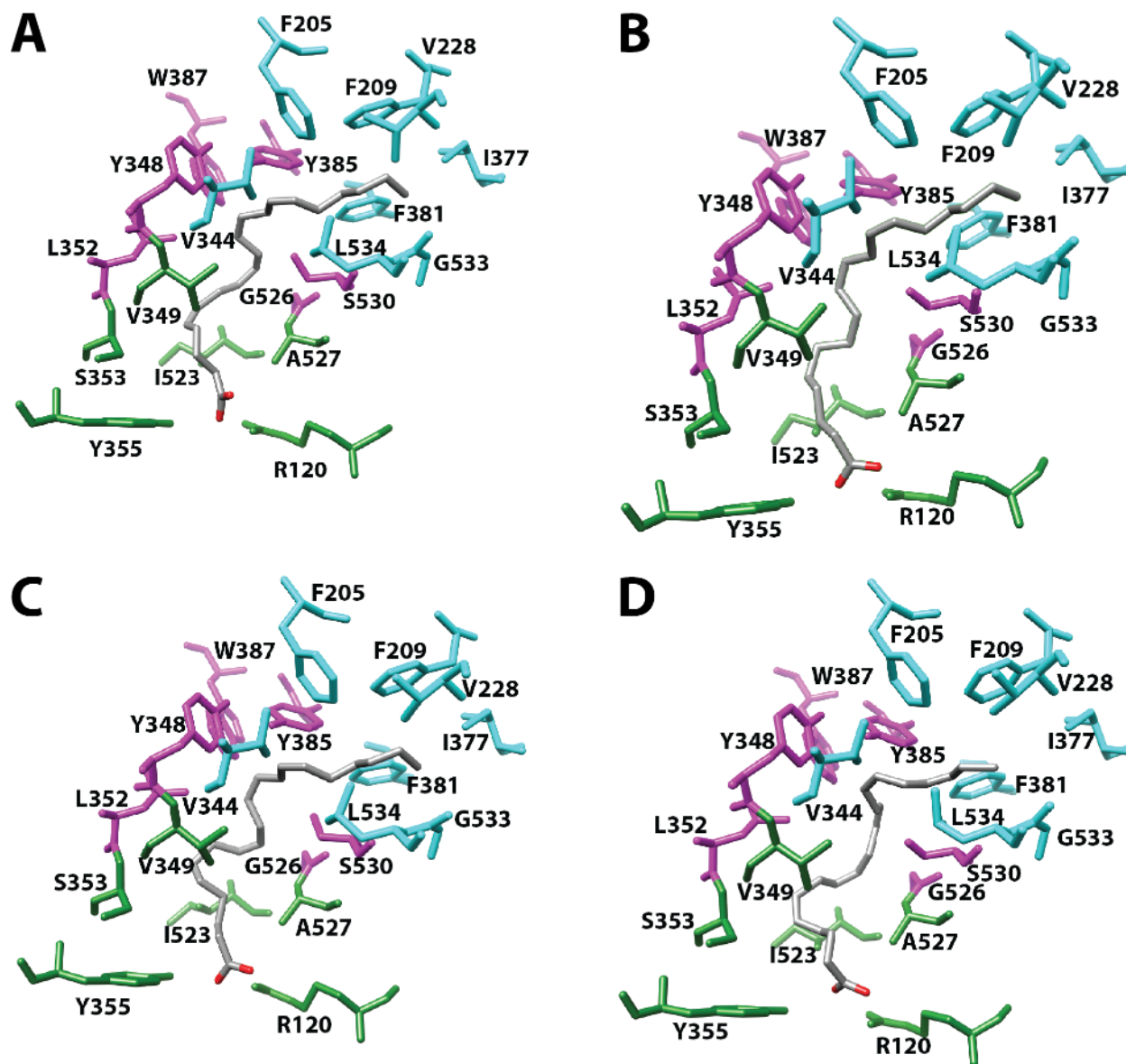


Figure S1. Structure of (A) AA, (B) LA, (C) DHLA, and (D) EPA, bound in the cyclooxygenase active site of COX-1 and the side chains that make up the proximal binding pocket (green), the central binding pocket (magenta), and the distal binding pocket (cyan). An overlay of these structures is provided in stereoscopic view in Figure 5B. From PDB #1DIY, #1IGZ, #1FE2, and #1IGX.

proximal binding pocket (green), the central binding pocket (magenta), and the distal binding pocket (cyan). An overlay of these structures is provided in Figure S3. From PDB #3HS5 (chain B), #4E1G, #3HS6 (chain B), #3HS7, and #3QH0.

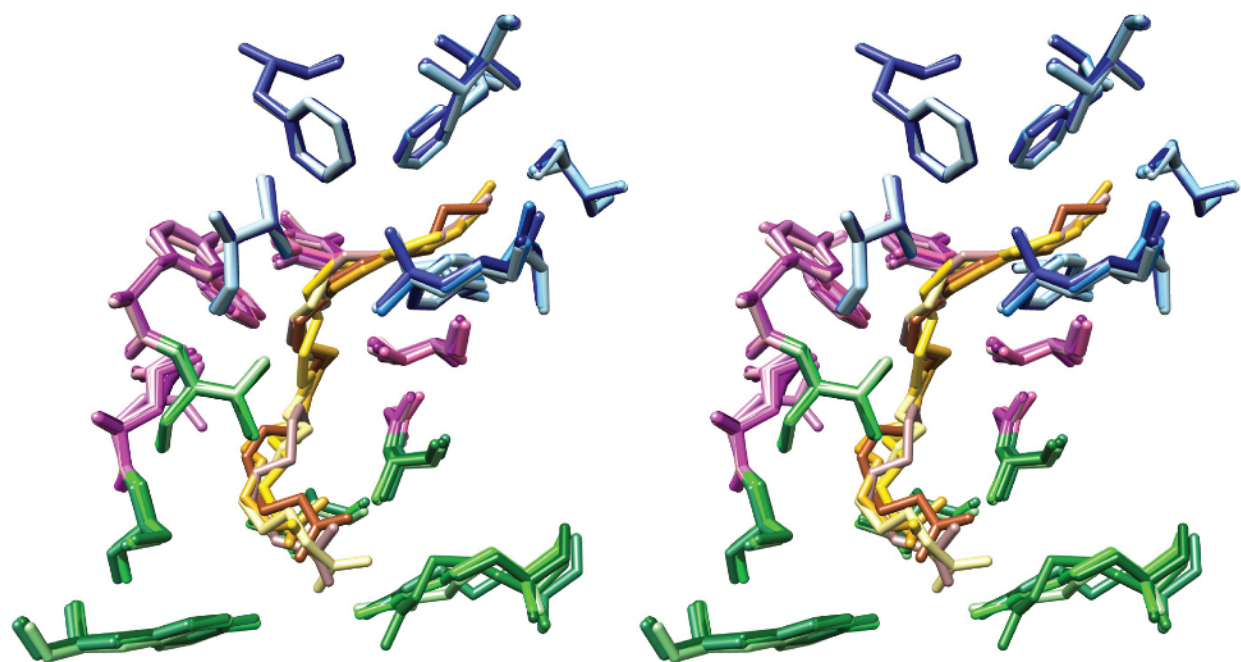


Figure S3. Cross-eyed stereo view of an overlay of the structures of five fatty acids in the cyclooxygenase active site of COX-2 and the side chains that make up the proximal binding pocket (green), the central binding pocket (magenta), and the distal binding pocket (blue). Fatty acids and amino acid side chains are colored from lightest to darkest in the order PA, α LA, EPA, DHA, and AA. Notable is the minimal movement of active site residues to accommodate the structural differences among the various fatty acids. Monoscopic views of the individual structures are provided in Figure S2. From PDB #3HS5 (chain B), #4E1G, #3HS6 (chain B), #3HS7, and #3QH0 (chain A).

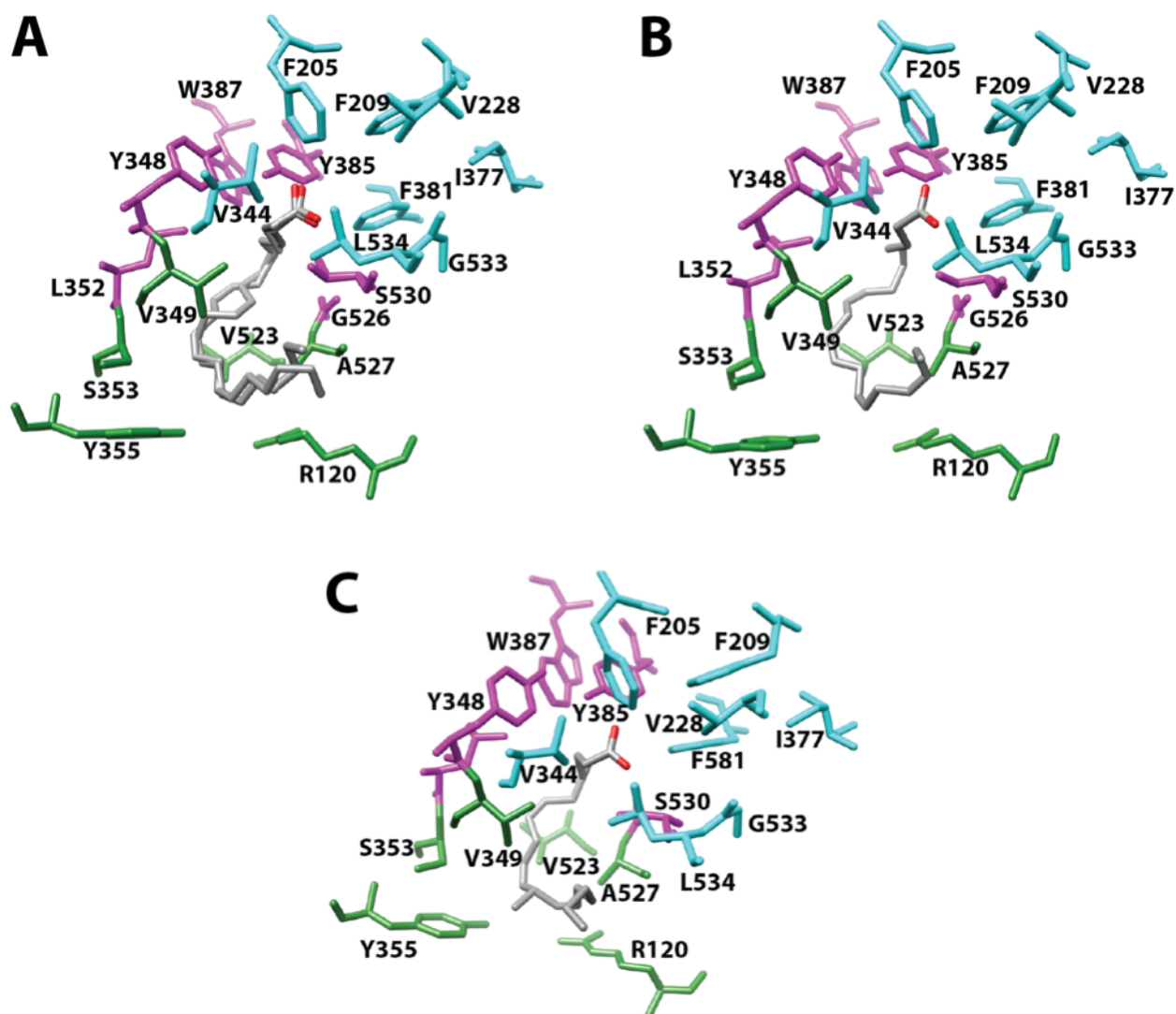


Figure S4. Structure of (A) AA (nonproductive conformation), (B) EPA (nonproductive conformation), and (C) 13-Me-AA bound in the cyclooxygenase active site of COX-2 and the side chains that make up the proximal binding pocket (green), the central binding pocket (magenta), and the distal binding pocket (cyan). Note that AA is observed in two slightly different conformations. From PDB #3HS5 (chain A), #3HS6 (chain A), and #4RUT.

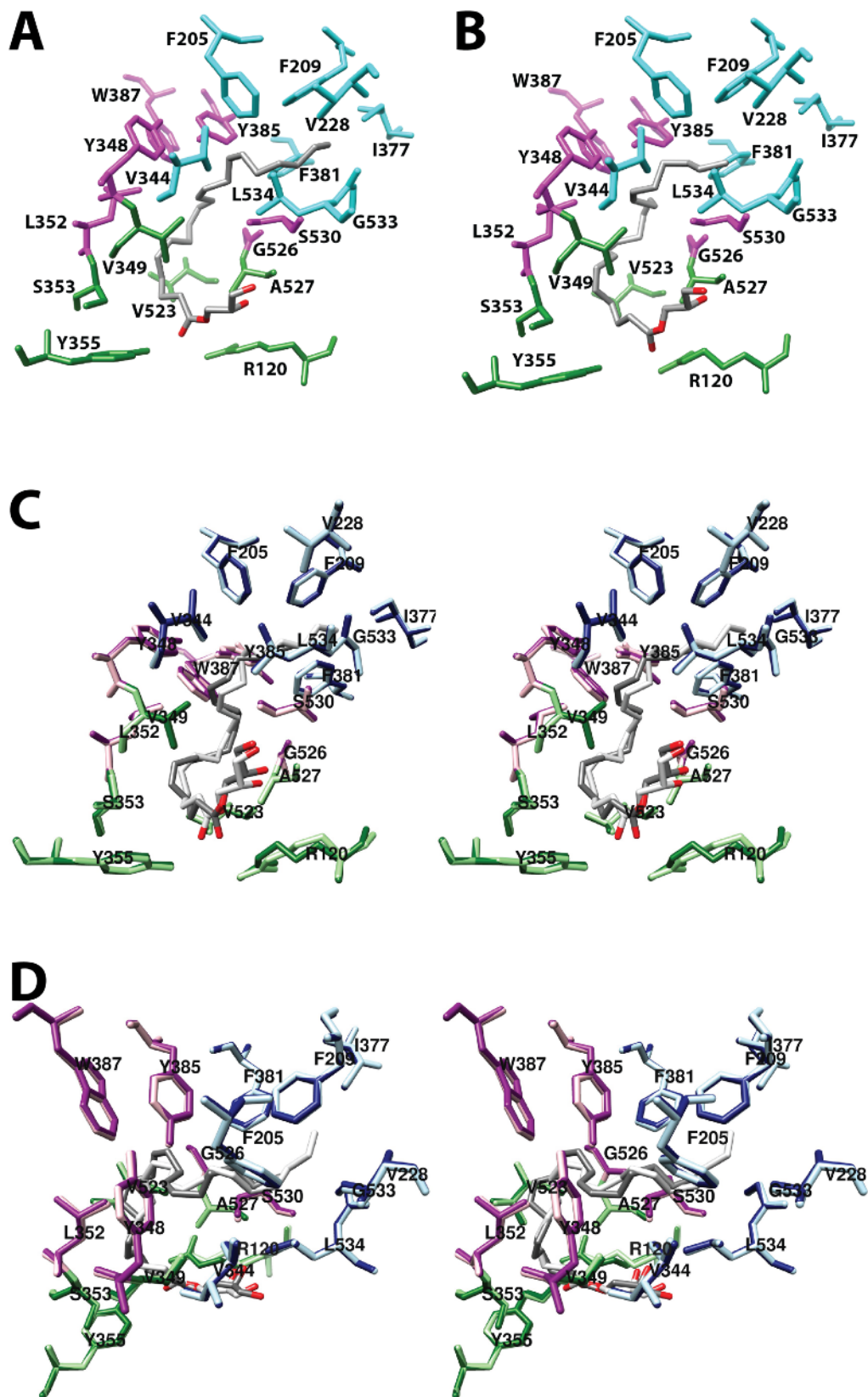


Figure S5. Structure of 1-AG in the (A) productive conformation and (B) nonproductive conformation

bound in the active site of COX-2 and the side chains that make up the proximal binding pocket (green), the central binding pocket (magenta), and the distal binding pocket (cyan). (C) and (D) Two different cross-eyed stereo views of the overlay of the structures of the nonproductive (dark gray) and productive (light gray) conformations of 1-AG bound in the cyclooxygenase active site. Residues in the surrounding binding pockets are colored similarly to those in (A) and (B) with the lighter and darker colors corresponding to the productive and nonproductive conformations, respectively. From PDB #3MDL.

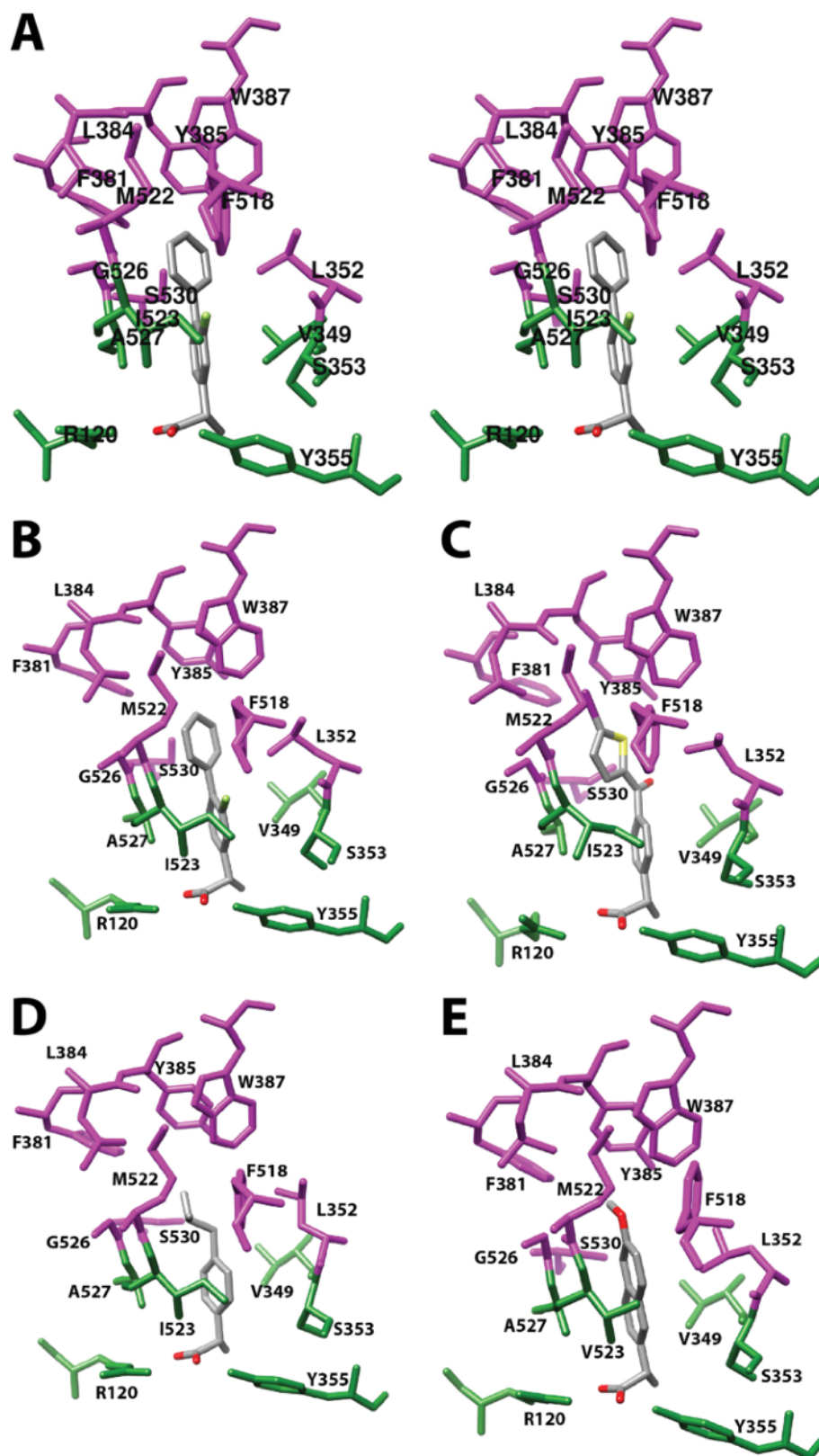


Figure S6. Cross-eyed stereo view of the structure of (*S*)-flurbiprofen bound in the cyclooxygenase active site of COX-1. Structures of (B) (*S*)-flurbiprofen, (C) (*S*)-iodosuprofen, (D) (*S*)-ibuprofen, and (E) (*S*)-

naproxen, bound in the cyclooxygenase active site of COX-1 (B, C, and D) or COX-2 (E). The side chains that make up the proximal binding pocket (green) and the central binding pocket (magenta) are shown. From PDB #1EQH (A and B), #1PGE, #1EQG, and #3NT1.

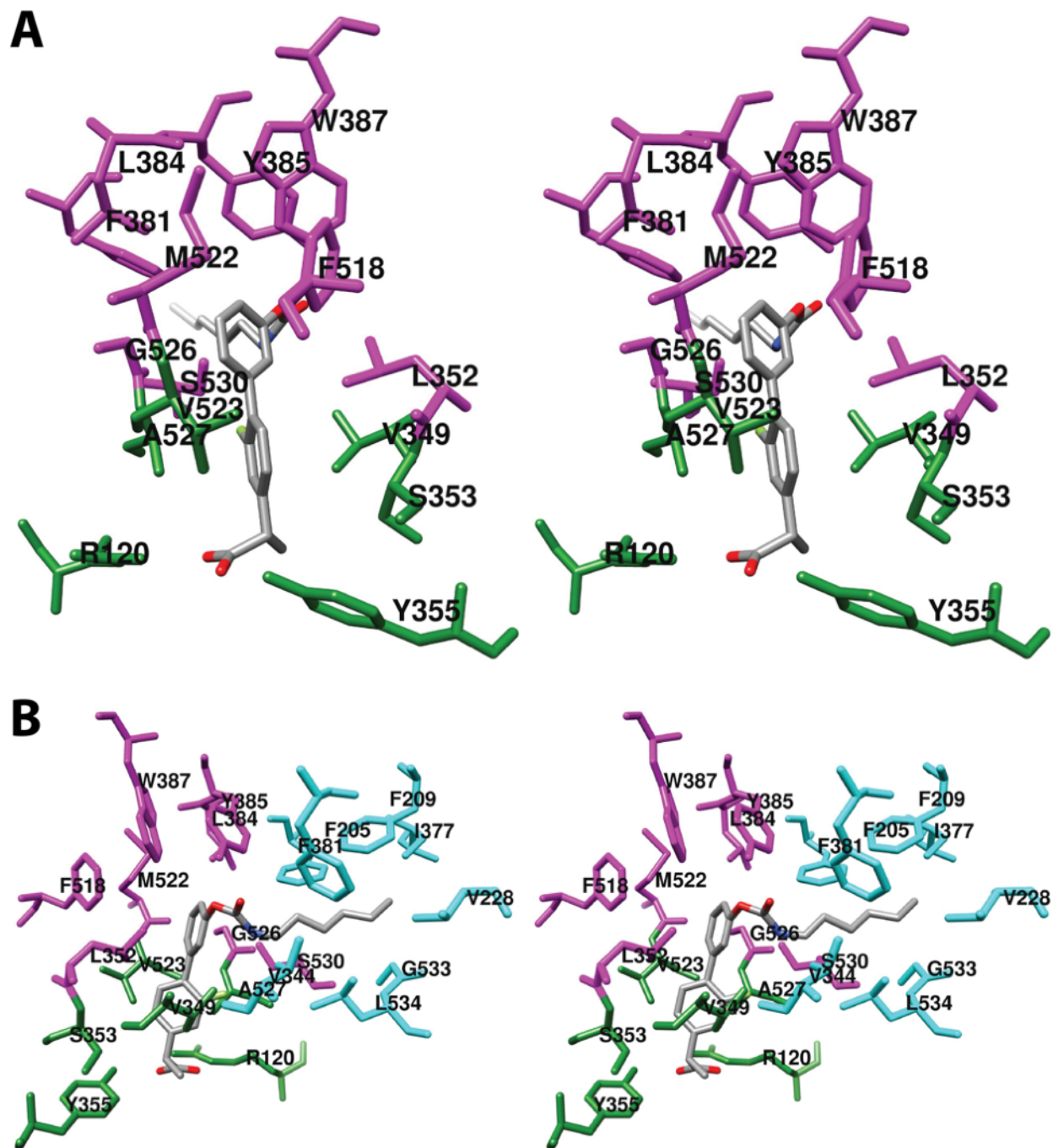


Figure S7. (A) Cross-eyed stereo view of the structure of ARN-2508 bound in the cyclooxygenase active site of COX-2 and the side chains that make up the proximal binding pocket (green) and the central binding pocket (magenta). (B) Same as (A) from a different perspective. Residues belonging to the distal AA binding pocket have been added and highlighted in cyan to reveal the localization of the hydrocarbon tail of ARN-2508 in this pocket. From PDB #5W58.

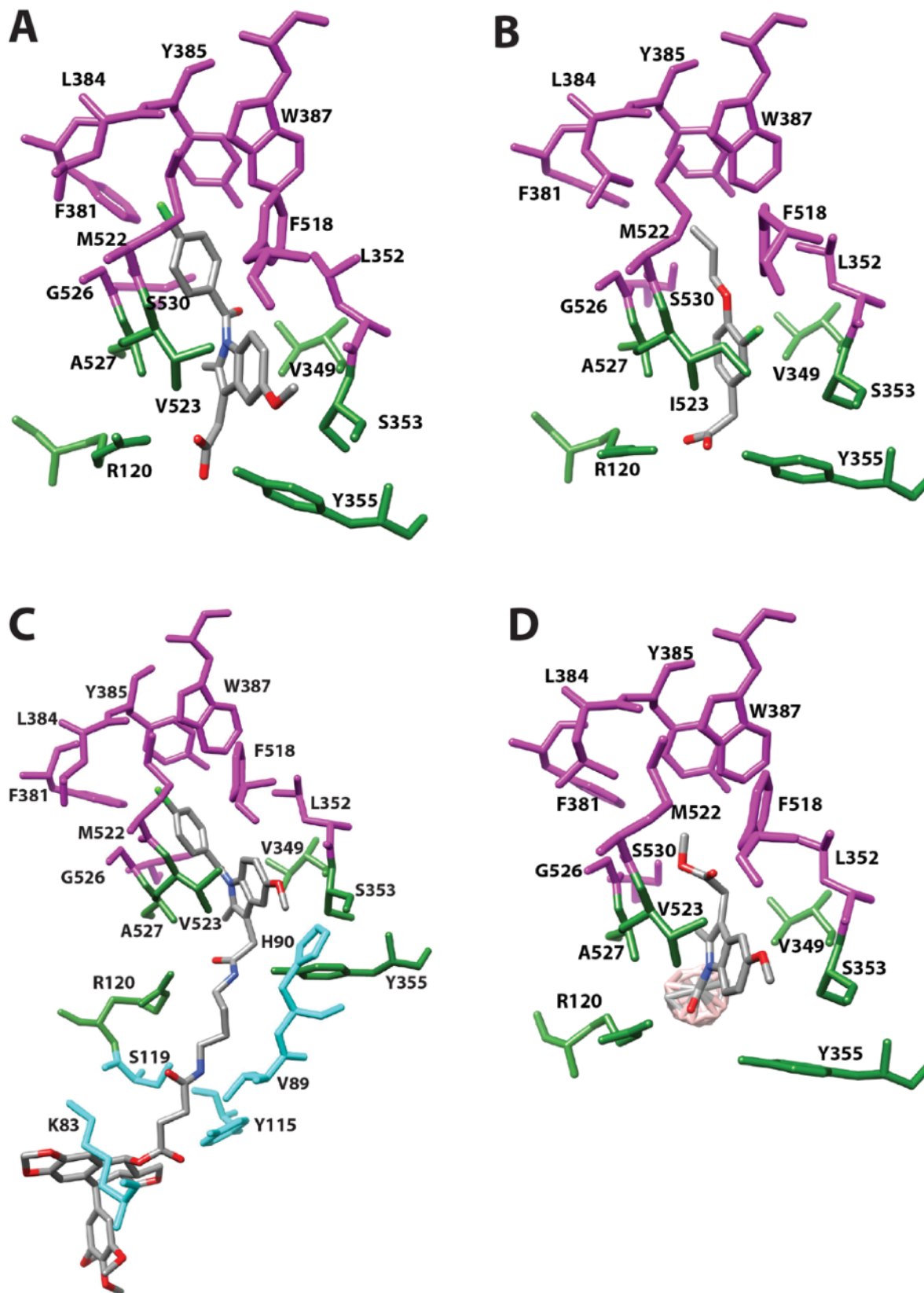


Figure S8. Structure of (A) indomethacin, (B) alclofenac, (C) an indomethacin-podophyllotoxin conjugate,

and (D) a *nido*-dicarbaborate derivative of indomethacin bound in the cyclooxygenase active site of COX-2 (A, C, & D) or COX-1 (B). The side chains that make up the proximal binding pocket (green), the central binding pocket (magenta), and membrane-binding domain residues that are predicted by molecular modeling to interact with the podophyllotoxin moiety (cyan) (C) are shown. From PDB #4COX, #1HT8, #4OTJ, and #4Z0L.

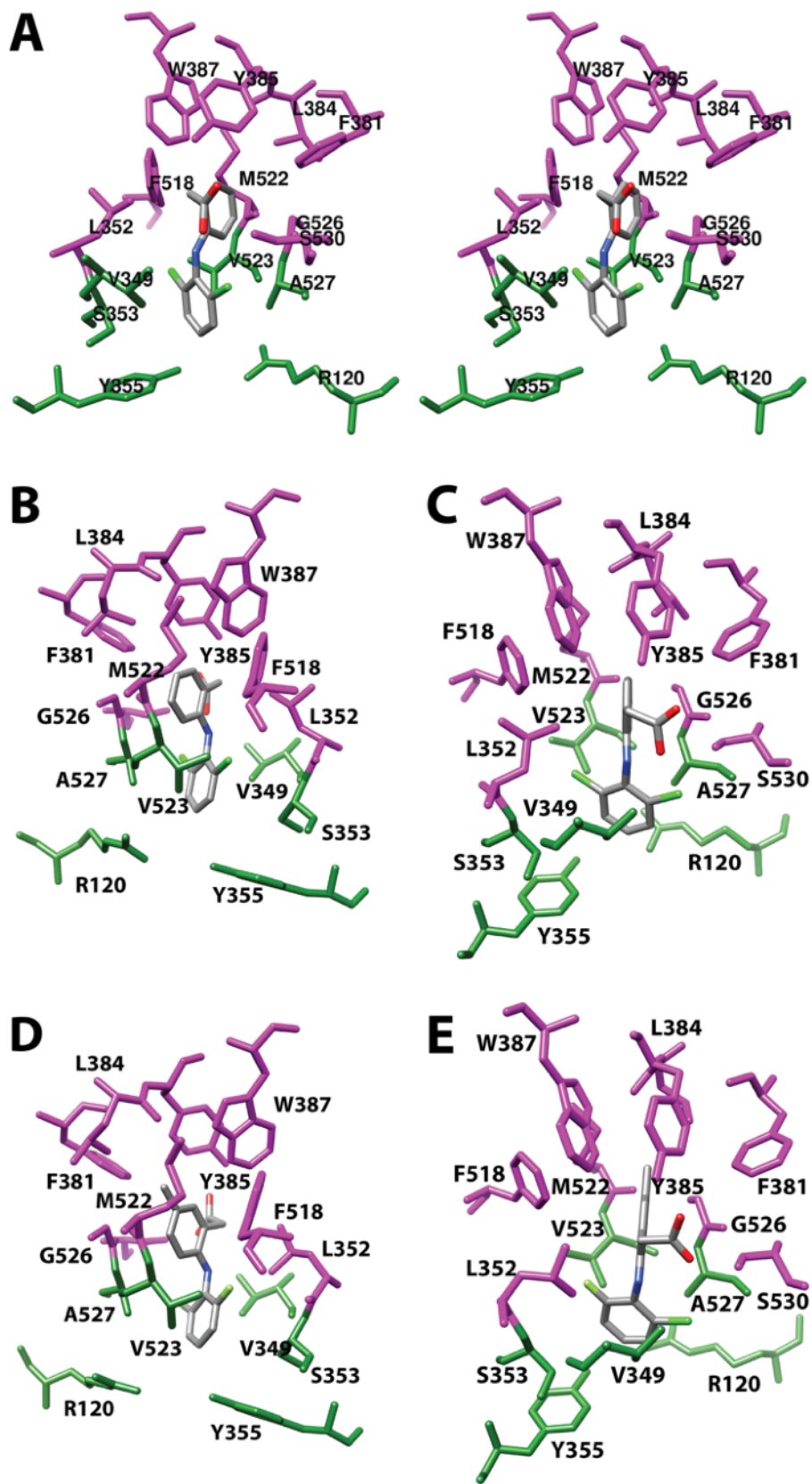


Figure S9. (A) Cross-eyed stereo view of diclofenac bound in the cyclooxygenase active site of COX-2.

Structures of (B & C) diclofenac and (D & E) lumiracoxib bound in the cyclooxygenase active site of COX-2. The side chains that make up the proximal binding pocket (green) and the central binding pocket (magenta) are shown. In each case, two views of the inhibitor are provided. Both are from the side (i.e., parallel to the plane of the membrane). Views (A, C, and E) highlight the proximity of the carboxylate of the inhibitor to the side chains of Ser-530 and Tyr-385. From PDB #1PXX and #4OTY.

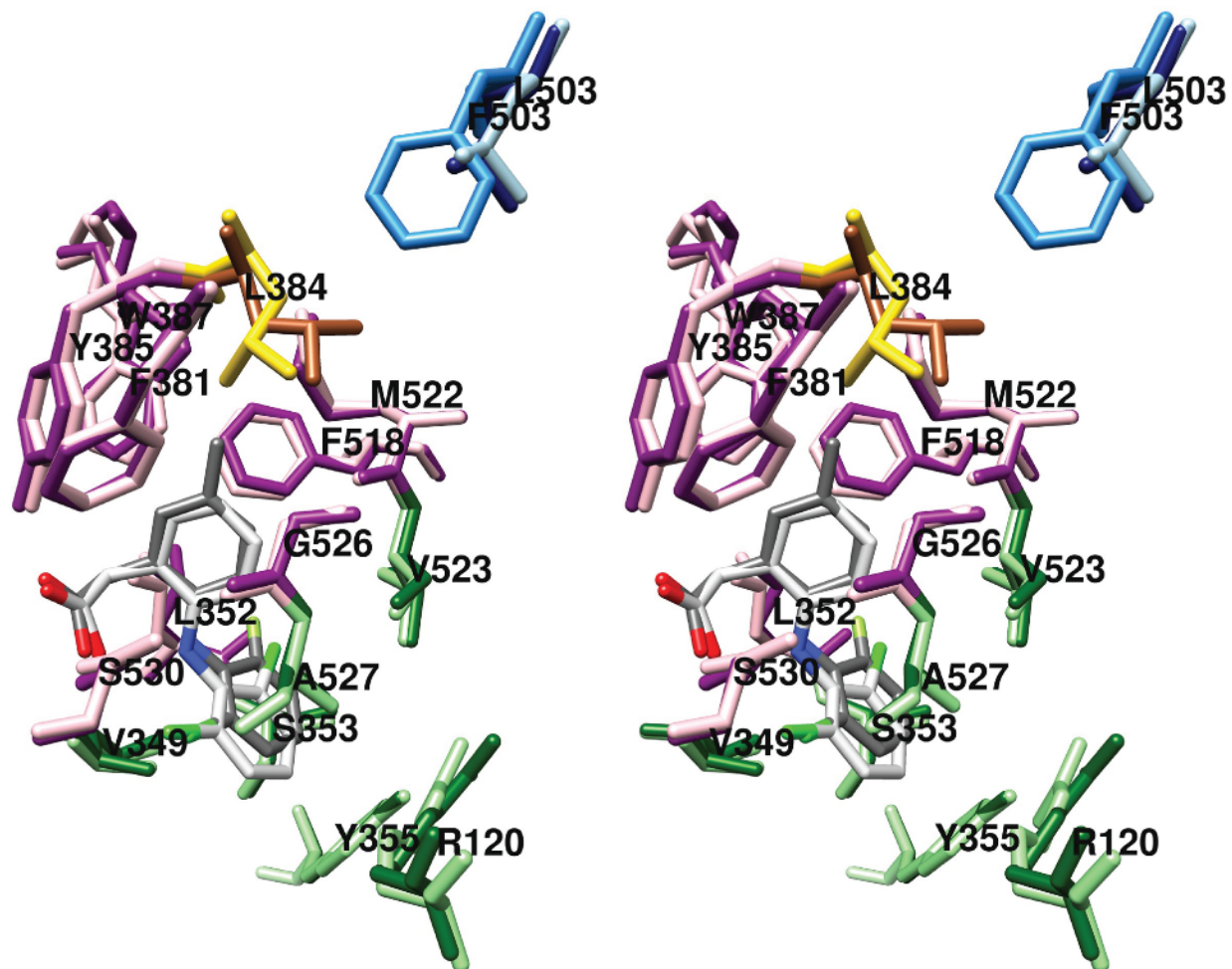


Figure S10. Cross-eyed stereo view of the overlay of the structures of diclofenac and lumiracoxib, bound in the cyclooxygenase active site of COX-2 and the side chains that make up the proximal binding pocket (light/dark green) and the central binding pocket (pink/magenta). Leu-384 is highlighted in gold/sienna, and Leu-503 is shown in light blue/navy blue. Also shown is the position that Phe-503 (dodger blue) occupies in the structure of diclofenac bound in the cyclooxygenase active site of COX-1. In each case, structures related to diclofenac (light gray) are shown in the lighter color and those related to lumiracoxib (dark gray) are shown in the darker color. From PDB #1PXX, #4OTY, and #3N8Y.

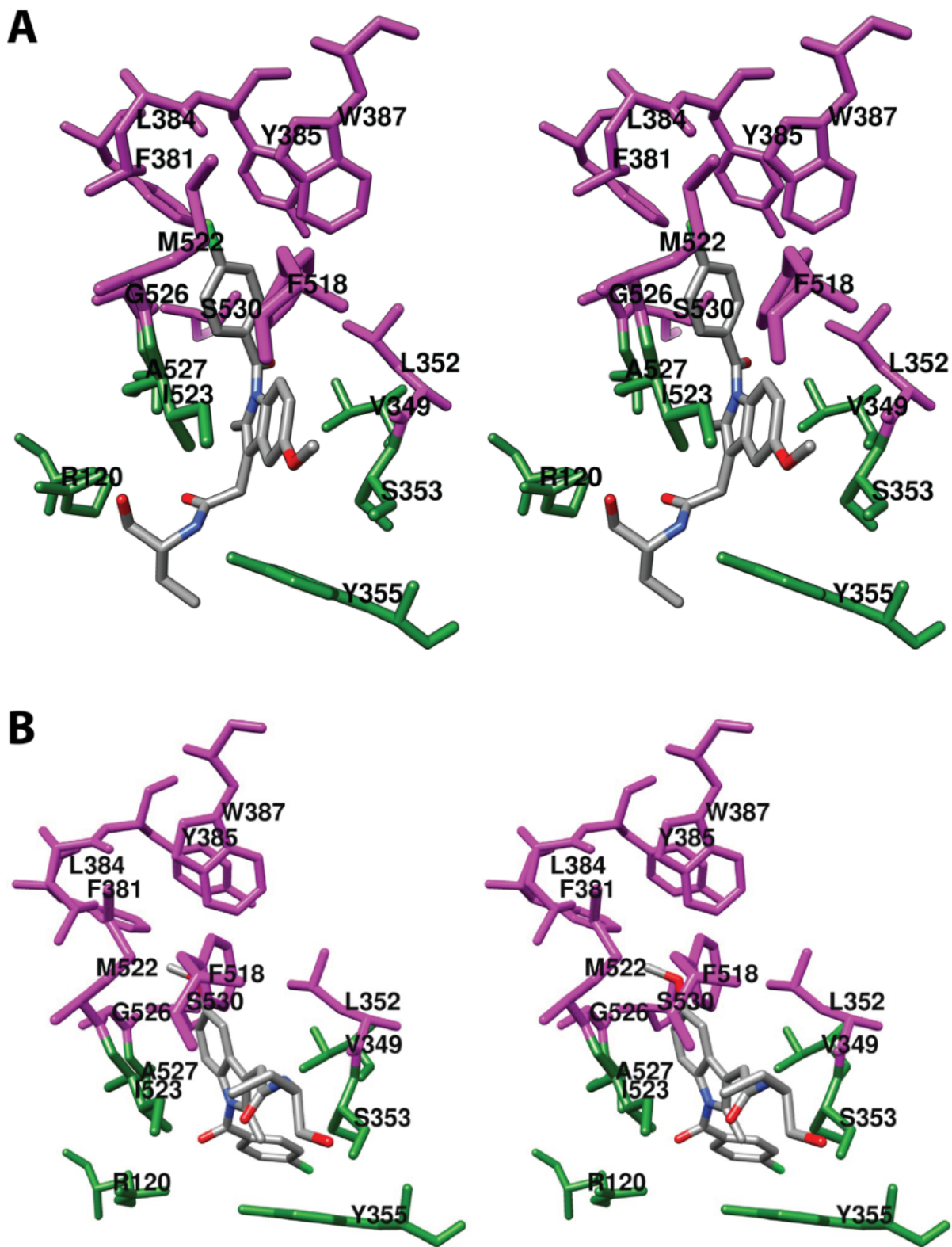


Figure S11. Cross-eyed stereo view of the structure of (A) indomethacin-(*R*)- α -ethyl-ethanolamide and (B) indomethacin-(*S*)- α -ethyl-ethanolamide bound in the cyclooxygenase active site of COX-1 and the

side chains that make up the proximal binding pocket (green) and the central binding pocket (magenta).
From PDB #2OYE and #2OYU.

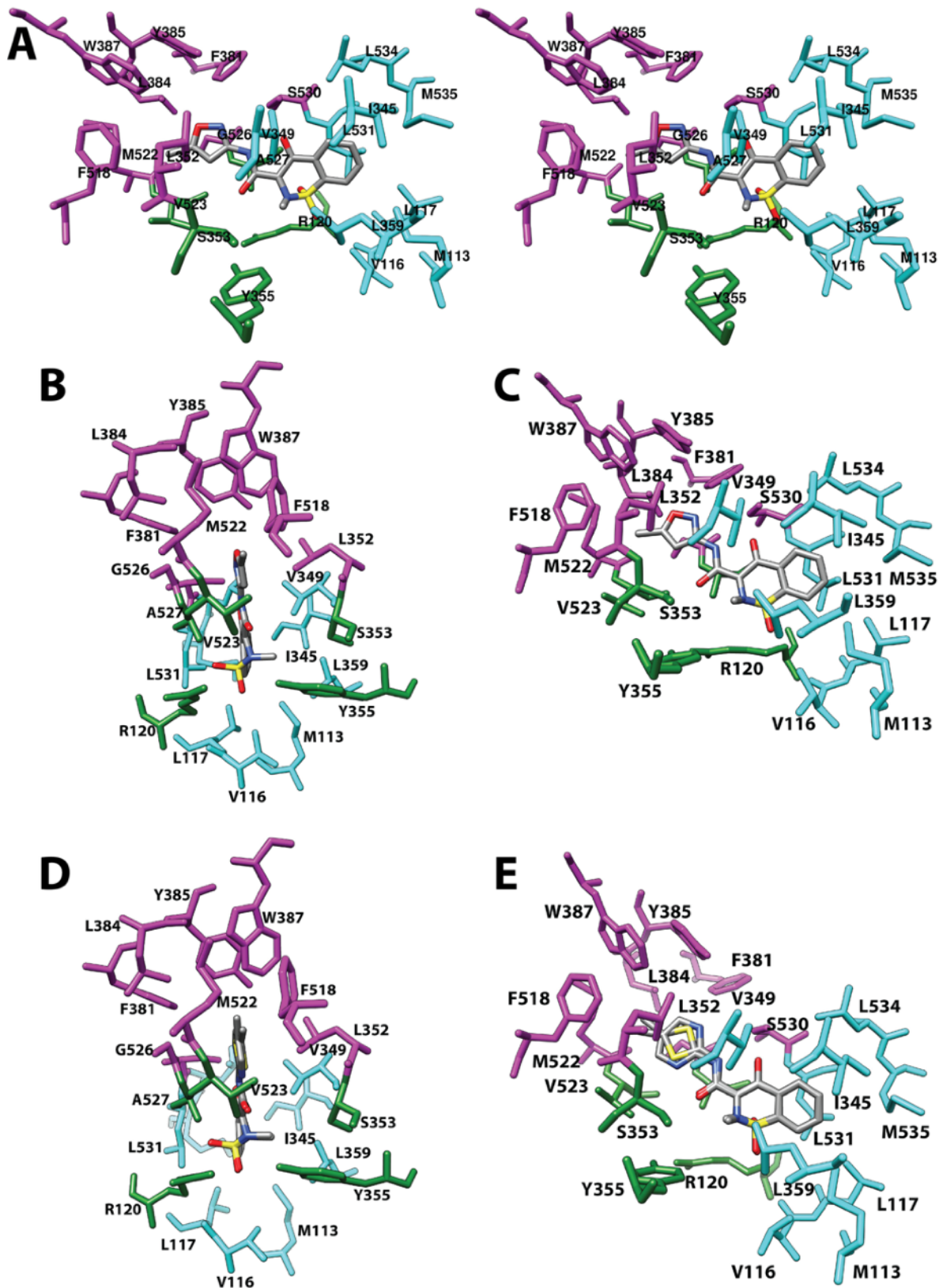


Figure S12. (A) Cross-eyed stereo view of isoxicam bound in the cyclooxygenase active site of COX-2. Structure of (B & C) isoxicam and (D & E) meloxicam bound in the cyclooxygenase active site of COX-2.

The side chains that make up the proximal binding pocket (green), the central binding pocket (magenta), and the oxicam pocket (cyan) are shown. Note that Val-349 is part of both the proximal pocket and the oxicam pocket. It is colored in cyan. The exact conformation of the thiazole ring of meloxicam could not be determined. From PDB #4M10 and #4M11.

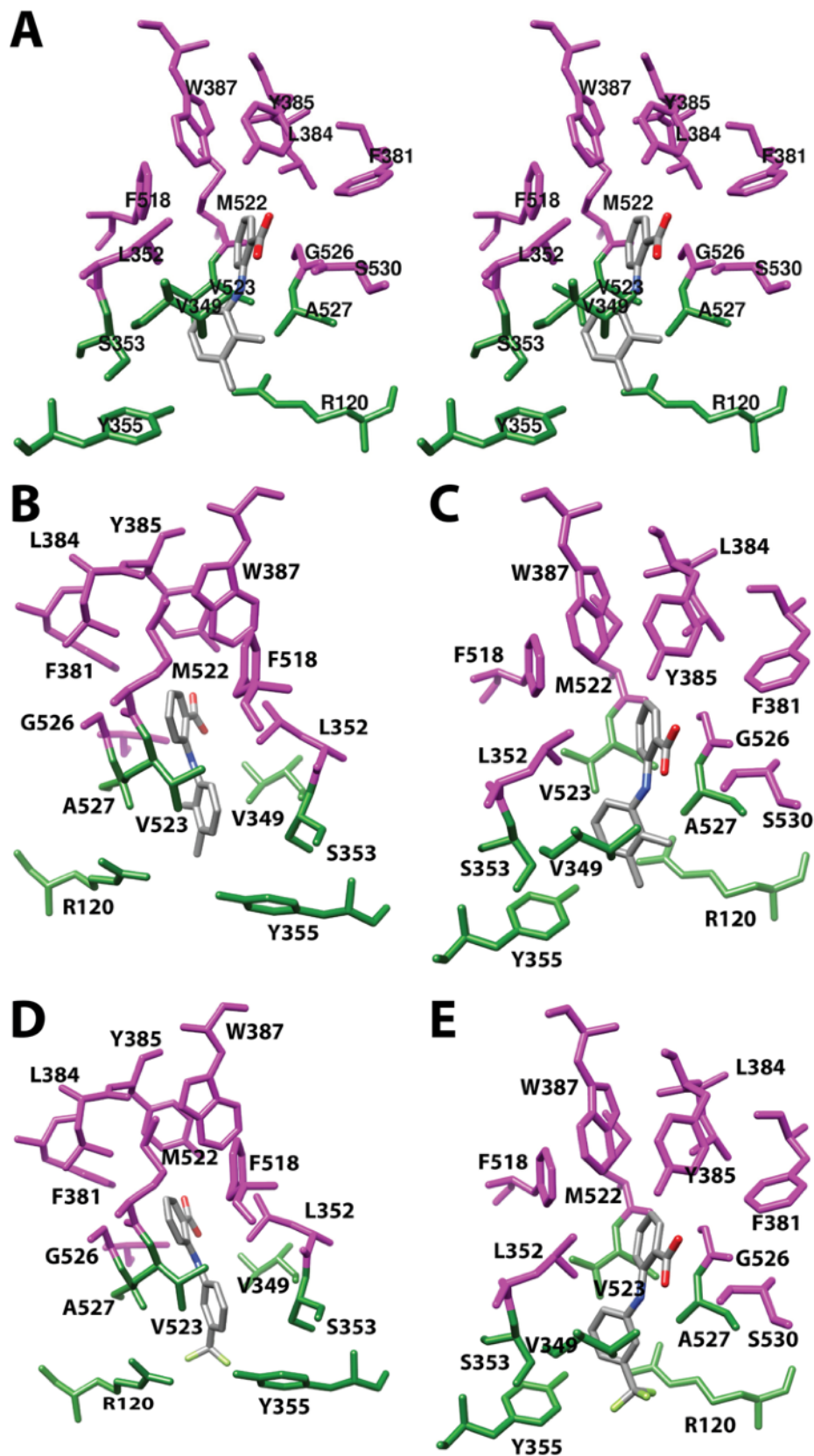


Figure S13. (A) Cross-eyed stereo view of mefenamic acid bound in the cyclooxygenase active site of

COX-2. Structures of (B & C) mefenamic acid and (D & E) flufenamic acid bound in the cyclooxygenase active site of COX-2. The side chains that make up the proximal binding pocket (green) and the central binding pocket (magenta) are shown. In each case, two views of the inhibitor are provided. Both are from the side (i.e., parallel to the plane of the membrane). Views (A), (C), and (E) highlight the proximity of the carboxylate of the inhibitor to the side chains of Ser-530 and Tyr-385. From PDB #5IKR and #5IKV.

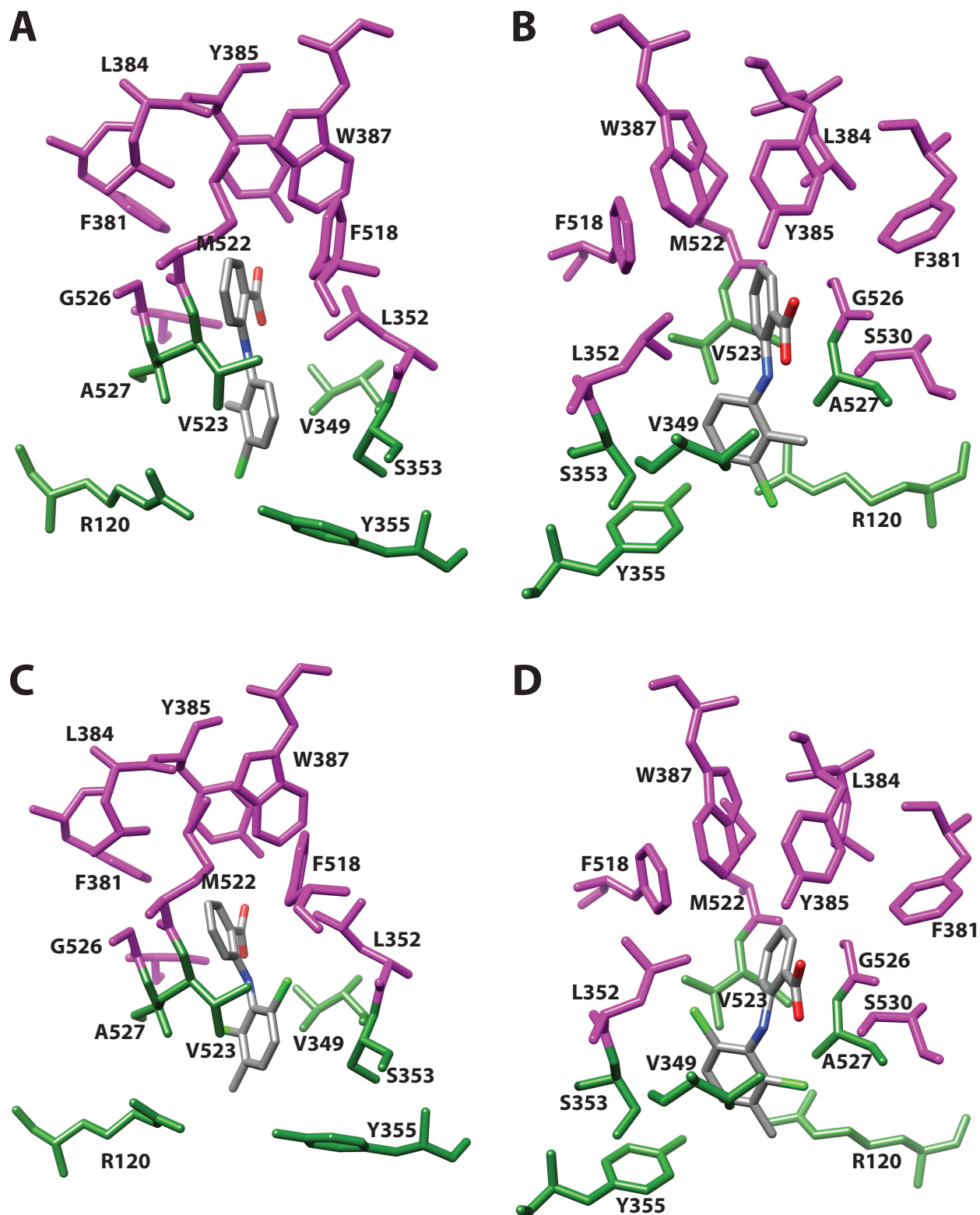


Figure S14. Structure of (A & B) tolfenamic acid and (C & D) meclufenamic acid bound in the cyclooxygenase active site of COX-2 and the side chains that make up the proximal binding pocket (green) and the central binding pocket (magenta). In each case, two views of the inhibitor are shown.

Both are from the side (i.e., parallel to the plane of the membrane). Views (B) and (D) highlight the proximity of the carboxylate of the inhibitor to the side chains of Ser-530 and Tyr-385. From PDB #5IKT and #5IKQ.

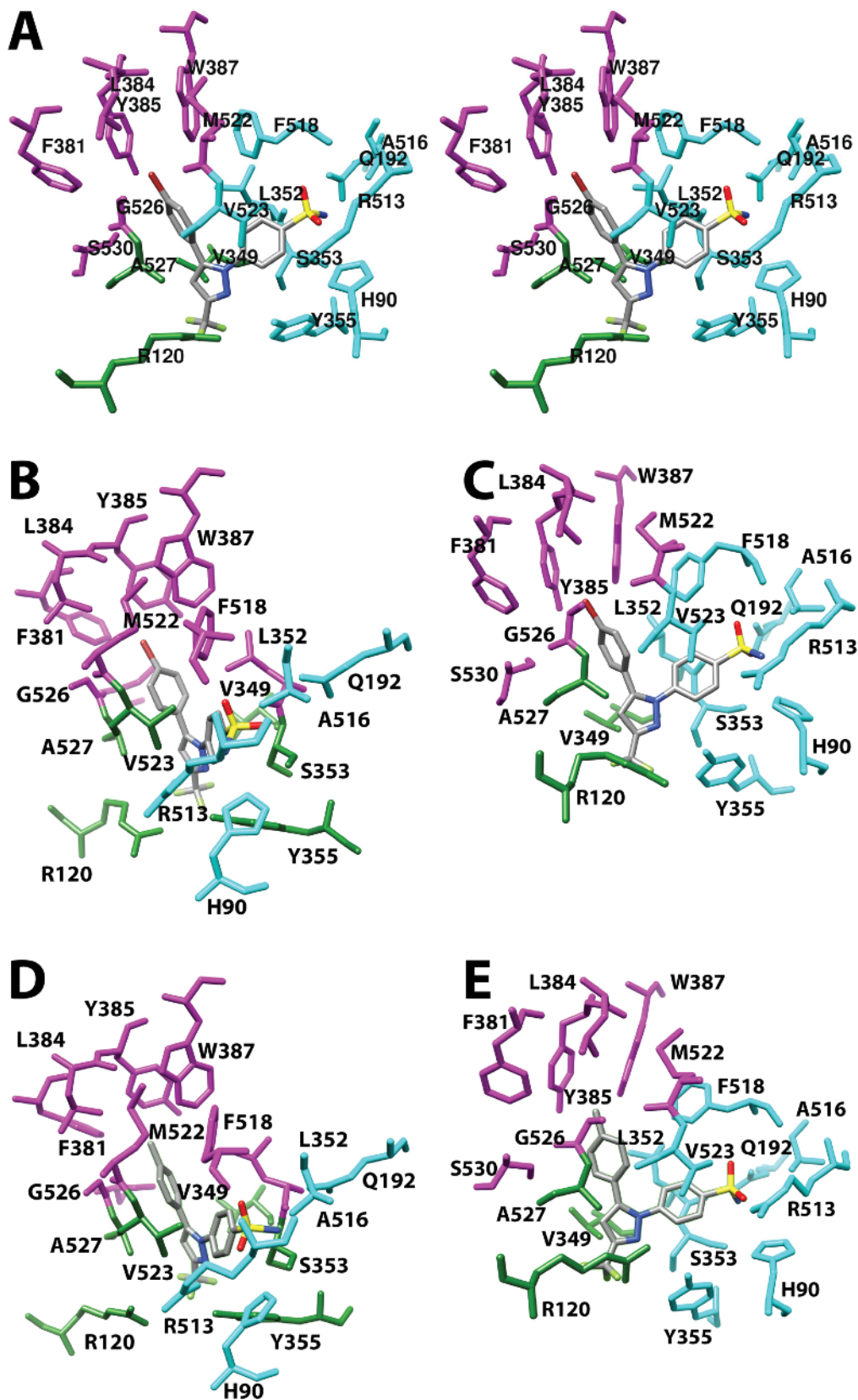


Figure S15. (A) Cross-eyed stereo view of SC-558 bound in the cyclooxygenase active site of COX-2.

Structures of SC-558 (B & C) and celecoxib (D & E) bound in the cyclooxygenase active site of COX-2. The side chains that make up the proximal binding pocket (green), the central binding pocket (magenta), and the COX-2 side pocket (cyan) are shown. In (B) and (D), the residues are colored as in most previous figures. In (A), (C), and (E), some residues in the proximal and central binding pockets that are shared with the COX-2 side pocket are colored cyan to highlight the interaction with the phenylsulfonamide group of each inhibitor. From PDB #6COX and #3LN1.

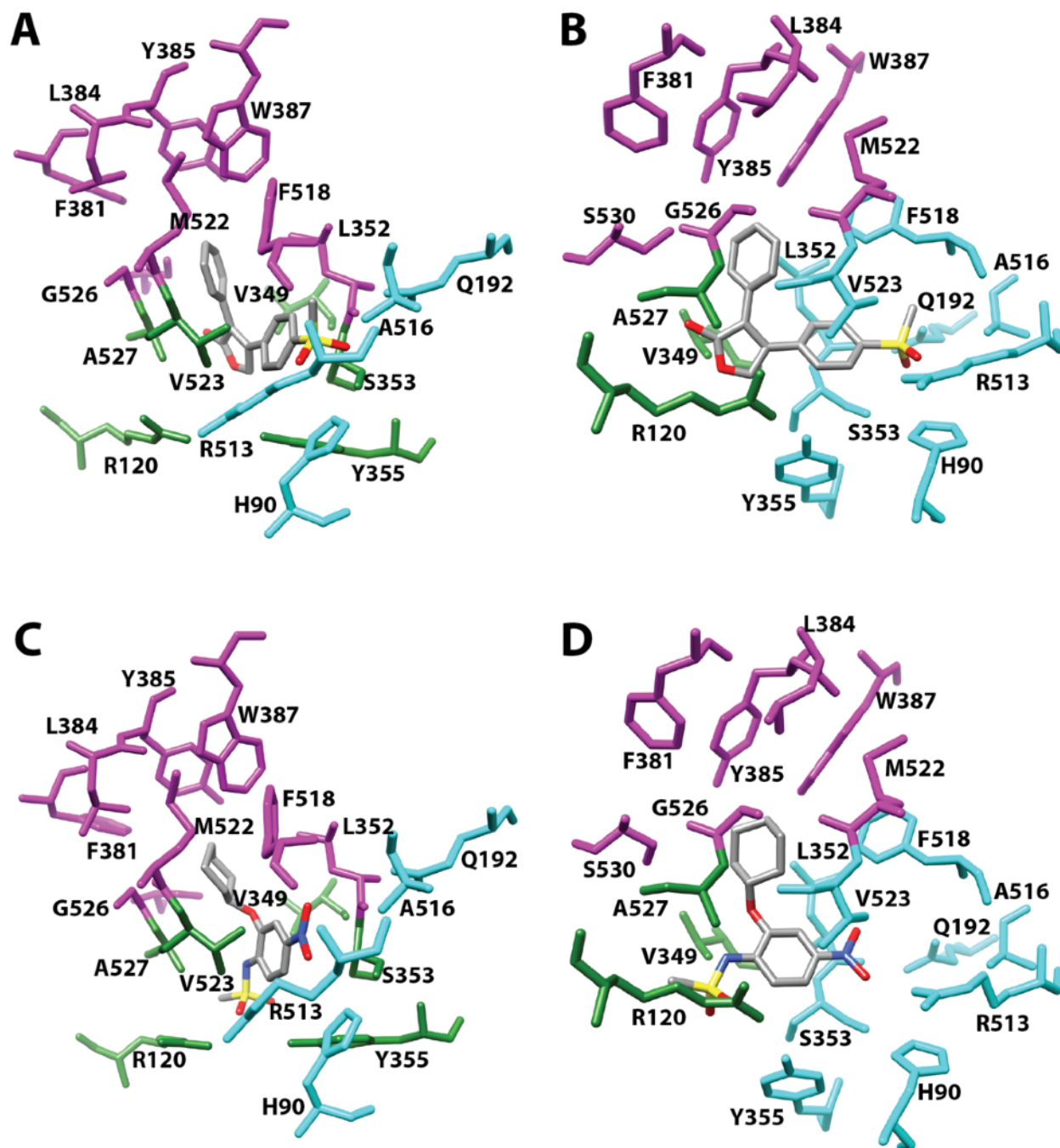


Figure S16. Structure of (A & B) rofecoxib and (C & D) NS-398 bound in the cyclooxygenase active site of COX-2 and the side chains that make up the proximal binding pocket (green), the central binding pocket (magenta), and the COX-2 side pocket (cyan). In (A) and (C), the residues are colored as in most previous figures. In (B) and (D), some residues in the proximal and central binding pockets that are shared with the COX-2 side pocket are colored cyan to highlight the interaction with the phenylmethylsulfone group of rofecoxib and the absence of an interaction with the side pocket in the case of NS-398. From PDB #5KIR and #3QMO.

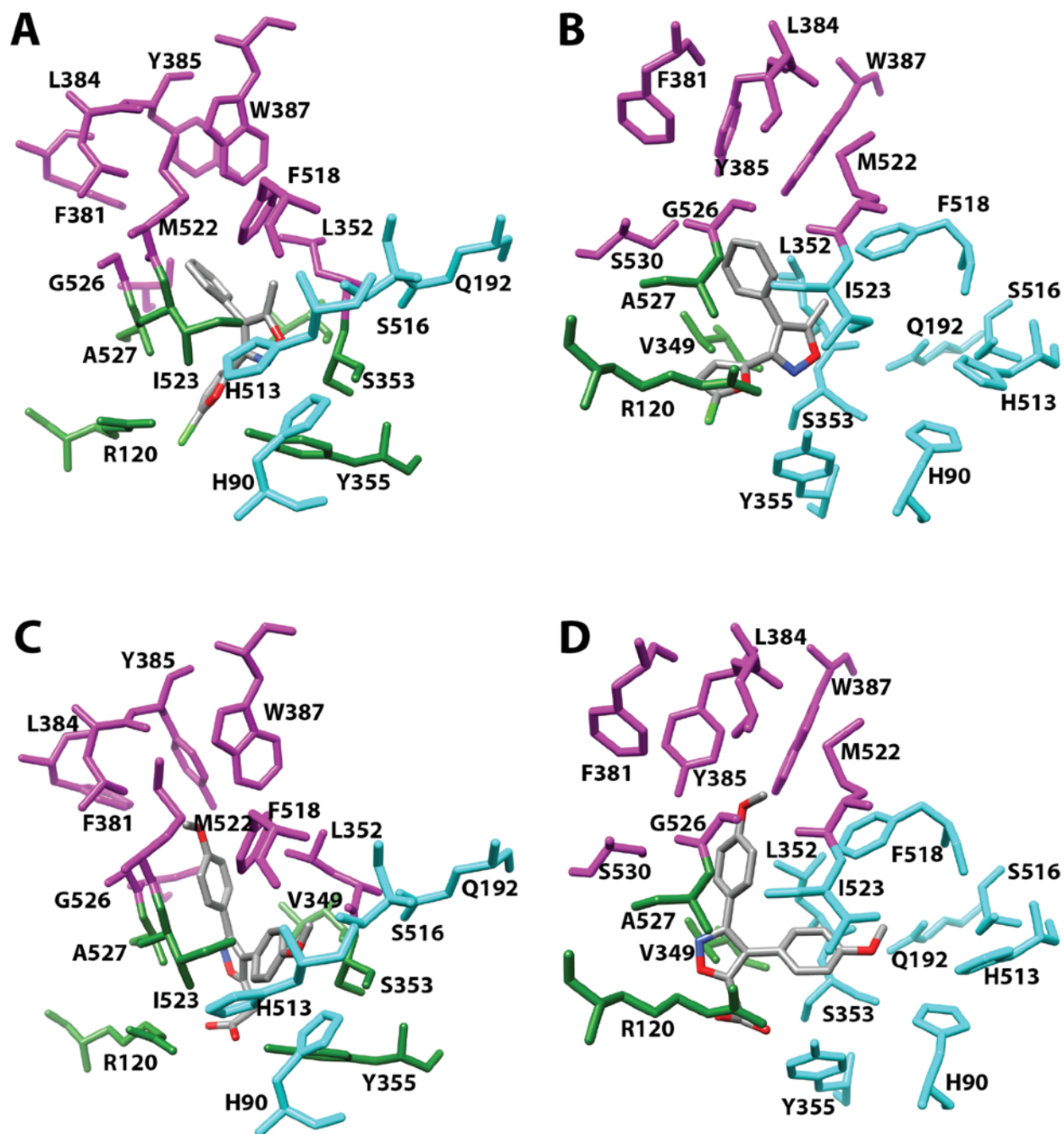


Figure S17. Structure of (A & B) P6 and (C & D) mofezolac bound in the cyclooxygenase active site of COX-1 and the side chains that make up the proximal binding pocket (green), the central binding pocket (magenta), and residues corresponding to the COX-2 side pocket (cyan). In (A) and (C), the residues are colored as in most previous figures. In (B) and (D), some residues in the proximal and central binding pockets that are shared with the COX-2 side pocket are colored cyan to highlight the interaction with the methoxybenzyl group of mofezolac and the absence of a significant interaction with the side pocket in the case of P6. From PDB #5U6X and #5WBE.

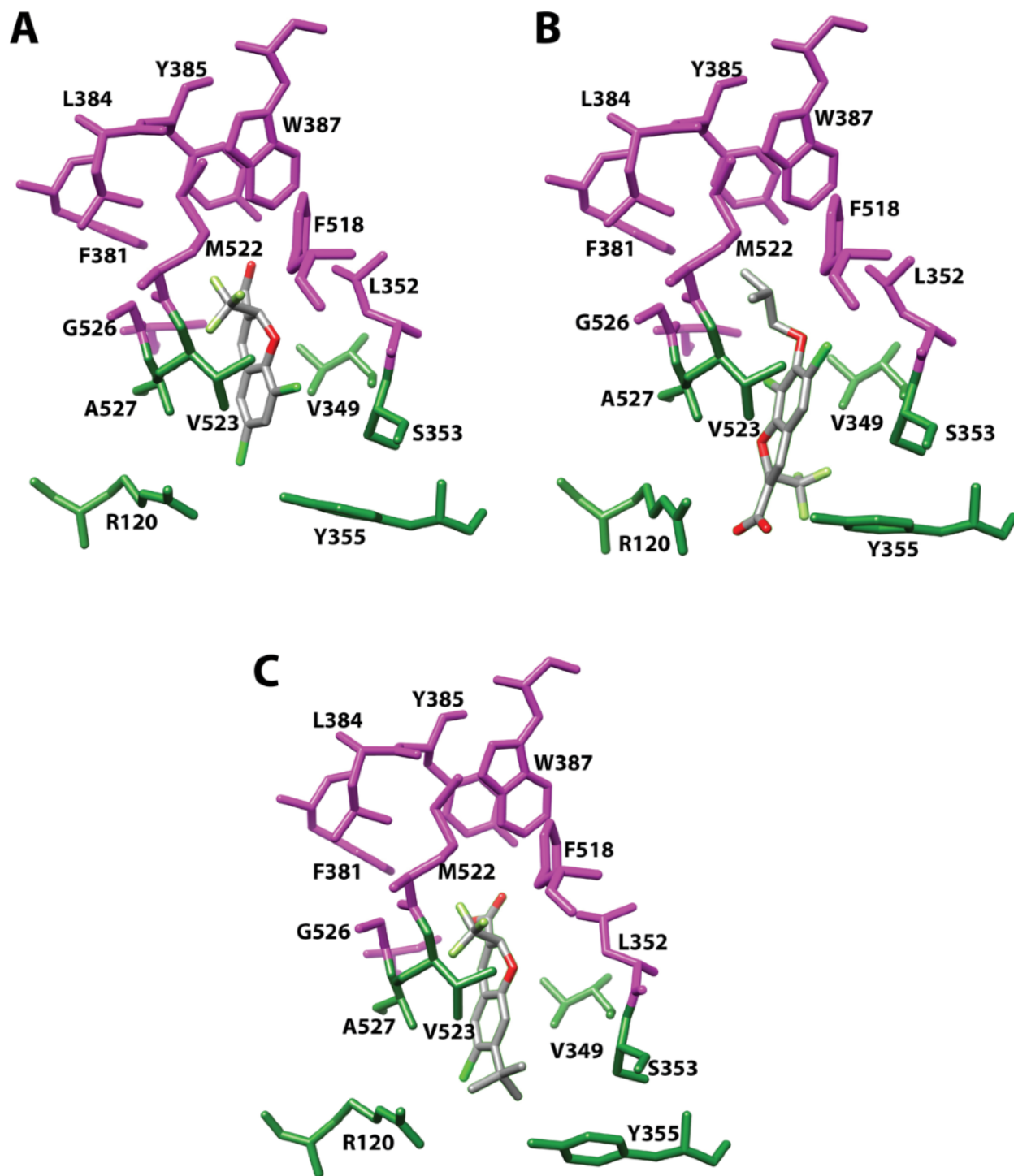


Figure S18. Structure of (A) (*S*)-5c, (B) (*R*)-23d, and (C) (*S*)-SC-75416 bound in the cyclooxygenase active site of COX-2 and the side chains that make up the proximal binding pocket (green) and the central binding pocket (magenta). From PDB #3LN0, #3NTG, and 3MQE.

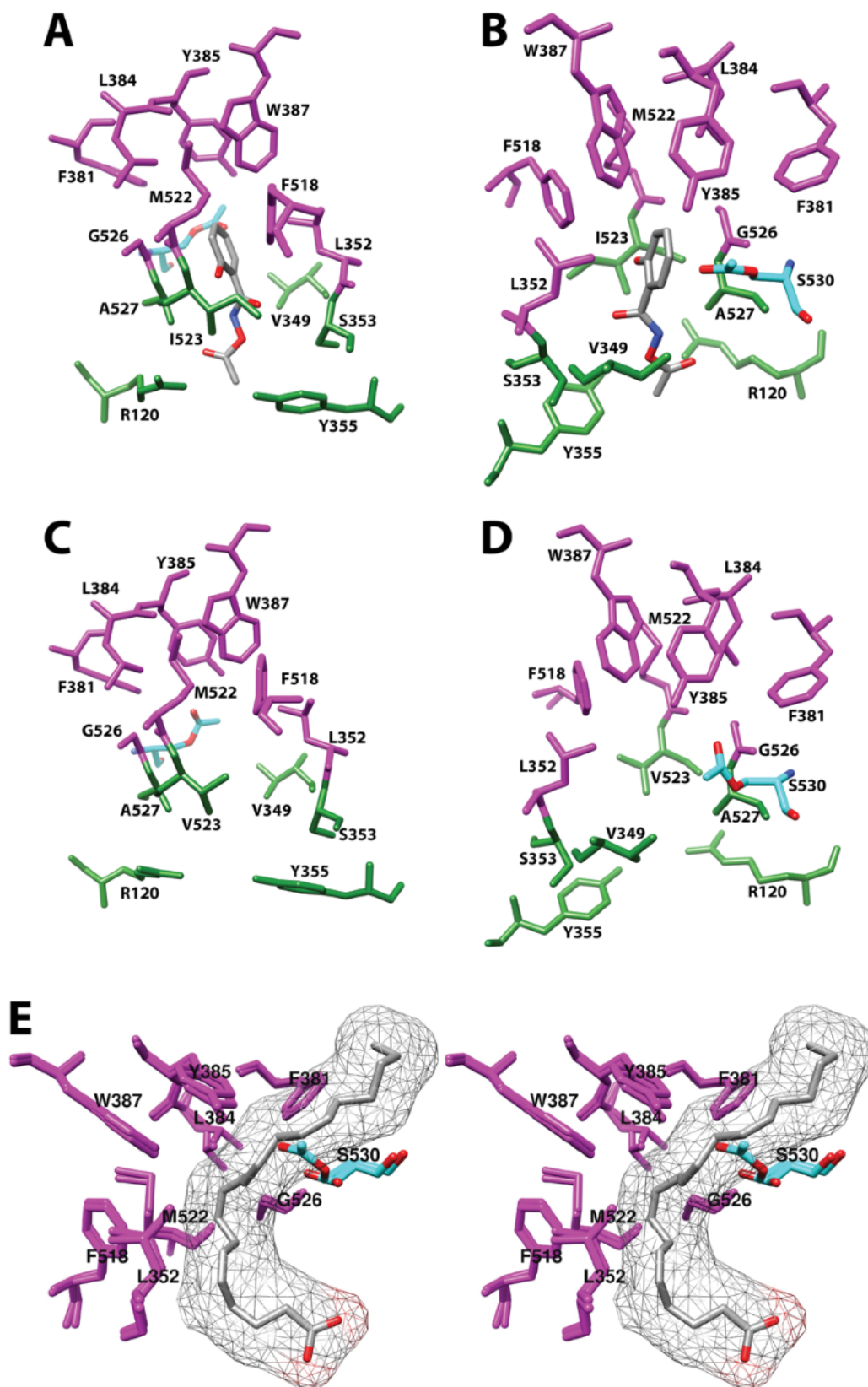


Figure S19. Structure of (A & B) acetylated COX-1 containing *O*-acetylsalicylhydroxamic acid bound in

the cyclooxygenase active site and (C & D) acetylated COX-2. (E) Cross-eyed stereo view of the structure of acetylated COX-2 superimposed over the structure of the productive conformation of AA complexed with COX-2. AA is colored by atom, with its surface shown in mesh. The steric clash between AA and the acetyl group on Ser-530 can be readily seen. The side chains that make up the proximal binding pocket (green, A-D) and the central binding pocket (magenta, A-E) are shown. The acetylated Ser-530 residue is colored by element on a cyan background. From PDB #1EBV and #5F19.

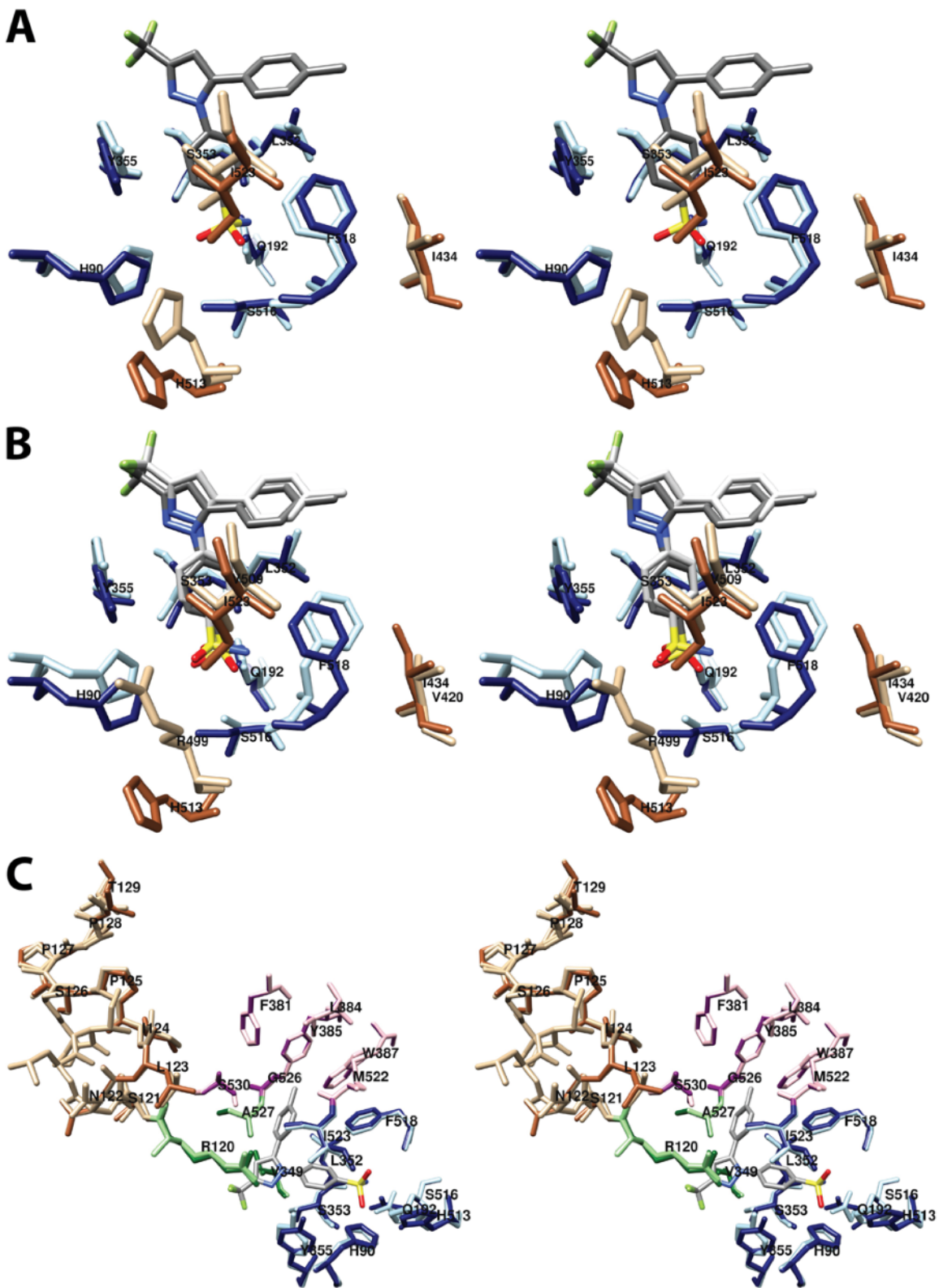


Figure S20. Cross-eyed stereo views of the structure of COX-1 complexed with celecoxib overlaid with (A) the structure of COX-1 complexed with (S)-flurbiprofen or (B) the structure of COX-2 complexed with

celecoxib. Key residues making up the side pocket are shown in dark blue (COX-1-celecoxib complex) or light blue (alternative complexes). The residues that differ between COX-1 and COX-2 (Ile/Val-434, His/Arg-513, Ile/Val-523) are shown in sienna (COX-1-celecoxib complex) or tan (alternative complexes). Celecoxib is colored by heteroatom on a dark gray (COX-1-celecoxib complex) or light gray (COX-2-celecoxib complex) background. (S)-Flurbiprofen is not shown. Note that the numbering in the COX-2-celecoxib complex, for residues Val-434, His-513, and Val-523 use the actual COX-2 residue numbers of 420, 499, and 509, respectively, reflecting the numbers in the PDB file. (C) Cross-eyed stereo view of COX-1 complexed with celecoxib The side chains that make up the proximal binding pocket (green) the central binding pocket (magenta), and the side pocket (blue) are shown. The structures of the two subunits are overlaid with subunit A (containing celecoxib) shown in the darker colors. Also shown are residues 121-129, which exist in two conformations in subunit B depending on the presence or absence of bound celecoxib. Subunits containing inhibitor exhibit the same conformation as is observed in subunit A (sienna), whereas those lacking inhibitor diverge between Ser-121 and Pro-125. From PDB #3KK6, #1EQH, and #3LN1.